12-2012

Examination of Nonpoint Source Nutrient Export from a Snowfall-Dominated Watershed

Lindsey DeBoer Carrigan
Utah State University

EXAMINATION OF NONPOINT SOURCE NUTRIENT EXPORT FROM A SNOWFALL-DOMINATED WATERSHED

by

Lindsey DeBoer Carrigan

A thesis submitted in partial fulfillment
of the requirements for the degree

of

MASTER OF SCIENCE

in

Civil and Environmental Engineering

Approved:

Darwin L. Sorensen Major Professor	David K. Stevens Committee Member
Grant E. Cardon Committee Member	Mark R. McLellan Vice President for Research and Dean of the School of Graduate Studies

UTAH STATE UNIVERSITY
Logan, Utah

2012

ABSTRACT

Examination of Nonpoint Source Nutrient Export from a Snowfall-Dominated Watershed

by

Lindsey DeBoer Carrigan, Master of Science

Utah State University, 2012

Major Professor: Darwin L. Sorensen
Department: Civil and Environmental Engineering

This study examined nonpoint source pollution via tributaries to Pineview Reservoir. Since few literature values of export coefficients are available for snowfall-dominated watersheds such as Pineview, locally scaled rates were quantified using an upstream-downstream bracketing technique. Nitrogen and phosphorus grab samples were manually collected and discharge measurements were conducted during the annual study period. Additionally, high-frequency monitoring sensors that measured EC, temperature, turbidity, and water level were deployed at the up- and downstream sites to represent short-duration transport events and to examine watershed processes on a more representative time scale.

Daily nutrient loads were estimated from grab samples and flow rates using the Rank-Data (RD) distribution method and, using surrogate relationships for discharge and total phosphorus (TP) concentration from high-frequency sensors, half-hour TP loads were calculated. Short-duration snow melt events were identified by turbidity spikes and increased air temperatures as well as, in some cases, hydrograph peaks. During these events, export coefficients from 0.31 to 0.54 g TP/ha/hr were observed for low and high elevation snow melt events. While losses to ground water were observed for one study reach, the study reach with positive load gains had annual export coefficients of 0.018 g TP/ha/hr from

high-frequency loads and 7.5e-5 g NO_x-N/ha/hr, 3.5e-6 g SRP/ha/hr, and 9.1e-6 g TP/ha/hr from RD loads. These rates were 1,000 to 2,000 times greater than available literature values typical of rainfall-dominated watersheds. This study showed the importance of erosive, snow melt events on nutrient transport and the need for high-frequency monitoring representing short-duration events for accurate estimation of export coefficients. Management strategies to reduce nutrients from tributaries should focus on erosion control in the Pineview Reservoir watershed.

(148 pages)

PUBLIC ABSTRACT

Examination of Nonpoint Source Nutrient Export from a Snowfall-Dominated Watershed

by

Lindsey DeBoer Carrigan, Master of Science

Utah State University, 2012

Major Professor: Darwin L. Sorensen
Department: Civil and Environmental Engineering

This study examined pollution from surface runoff water transported to the Pineview Reservoir by rivers and streams. Since few past studies have been conducted on watersheds of this climate, locally applicable nutrient export rates were quantified. The study was conducted by isolating river segments and monitoring changes in water quality between the top and bottom of the segments. Samples of nitrogen and phosphorus concentrations were collected and flow rate measurements were made during the annual study period. Additionally, monitoring sensors which took frequent measurements of characteristic water quality parameters were deployed at the top and bottom of the river segments. These served to monitor changes in water quality occurring between site visits.

Daily loads of nitrogen and phosphorus were estimated from sample concentrations and flow rates. Half-hour phosphorus loads were also calculated using a correlation observed between sample concentrations and monitoring sensor values. Snow melt events were identified by muddy water conditions and increased air temperatures as well as, in some cases, increased flow rates. During these events, nutrient export rates from 0.31 to 0.53 g total phosphorus/ha/hr were observed for low and high elevation snow melt events. In one study reach, loads at the bottom of the river segment were less than those at the

top and it was assumed that the surface water was being routed to ground water. In the study reach that had greater loads at the bottom of the river segment than at the top, annual nutrient export rates were 0.018 g total phosphorus/ha/hr from loads estimated from sensor values and 0.000075 g nitrogen/ha/hr, 0.0000035 g bioavailable phosphorus/ha/hr, and 0.0000091 g total phosphorus/ha/hr from loads based on grab samples only. These rates were 1,000 to 2,000 times greater than available literature values typical of watersheds receiving the dominant portion of their precipitation as rainfall. This study showed the importance of snow melt events, and subsequent erosion, on nutrient transport and the need for sensor monitoring in order to represent short-duration events in nutrient export rates. Management strategies to reduce nutrients from tributary contributions should focus on reducing erosion in the Pineview Reservoir watershed.

ACKNOWLEDGMENTS

I express my gratitude to my advisor, Dr. Sorensen, for his mentoring and making it possible for me to continue to explore the science world. I am also grateful to my committee members for their guidance and suggestions, which have broadened my perspectives. Thank you to my colleagues for their generous contributions to this research including, but not limited to, enduring sub-zero temperatures during sampling trips. I also express my gratitude to my family and friends who have supported me on this journey and through the journey of life. Ultimately, I could do nothing without the grace of the Lord for which I will be eternally grateful.

Lindsey DeBoer Carrigan

To promoting a better world for future generations to enjoy.

CONTENTS

LIST OF TABLES

LIST OF FIGURES

CHAPTER 1

INTRODUCTION

Water is extremely valuable and all life depends upon it. As less than one percent of the planet's water is located on land accessed by humans (*Dodds*, 2002), the need for sufficient supplies of good quality is extremely important. Reservoirs are constructed to store water for drinking, agriculture, and industry, as well as for power generation, flood control, navigation, and recreation (*UNEP*, 2010). Most reservoirs in North America are located in the mid-latitudes of the continent and are used for water storage where natural lakes do not adequately supply water (*Thornton et al.*, 1990). These regions also coincide with erodible soils where watershed nutrient export is high and, inherently, the dominant portion of phosphorus loading is particulate (*Thornton et al.*, 1990).

Lakes and reservoirs naturally accumulate sediments and organic debris thereby obtaining nutrients from their watersheds and increasing biological productivity (*Dodds*, 2002; *Masters and Ela*, 2008). This process can also be accelerated by anthropogenic sources such as wastewater flows, agricultural returns, or urban runoff (*Masters and Ela*, 2008). Reservoirs are highly susceptible to anthropogenic inputs due to their locations. While the regulation of point source pollution has improved the quality of surface waters, the nature of nonpoint source pollution makes it particularly difficult to control and regulate, causing some water bodies to still not meet the goals of the Clean Water Act (*Federal Water Pollution Control Act 33 U.S.C.*, 1972; *Masters and Ela*, 2008). Reservoir water quality is often controlled by its external nonpoint source nutrient loadings which echo climatic and watershed characteristics (*Thornton et al.*, 1990).

Many nutrients are essential for aquatic life but nitrogen and phosphorus are usually the nutrients limiting algal growth (*Pierzynski et al.*, 1993; *Masters and Ela*, 2008) and are co-limiting in some cases (*Dodds*, 2002; *Lewis and Wurtsbaugh*, 2008; *Conley et al.*,

2009). Nutrient availability is influenced by system chemical parameters, geology, and land use (*Dodds*, 2002). Most freshwater systems tend to be phosphorus-limited and those with naturally low concentrations are especially sensitive to anthropogenic nutrient enrichment (*Pierzynski et al.*, 1993).

Discharge of nitrogen and phosphorus from runoff and ground water are known to contribute to eutrophication (*Pierzynski et al.*, 1993). In a survey conducted by the USEPA to identify impaired lakes and reservoirs, the dominant pollutants were nutrients and the chief contributing source of pollution was agricultural runoff with urban runoff also posing a concern (*Masters and Ela*, 2008). These runoff and erosion events decrease soil structure and accelerate the transport of chemicals and pollutants (*Lal and Stewart*, 1994) as flowing water dissolves soluble constituents or erodes particles (*Pierzynski et al.*, 1993).

Particles are delivered from watershed runoff and stream bank erosion (*Pierzynski et al.*, 1993). This is a function of the energy of flowing or impacting water and the energy required to detach a particle based on the soil texture and structure (*Pierzynski et al.*, 1993). Both water availability and soil properties are influenced by land use and climate and these can vary by season, impacting transport processes. For example, upstream agricultural practices in the spring have been shown to result in higher sediment transport with the portion of large particles greater than usual (*Thornton et al.*, 1990).

While sediment itself is a major pollutant, it is also a carrier of nutrients, pesticides, and pathogens (*Thornton et al.*, 1990) due to its net surface charge and the large surface area of clay particles. Soluble and particulate phosphorus is transported in runoff and during flood events and, due to the selective transport of clay-sized material and its high adsorption potential, the phosphorus content in the delivered material becomes enriched (*Thornton et al.*, 1990; *Lal and Stewart*, 1994). Most nitrogen loss is due to the erosion of sediment-associated nitrogen but a reduction in soluble nitrogen, in addition to particulate, has been observed when practices preventing erosion and runoff were implemented (*Lal*

and Stewart, 1994). Nitrogen from fertilizer has also been shown to be transported in runoff water with a significant fraction of the organic nitrogen associated with particles (*Lal and Stewart*, 1994).

Pineview Reservoir is located in the Wasatch Front region of Utah. Originally constructed in 1937 and expanded in 1957, Pineview Reservoir is used primarily for irrigation water and flood control but also for drinking water and recreation (*Tetra Tech Inc.*, 2002). Similar to other reservoirs in this region, the dominant portion of reservoir inflows occurs during the spring runoff season when snow melts from the valley floor and successively higher elevations. Water quality of the reservoir is typically good but conditions during the late summer to early fall often result in algae blooms. Temperature stratification in the reservoir provides conditions for the development of anoxia in the hypolimnion and, following mixing of the water column, previously sediment-bound nutrients are entrained. Nitrogen and phosphorus are thought to be co-limiting in this system (*Tetra Tech Inc.*, 2002). As no point source pollution discharge permits have been issued for Pineview Reservoir or its tributaries, nutrient enrichment of the system is assumed to occur via nonpoint source contributions.

1.1 Literature Review

1.1.1 Study Area: Pineview Reservoir Watershed

This research was conducted in the Pineview Reservoir watershed, located in Weber County, Utah, USA, part of the Lower Weber River Basin, Hydrologic Unit Code 16020102. The Ogden River is impounded by Pineview Reservoir in Ogden Valley and has three sub-drainages converging at the reservoir. Flows from these three rivers, the North, Middle, and South Forks of the Ogden River, are diverted during the irrigation season and the channels are frequently dry until recharged by ground water (*Tetra Tech Inc.*, 2002). Agriculture has historically dominated this area but has been decreasing with increasing recreational and residential developments (*Tetra Tech Inc.*, 2002). Ogden Valley is the home of the communities of Eden, Liberty, and Huntsville, the largest and only incorporated town, as well as lands managed by the U.S. Forest Service and Utah Division of Wildlife Resources (*Weber County*, 2008). The population of Huntsville in 2010 was 608 (*U.S. Census Bureau*, 2010), experiencing a 6.0% decrease since 2000 in comparison to the 16% increase from the years 1990 to 2000 (*U.S. Census Bureau*, 2009). The total population in the Ogden Valley was 6,604 in 2010 (*U.S. Census Bureau*, 2010).

Pineview Reservoir watershed is situated in the Wasatch and Uinta Mountains with a maximum elevation of about 3,000 meters at Willard Peak (*Tetra Tech Inc.*, 2002). The elevation of the reservoir is 1,500 meters at full capacity. Average watershed slope is estimated at 5.6% (18°). Ogden Valley was created by normal faults and has been accumulating fluvial and lacustrine sediments, up to about 230 meters thick in some areas (*Lowe et al.*, 1999). Notable geologic deposits include quartzite, dolomite, limestone, sandstone, shale, and Norwood tuff (*Lowe et al.*, 1999). In the western side of the valley, lacustrine silts form a confining layer under which the aquifer behaves uniformly (*Lowe et al.*, 1999). Figure 1 shows the location and boundary of this confining layer below the reservoir. Outside of

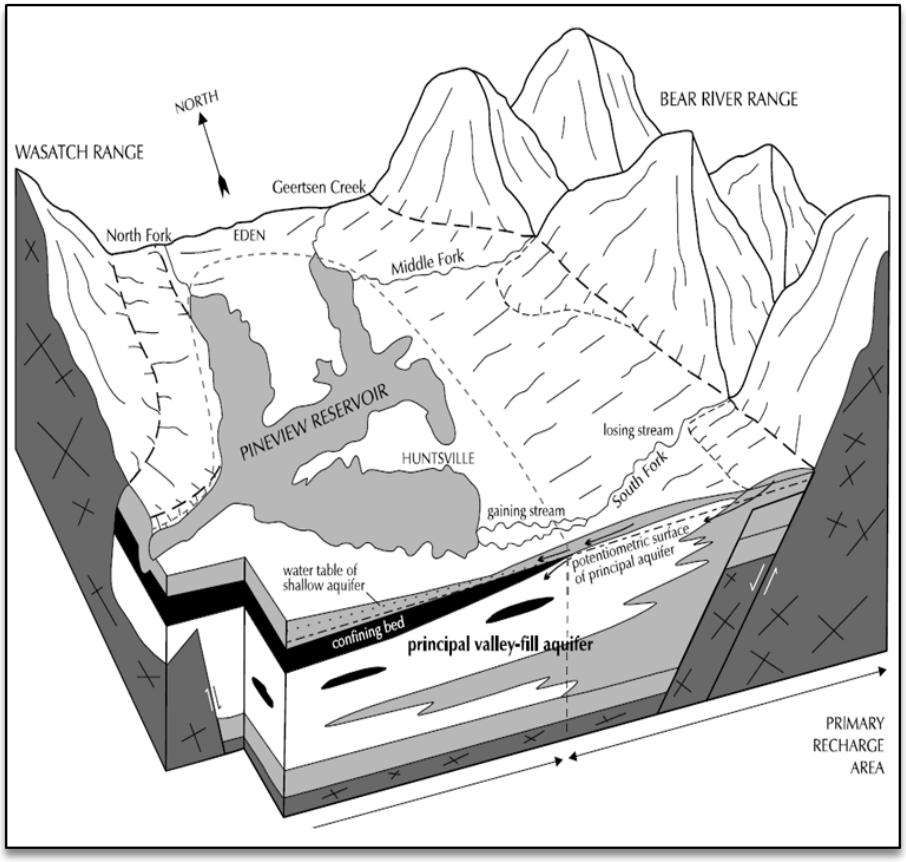

Fig. 1: Pineview Reservoir unconfined and confined aquifers (*Lowe et al.*, 1999).

this confining layer, ground water acts under unconfined conditions (*Lowe et al.*, 1999). Ground water is recharged by snow melt, seepage from streams, and irrigation infiltration while discharge from the aquifer is by seepage to streams and springs, pumping from wells, and evapotranspiration (*Avery*, 1994). *Avery* (1994) identified seepage rates from the South Fork Ogden River along the valley floor as 0.31 cms to 0.70 cms during November through February of 1960-64, this tributary exhibiting the highest rates compared to other tributaries.

The climate is generally hot and dry in the summer with most precipitation falling during the colder, winter months as snow. Daily maximum summer temperatures near Huntsville averaged 31°C and winter lows −12°C (*WRCC*, 2009). Annual precipitation at the Huntsville Monastery (elevation 1567 m) averages 55 cm (*WRCC*, 2009) while up-

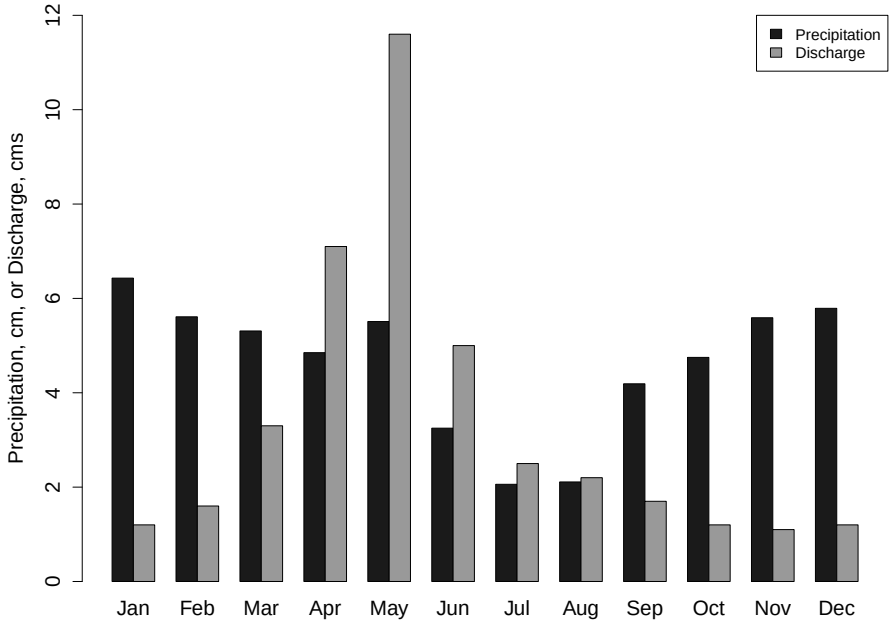

Fig. 2: Average total precipitation and stream discharge data by month (*WRCC*, 2009; *U.S. Geological Survey*, 2010).

per elevations receive approximately double that amount (*Avery*, 1994). Average annual snowfall at this valley-level station equaled 180 cm from 1976 to 2009 (*WRCC*, 2009). Figure 2 displays monthly average precipitation totals at the Huntsville Monastery alongside monthly average stream flow rates for the South Fork Ogden River for 1976 to 2009.

As illustrated in Figure 2, about 60% of the total average precipitation occurred during the winter months from November to April, the six months which received the highest average snowfall. During the six months of greatest discharge from March to August, 80% of the total average stream flow occurred. Spring melting of snow received during winter months generates the major portion of reservoir inflows. Stream flows during winter months are more consistent and reflect the system's baseflow conditions.

The reservoir was identified in 2000 as an impaired water not meeting its beneficial use as a cold water fishery due to summer hypolimnetic anoxia and warm temperature; reductions in the total phosphorus and nitrogen loads were identified to remedy this problem

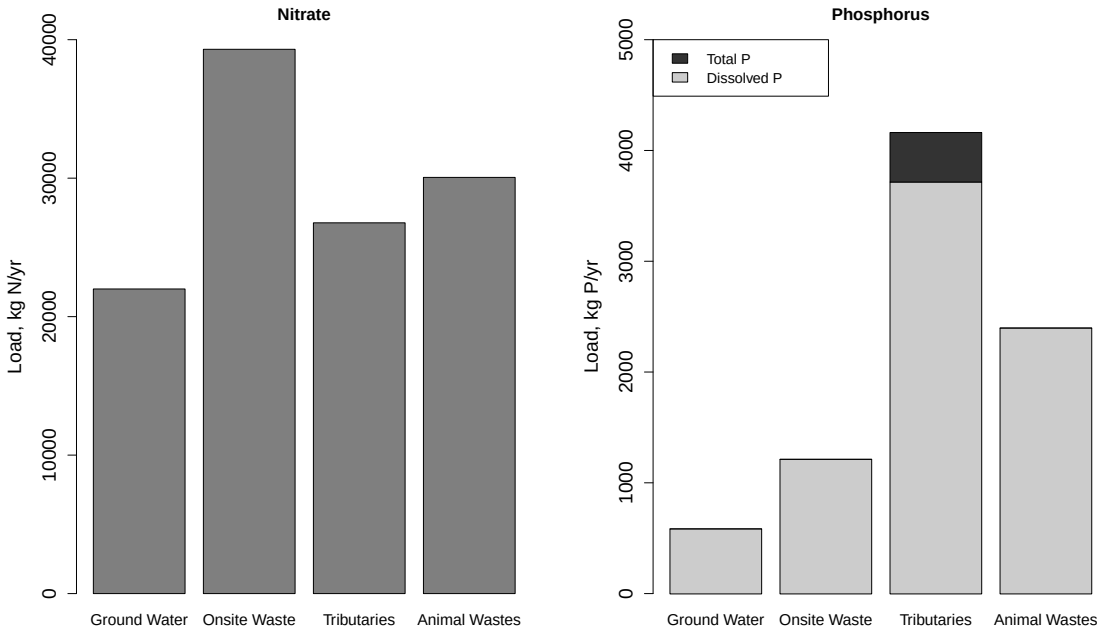

Fig. 3: Sources of dissolved N and dissolved P to Pineview Reservoir, adapted from *Tetra Tech Inc.* (2002).

(*Tetra Tech Inc.*, 2002). Pineview is currently listed as partially supportive of its designated use (*UDEQ Division of Water Quality*, 2008) and is managed as a warm water fishery. Due to their impact on algal growth, the Total Maximum Daily Load (TMDL) conducted by *Tetra Tech Inc.* (2002) identified nitrogen and phosphorus from nonpoint pollution sources, illustrated in Figure 3, as there are no point source pollution discharge permits within the watershed.

Discharge from the shallow aquifer has greater influence on tributary water quality as irrigation diversions drain tributaries and inflows become primarily ground water near their confluence with the reservoir. Surface water nutrient loads predicted in the TMDL study conducted by *Tetra Tech Inc.* (2002) showed the greatest rates of transport during the winter months of December through March. In this study, *Tetra Tech Inc.* (2002) used precipitation and temperature data representing the valley elevations. While these data would reflect warmer temperatures, less precipitation, and different snow melt events than the large areas

of upper elevations in the watershed, *Tetra Tech Inc.* (2002) assumed total annual loads were still considered accurate and that only the timing of their transport was altered. However, this hydrologic pattern does not represent the high peak flows and corresponding erosion which typically occur in this watershed during the spring snow melt season. Particles containing sorbed and mineral phosphorus are carried by tributaries to the reservoir during these erosive events. These particles settle and anoxia of late summer creates reducing conditions wherein ferrous iron and phosphates, previously-complexed with ferric iron and insoluble under oxygenated conditions, are released into the water column. This is the basis of the internal phosphorus loading from sediments which *Tetra Tech Inc.* (2002) identified as another potential source of phosphorus to Pineview Reservoir.

The TMDL study (*Tetra Tech Inc.*, 2002) estimated that the South Fork Ogden River delivered 73% of the surface water flows to the reservoir and represented 60% of the total watershed; the report by *Avery* (1994) was in agreement that the South Fork is the largest tributary and drainage area. In addition, runoff load modeling conducted by *Tetra Tech Inc.* (2002) showed the South Fork subbasin to be the greatest contributor of surface water loads due to its large size. When examining the *Tetra Tech Inc.* (2002) modeled mass of pollutants on a per area basis of the respective subbasin, the North, Middle and South Fork subbasins were comparable.

After exiting Causey Reservoir, the South Fork Ogden River flows approximately 12 km where, during irrigation season, it is initially diverted into three irrigation canals. From this point, the river flows an additional 2 km and splits into two separate channels, the North and South Branches of the South Fork Ogden River, that each converge with Pineview Reservoir approximately 5 km downstream.

1.1.2 High-Frequency Monitoring

In order to be able to understand watershed and stream processes, it is necessary to

examine the results of these processes on a time scale corresponding to their reactions while doing so within logistical and economical constraints (*Horsburgh et al.*, 2010). As the need for reliable, quality water sources increases, protecting and managing these systems becomes of vital importance. As such, timely information about hydrologic systems is important to examine the effects of anthropogenic influences and to protect valuable resources (*Christensen et al.*, 2002). Often grab sampling events, even as frequent as weekly, miss constituent fluxes which occur on time scales less than one day. This can be due to changes in constituent concentrations, flow rates, or both as rapid melt events or storms alter watershed processes. In-situ monitoring enables these events to be captured and the use of surrogate variables, where adequate technology does not exist, further increases the availability of needed data (*Horsburgh et al.*, 2010).

Using the sensor values and manually collected samples for each constituent, regression equations can be developed to estimate variables when no samples are available (*Christensen et al.*, 2000, 2002). Temporal and spatial factors require consideration in the identification of explanatory variables. Unique geologic, hydrologic, and geographic conditions at each site can require site-specific relationships to be developed. *Christensen et al.* (2002) recommended a sampling regime such that 90% of the stream flow's characteristics are represented by manual sampling.

Since turbidity measures light scatter and particulates associated with such are also means of transporting N and P, relationships between total P and N with turbidity have been observed by *Christensen et al.* (2002),*Ryberg* (2006), and *Horsburgh et al.* (2010). Dissolved species did not typically show turbidity as an explanatory variable (*Rasmussen et al.*, 2005; *Ryberg*, 2006). However, *Rasmussen et al.* (2005) observed specific conductance as an explanatory variable for ionized constituents and concentrations of which decreased during high flow periods generated by runoff. *Christensen et al.* (2002) explained the influence of inverse specific conductance on a few observed N and P regressions since

the transport of these nutrients occurs predominantly during the runoff season when specific conductance is low. N and P concentrations have also been observed to be influenced by other seasonal variables such as flow or water temperature and, even more directly, day of the year (*Christensen et al.*, 2000; *Ryberg*, 2006). These real-time estimates of water quality can be combined with estimates of stage-discharge relationships (*Ryberg*, 2006) and used to improve load calculations (*Christensen et al.*, 2000, 2002).

1.1.3 Export Coefficients

The rate of nutrient transport according to land area is one way to simulate pollutant loads in a watershed; however, it is important that these rates be representative of the geography and climate of the region in which they are being modeled as these factors control the characteristic pollutant yield (*Shrestha et al.*, 2008). *Beaulac and Reckhow* (1982) noted the wide range of nutrient export values and attributed observed variability to the natural spatial and temporal differences of the study watersheds. They also proposed the dominant factor controlling the export from undisturbed watersheds, such as forestland, is climate and that as watersheds become more subject to anthropogenic impacts nutrient transport becomes more complex (*Beaulac and Reckhow*, 1982).

Nutrient transport rates have typically been expressed as export coefficients (ExCs) (mass of constituent per unit area and time) for large rural areas or as expected mean concentrations (mass per volume) used for urban areas and based on runoff from storm events. These rates vary by land use and hydrologic event (*Tang and Liu*, 2008) and are typically expressed as annual averages. Advances in GIS technology has facilitated doing these types of analyses for large areas of mixed land use.

Because the transport of pollutants and sediments are closely linked and their mechanisms are influenced by surface runoff, erosion models, such as the Universal Soil Loss Equation, can be used to locate landscapes with high nonpoint pollution potential (*Sivertun*

and Prange, 2003). Factors impacting these critical landscapes include soil type, terrain slope, distance to the body of water, and land use (*Sivertun and Prange*, 2003). Typical land use types which are acknowledged as dominant pollutant contributors are agriculture, forest, grassland/meadow, urban and barren (*Shrestha et al.*, 2008; *Tang and Liu*, 2008). Considering these many significant factors, a wide range of landscape types exists and often the land use type simply becomes the major qualifier. *Beaulac and Reckhow* (1982) reviewed 40 export coefficients of total nitrogen (TN) and total phosphorus (TP) for generally agricultural land use and included data on precipitation and runoff. Figure 4 shows the relationship observed between runoff and watershed precipitation while Figure 5 shows TN and TP export coefficients in relation to precipitation received.

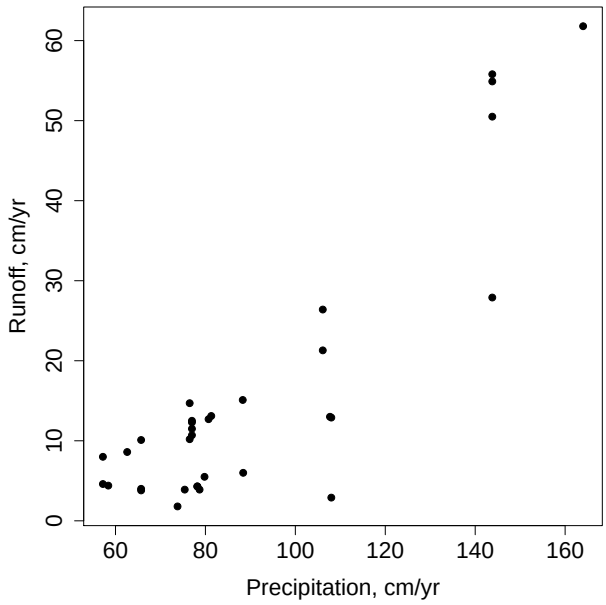

Fig. 4: Watershed precipitation versus runoff, adapted from *Beaulac and Reckhow* (1982).

Figure 4 shows a relationship between precipitation and runoff as would be expected; however, the export rates shown in Figure 5 cannot be predicted accurately by precipitation alone. As noted previously, the Pineview watershed receives 55 cm (in lower elevations)

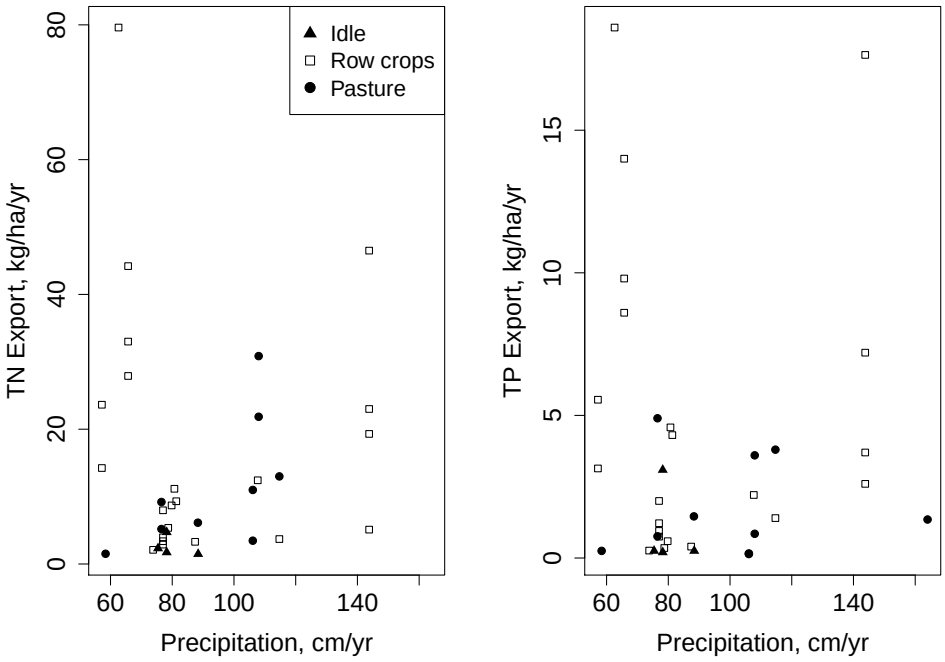

Fig. 5: TN and TP export as a function of precipitation, adapted from *Beaulac and Reckhow* (1982). Land use classifications for rotational grazing were labeled 'Idle' and all other grazing as 'Pasture'.

to greater than 100 cm (at higher elevations) of precipitation annually. The data reviewed by *Beaulac and Reckhow* (1982) show relatively few data points where the study area received greater than 100 cm precipitation with export coefficients from 3.5 to 47 kg/ha/yr for TN and 0.14 to 18 kg/ha/yr for TP. In general, nutrient export rates can vary by two orders of magnitude and few rates are available for watersheds dominated by snowfall and subsequent melting events.

1.1.4 Watershed-Based Models

In mountainous regions a vital part of the water supply comes from snow melt and a critical part of managing this resource is based on understanding the interactions between landscape, snow accumulation, and stream flow generation (*Ahl et al.*, 2008). Simulation models can be useful tools to systematically examine these interactions and the effects which natural or anthropogenic changes on landscapes within a watershed may induce (*Ahl et al.*, 2008). In such situations, models use previously determined rates of nutrient transport from diffuse sources and known land use parameters, as well as loadings from point sources, to simulate the constituent loads at a desired location. Such an approach allows concerns about water amounts, quality, and timing to be addressed. However, given in-stream locations of known flow and nutrient concentration along with upstream watershed information, nonpoint source contributions as runoff based on land area can be determined.

Several approaches have been used in quantifying rates of nutrient export from watersheds and various land uses. Monitoring the major tributaries of smaller watersheds enables the contributions of sub-catchments within larger watersheds to be examined (*Shrestha et al.*, 2008). The advantage to monitoring catchments containing heterogeneous land uses, as opposed to homogeneous catchments or field plot studies, is that results represent an average of conditions and processes of the whole catchment (*Shrestha et al.*, 2008) as well as more accurately representing the natural attenuation occurring in larger basins (*Beaulac*

and Reckhow, 1982).

Lal and Stewart (1994) state that although several physically-based models exist to describe phosphorus transport, the processes have been oversimplified due to a general lack of data. However, *Ahl et al.* (2008) applied SWAT in a Rocky Mountain watershed, separating periods of runoff and base flow, and found it performed reasonably well during the runoff period but was less accurate during base flow periods. *Tang and Liu* (2008) proposed a method using GIS whereby runoff is predicted from land use and precipitation and combined with known event mean coefficients to predict nonpoint source loadings and average annual in-stream concentrations. Their method compared flow rates during non-precipitation periods to that during precipitation events to separate runoff contributions from base flow and found good agreement between modeled surface runoff and measured surface runoff; however, modeled pollutant concentrations compared to measured concentrations were less accurate due to point source contributions and the assumption that pollutant transport was conservative (*Tang and Liu*, 2008).

1.2 Objectives

The main objective of this study centralized around identifying and quantifying sources and timing of nonpoint nutrient loading to Pineview Reservoir. Such information has the potential to be used to examine future land use and climate scenarios and to be helpful to resource managers in developing practical strategies for protecting water quality. Specific objectives were:

1. Use identified critical landscapes to determine sub-watersheds contributing nonpoint nutrient loads within the valley. Within these sub-watersheds, areas typical of land use types associated with nutrient runoff were quantified with the aid of GIS software.

2. Determine if separate stations of high-frequency sensors originating from the same

headwater were duplicates. Up and downstream sites were also compared to determine if changes in high-frequency measurements could be observed across the study reaches.

3. Examine the effect of snow melt events and characteristic land use types on nutrient load rates. This was based on field measurements and grab sampling but especially high-frequency monitoring using surrogate measurements in tributaries.

4. Quantify nitrogen and phosphorus nonpoint source pollution expressed as mass per area per time based on characteristic land use types from two study watersheds. Irrigated and non-irrigated conditions were considered in the determination of land use areas.

CHAPTER 2

METHODOLOGY

2.1 Study Design

Two stream reaches were isolated following the branching of the South Fork Ogden River and nonpoint source runoff generated in the two sub-watersheds was examined. Using an upstream-downstream bracketing technique to create study reaches where the rivers flowed through the valley, noise from upstream contributions was minimized so that runoff mainly originating from the valley floor and nearby, higher-elevation rangeland could be examined. Locally-scaled rates of nitrogen and phosphorus export according to land area were quantified using loads estimated from field measurements and grab sampling and with the aid of high-frequency surrogate measuring techniques.

Initially, a critical landscape analysis involving slope, land use/cover, soil type, and distance to stream bed was conducted following the approach of *Sivertun and Prange* (2003) to identify areas of high erosion potential. These areas were limited to the valley floor where the implementation of potential management strategies is more likely. The results of this analysis are shown in Figure 6.

Note that higher values on the scale represent areas of greater erodibility (colored red). Figure 6 shows areas near the South Fork exhibit a higher erosion potential in comparison to other areas on the valley floor. Due to this erosion factor and the large drainage area represented by the South Fork, it was selected for more intensive monitoring than other tributaries to Pineview Reservoir.

Hydrology and water quality measurements have been made on the South Fork Ogden River near the confluence with the reservoir since 2009. Additionally, more intensive data collection was conducted during 2010 including data collection at two additional upstream

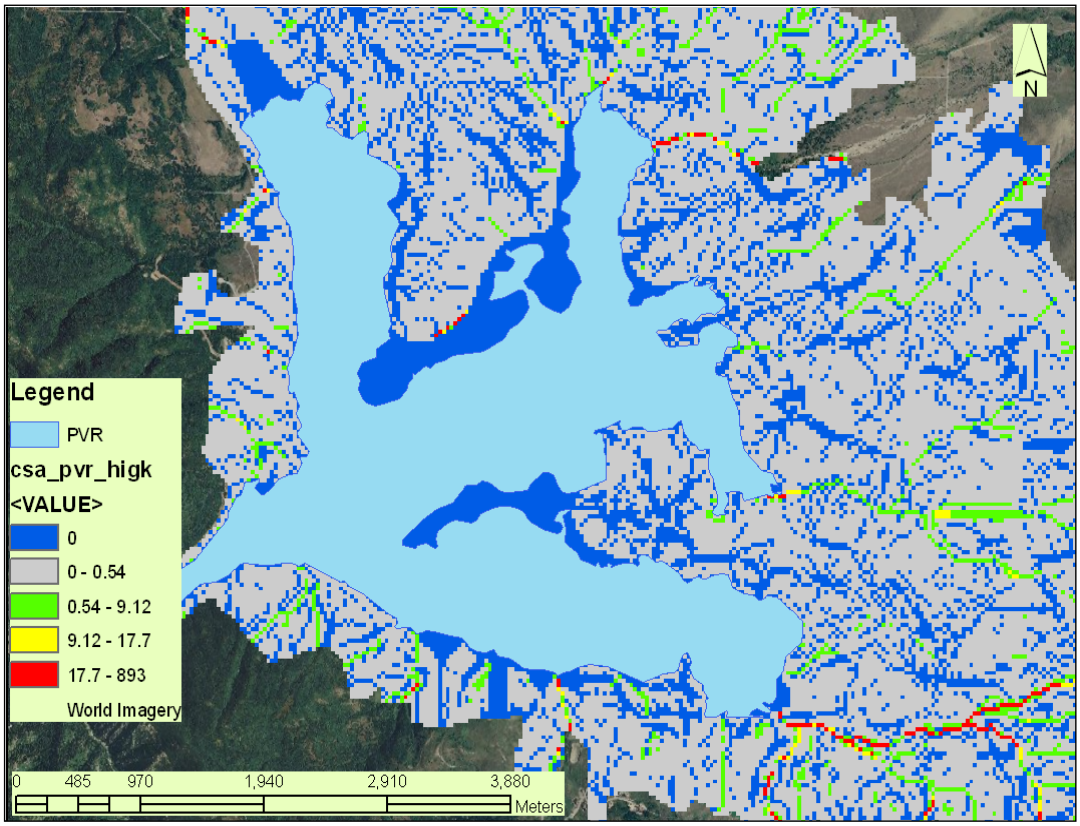

Fig. 6: Critical landscape analysis.

sites on the North Branch South Fork (NBSF) and South Branch South Fork (SBSF). Locations of the collective sampling sites are shown in Figure 7.

It was hypothesized that due to the close proximity of the upstream monitoring sites to the split in the South Fork Ogden River (0.25 km) that these two sites should represent the same water and that sensor measurements and grab samples of these sites could be tested as duplicates. Studying upstream and downstream points allowed changes occurring in water quality as the streams traveled through the valley to be examined and dominant contributions from overlapping upland elevations to be minimized. Although these two study reaches lie relatively close in proximity, they do not represent contributions from similar sub-catchments.

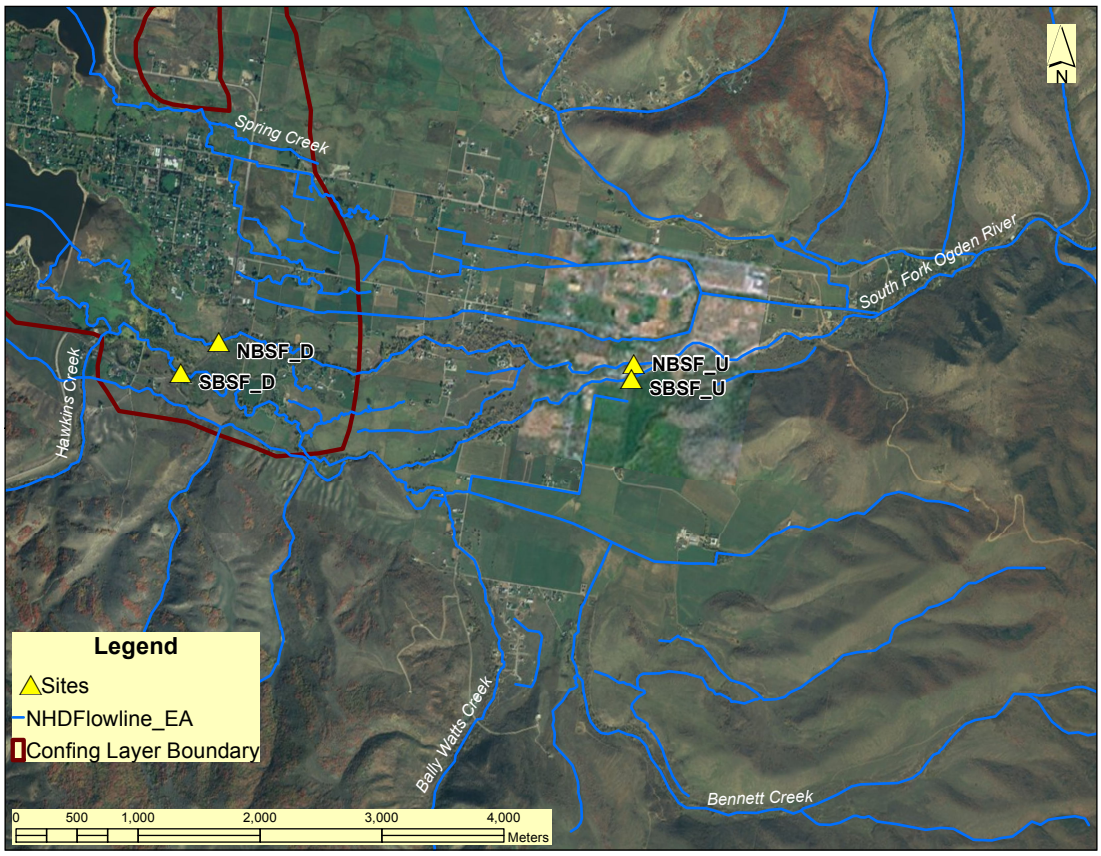

Fig. 7: Monitoring sites located on the South Fork Ogden River. Upstream sites are denoted by 'U' and downstream sites by 'D'.

Data collection included measurement of flows and collection of grab samples for nutrient analyses and measurement of pH, conductivity, and turbidity. Discharge estimates were obtained from point estimates across a stream transect (*Chapra*, 1997) using a top-reading depth gage with an attached velocity meter (Swoffer model 2,100) or by using an acoustic doppler current profiler (Teledyne RD Instruments StreamPro ADCP). Laboratory nutrient analyses included dissolved nitrate+nitrite (NO_x-N), dissolved ammonium (NH_4-N), soluble reactive phosphorus (SRP), and total phosphorus (TP). In addition, water quality data was recorded by fixed sensors. These sensors recorded conductivity, temperature, turbidity, and water pressure (depth) at half-hour intervals. Temperature-corrected electrical conductivity (EC) measurements were used to examine seasonal surface wa-

ter/ground water interactions. As phosphorus transport is commonly associated with sediments, high-frequency turbidity measurements were correlated with grab sample measurements of phosphorus in an attempt to predict in-stream concentrations of phosphorus at half-hour intervals. In a similar manner, a stage-discharge relationship for each site was generated using half-hour water level values for frequent estimations of flows. Using the rank-date distribution method (*Lee*, 2008), daily nutrient concentrations and flow rates were estimated from grab samples and measured flows. The product of these half-hour and daily concentrations and flows created estimates of the nutrient loads at each site. Difference in the loads between the downstream and corresponding upstream site represented the nutrient load gain across the study reach. Annual surface water load estimates from tributaries to Pineview Reservoir were also estimated from the product of daily concentrations and flow rates.

Water quality, hydrology, and land use data were integrated to determine ExCs for the South Fork/Pineview Reservoir watershed using GIS and other modeling techniques. Landscapes examined included agricultural lands, urban areas, and rangeland. Land use classification was as determined by the Utah Division of Water Resources (*Utah Division of Water Resources*, 2007) for lands influenced by irrigation. Remaining areas within the watersheds were assumed to be rangeland as this was not mapped by the Utah Division of Water Resources since these lands are not irrigated.

Hydrologic conditions of the South Fork/Pineview Reservoir watershed are very different among the snow melt/non-snow melt seasons and the irrigation/non-irrigation seasons. Assuming flow and proper weather data would reflect snow melt and runoff conditions, irrigation/non-irrigation conditions necessitated a representation in the physical change in flow paths. Irrigation canals, even with closed head gates, still act to collect and channel water running off fields; however, only with open head gates are canals able to divert a portion of the flow from the main channel. In GIS, runoff and stream flow generation

was forced to flow to certain mapped streams or irrigation canals by lowering the elevation of grid cells representing these channels. Using a spatial discontinuity greater than the analysis's grid size, irrigation canals were disconnected from natural streams to prevent water flowing into the canals during non-irrigation season while allowing the canals to act as a collection system for runoff. The canals were connected to the streams during the irrigation season to simulate diverting a portion of the flow. Watershed areas used as the basis for nutrient export rates were respective of these two hydrologic scenarios.

2.1.1 High-Frequency Sensors

Water quality sensors used for high-frequency monitoring were Campbell Scientific CS547A Conductivity and Temperature Probe, FTS DTS-12 Digital Turbidity and Temperature Sensor, and Campbell Scientific CS450 Submersible Pressure Transducer. The Campbell Scientific CR800 Measurement Control System was used at each station to initiate measurements and store each set of half-hour data until it was manually uploaded. Monitoring sensors were suspended inside HDPE pipe and, where a continuous supply of fresh water was necessary for representative measurements, pump screens protected sensors extending outside the pipes (*Horsburgh et al.*, 2010). This protective housing extended into continuously flowing zones of the river. Each of these systems was fastened to a bridge for stability and further protection. Figure 8 shows the general orientation of each high-frequency monitoring site. Permission from the government agencies managing the respective bridges was obtained prior to installation. During site visits, data was uploaded, sensors were cleaned and reinstalled, and debris was removed from the sensor protective housing to ensure optimal function.

Fig. 8: High-frequency monitoring equipment at the SBSF_U site.

2.1.2 Laboratory Analyses

Principal analytical methods focused on identifying forms of nitrogen and phosphorus. These are summarized in Table 1. Other laboratory analysis methods for pH, conductivity, and turbidity measurements were made at 25°C using potentiometric probes and a nephelometer.

Table 1: Summary of laboratory nutrient analyses.

Analysis	Method	Reference
Dissolved Ammonium-N	AQ2 Method No: EPA-103-A Rev. 4	*APHA* (1995a), *Seal Analytical* (2009)
Dissolved Nitrate+Nitrite-N	AQ2 Method No: EPA-127-A Rev. 5	*APHA* (1995b), *Seal Analytical* (2006)
Soluble Reactive Phosphorus	Modified EPA 365.3	*U.S. EPA* (1978), *APHA* (1995c)
Total Phosphorus	Modified EPA 365.3	*U.S. EPA* (1978), *APHA* (1995c)

The quality control plan included routine equipment cleaning and maintenance. Trip blanks were incorporated for each type of sample used on each sample collection event to verify samples were not contaminated from unclean containers. As was appropriate for the analysis method, instruments were calibrated and/or calibration verification was conducted with each batch of samples processed. Method blanks, matrix spikes, and control samples were also included as necessary to verify proper laboratory performance was maintained. Quality control charts were developed to track and monitor the consistency of control samples.

2.2 Data Management

2.2.1 Relational Database

Datasets from field measurements, grab samples, and high-frequency monitoring were stored in a relational database. Organization of this database followed the structure of the observations data model outlined by *Horsburgh et al.* (2008) where observations are stored with corresponding metadata such that they are unambiguous and can be manipulated and interpreted. High-frequency data values entered into the database were quality controlled using ODM Tools (*Horsburgh et al.*, 2011) by the removal or interpolation of erroneous points (those not representative of the true sample matrix or outliers from obvious trends), applying linear drift corrections between instrument servicing, and linear interpolation to fill data gaps. When water temperatures were below freezing, anomalous EC, mean turbidity, and water level values were also replaced by interpolation since the presence of ice was suspected to interfere with accurate measurements.

2.2.2 Quality Control

Data in this study was constrained and censored due to three reasons: limitations of the datalogger, applicable range of temperature-corrected EC measurements, and method detection limits of laboratory analytical procedures. As the constraints placed on these measurements varied in nature, so did corresponding response methods.

Most variables of interest recorded by the Campbell Scientific CR800 datalogger were sufficiently stored as floating point numeric type which has the limits of $\pm$7999 (*Campbell Scientific*, 2010). The turbidity sensor records 100 values during a five second active measurement period to produce a mean turbidity value for each half-hour measurement cycle; however, when the variance of the 100 values exceeded 7999, it was only recorded as 7999 by the datalogger. Variance values of 7999 comprised less than 1% of the total variance

measurements and were thought to be caused by random interference to the optical sensor by such things as debris, insects, or fish passing within range of the sensor optics during the five second measurement. This occurrence was assumed to be not representative of the true turbidity. As such, the corresponding five second mean turbidity value was rejected from further analysis and was replaced via linear interpolation as described above.

EC measurements were temperature-corrected according to equation 1:

$$EC = \frac{Cond \times 100}{(T - 25) \times C_T + 100} \tag{1}$$

where *Cond* is raw conductivity in mS/cm, T represents the water temperature recorded at the time of conductivity measurement in °C, and C_T represents a correction coefficient based on average system temperatures (*Campbell Scientific*, 2009). Measurements are programmed to have a minimum EC value of 0.005 mS/cm since ionization errors are mathematically corrected in conductivity measurements as low as this value (*Campbell Scientific*, 2009). Values below 0.005 mS/cm represented 1% of the original dataset during the study period at all four high-frequency monitoring sites and were substitubed using linear interpolation. An example of the raw conductivity, temperature-corrected EC, censored values, and final interpolated values are shown in Appendix A Table A.1.

Analytical results below method detection limits included concentrations of NO_x-N and SRP. Censored points contributed 11% and 2%, respectively, of the datasets at all sites where grab samples were collected and 3% for both constituents at the four high-frequency monitoring sites. Although NH_4-N was measured, greater than 90% of the values were censored and less than 50 non-censored values were present for each site; these data were not imputed or used in loading determinations (*Helsel*, 2005). Censored values were imputed based on regressions of normal order scores and logarithmic concentrations as proposed by *Gilliom and Helsel* (1986). Imputed results with corresponding censored values, along with

all measured concentrations and flow rates used in the study, can be found in Appendix A Tables A.2 through A.5.

No high-frequency measurements at the upstream sites were collected during the majority of the irrigation season when the streambeds were dry. This period of no flow was determined based on collected values of mean turbidity and water level which were zero. Beginning late in the day on 29 June to 9 November the turbidity and water level values were set to zero so that upstream calculated loads would be zero. During this time, no values for raw conductivity, EC, and temperature were used.

2.3 Modeling Techniques

2.3.1 Geographic Information Systems

Geographic data was analyzed using ESRI's ArcGIS 10 (`http://www.esri.com/software/arcgis/arcgis10/index.html`). The base map was created from available datasets including a water-related land use map published in 2007 by the Utah Division of Water Resources (*Utah Division of Water Resources*, 2007), a 10-meter Weber County digital elevation model (DEM) (*Utah GIS Portal*, 2008) and National Hydrography Dataset flow lines (*Horizon Systems Corporation*, 2006) showing natural streams and irrigation canals. These data files were projected using USA Contiguous Albers Equal Area Conic USGS version for proper representation of polygon shape areas. Flow lines were edited to more closely match satellite imagery obtained from ESRI ArcGIS Map Service (*ESRI*, 2009). Polygon land use data were converted to raster values using the same resolution as the DEM (7.5 minutes, approximately 10 meters).

GIS modeling was conducted under two physical scenarios. Non-irrigation conditions were represented by disconnecting irrigation canal flow lines from headwaters using a spatial differentiation larger than the grid cell used in raster analysis (10 m). Flow lines con-

necting canals to sources represented irrigation conditions. These mapped flow lines were burnt into the DEM using terrain processing available from ArcHydro Tools (*ESRI*, 2011) in order to refine the DEM according to mapped flow lines. Further analyses were conducted for each scenario using the respective burnt DEM. The DEM was further processed by filling sinks, or places where flowing water would be trapped based on the elevations of grid cells, again using ArcHydro terrain processing (*ESRI*, 2011).

Following processing of the DEM, flow directions were determined according to the Spatial Analyst extension in ArcGIS 10 wherein the flow from each grid cell flows to one of eight nieghboring cells which has the lowest elevation. Using the processed DEM, a flow accumulation grid (cells of any land use) was created to show the total number of upstream grid cells contributing to points (or cells) of interest. A weighted grid was created for each land use of interest wherein cells of a particular land use were assigned a value of one and all cells of any other land use were assigned zero. Weighted flow accumulation grids were created for each land use using the weighted land use grids. A weighted flow accumulation grid sums the upstream cells from the weighted grid so that only grid cells of the land use of interest are represented since all others have a zero value. The fraction of weighted flow accumulation values versus total flow accumulation values resulted in the fraction of upstream area represented by each land use. Land uses of each watershed contributing to the study reaches on the North and South Branches of the South Fork Ogden River were determined as the difference in each land use area between the up and downstream sites. The GIS model had difficulty in representing the flow conditions at the fork where the North and South Branches diverge; however, the total number of upstream cells was unimportant since only the watershed contributing to the reach between the study sites was of interest.

Due to the different physical scenarios required for calculation of land use areas, the water year was broken down into three seasons. The runoff season (non-irrigation physical scenario) spanned 05 April to 20 June and was identified by the rising limb of the turbidity

and hydrograph peaks and ended prior to the beginning of the irrigation season. The irrigation season was from 21 June to 20 October based on the opening and closing of the South Bench Canal diversions (personal communication, Mr. Blane Green, South Bench Canal watermaster, 02 June 2011). Non-runoff and non-irrigation conditions were classified as baseflow which was the remainder of the year (21 October to 04 April).

2.3.2 Significant Difference Testing

Significant difference tests were conducted to test the hypothesis that the upstream sites on the North and South Branches contained water of similar quality and acted as duplicates. Similar tests were also conducted between each respective up and downstream site to show the effectiveness of selected parameter measurements to detect differences in water quality. Flow rates and depth measurements were not compared as the sites do not have similar morphometry and any similarity between the sites would be coincidental. Since most of the distributions were non-parametric (Appendix B Figures B.1 through B.3), the Wilcoxon rank sum test was used to compare the non-simultaneous grab sample measurements (*R Development Core Team*, 2010). High-frequency measurements do represent simultaneous measurements but were inherently auto-correlated and so the measurements corresponding in time were compared graphically. Also, since no actual high-frequency measurements were recorded at the upstream sites when they had no flow from 29 June to 9 November, this period of time was excluded from high-frequency significant difference tests and results are summarized for the periods prior to and following dry conditions.

2.3.3 Nutrient Load Estimations

Load estimations from grab samples of NO_x-N, SRP, and TP were made using measured concentrations and measured flow rates or from predicted concentrations and flow rates where surrogate measurements were available. Estimates made where surrogate mea-

surements were not available were used for comparison with loading rates generated using surrogate measurements. Nutrient loads were generated for all major reservoir tributaries as well as the four sites on the South Fork Ogden River so that contributions from the South Fork drainage could be compared to the other reservoir drainage areas and a total load to Pineview Reservoir could be estimated.

Using data from grab sampling events only, daily loads were simulated using the RD distribution method proposed by *Lee* (2008). Available data points were ranked in descending order and assigned a cumulative failure probability (CFP) as follows:

$$CFP_i = \frac{1-(r_i-1)}{n} \tag{2}$$

where r_i and n represent the individual rank of a data point and the total number of points, respectively. A CFP was found for each day of the year during the study period by linear interpolation between sampled data points. A regression equation (p=0.001 for coefficients) was then determined for concentrations or flow rates and CFPs of sampled points. These regressions were site-specific for each nutrient and flow rate. Using the interpolated daily CFPs, the concentration or flow on that given day was predicted using the regression equation (Figure 9). Cross-referencing the date associated with a given CFP, the TP concentrations were estimated for each day of the study period which illustrated seasonal patterns as in Figure 10.

Nutrient concentrations and flow rates on the upstream sites on the North and South Branches of the Ogden River were forced to be zero during periods of the irrigation season when stream beds were dry. This period was determined to be 30 June through 8 November 2010 based on high-frequency water level measurements at these sites. Using estimates of daily nutrient concentrations and flow rates, their product was used to create daily loads throughout the annual study period. The sum of each daily load created an estimate of

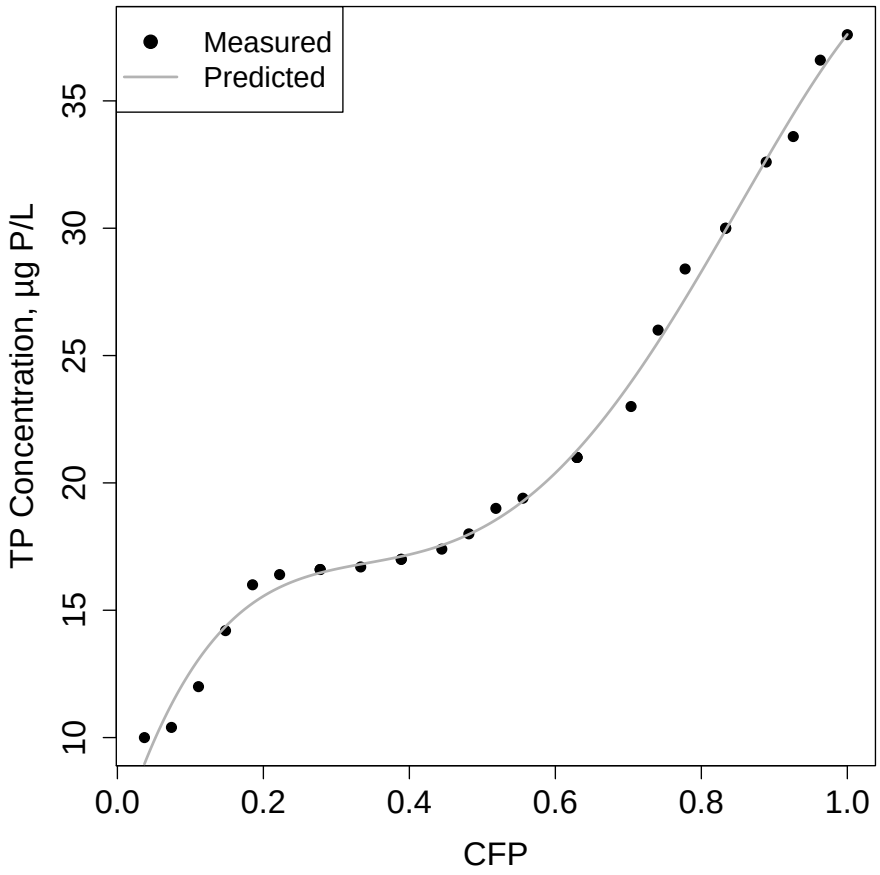

Fig. 9: TP concentrations predicted from daily interpolated CFPs at the NBSF_D site.

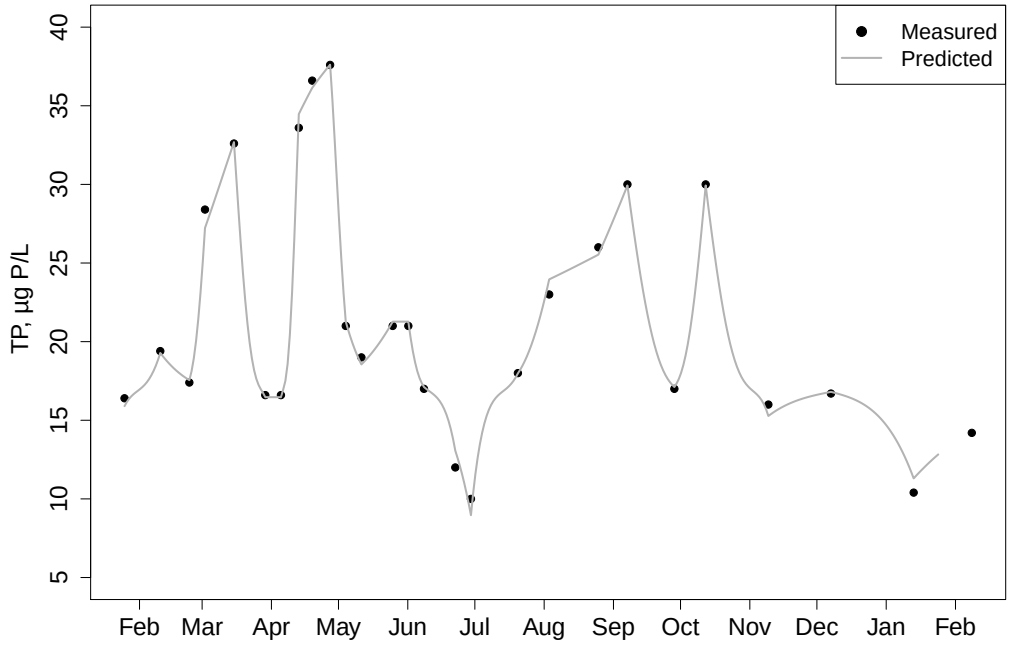

Fig. 10: Daily TP concentrations generated from CFPs at the NBSF_D site.

annual loads of NO_x-N, SRP, and TP.

Where surrogate measurements were available (turbidity and water level), regression equations were determined to predict half-hour values for TP concentration and flow rate. Assuming TP could be sufficiently described by turbidity, the data was fitted to a linear regression using high-frequency mean turbidity values as the independent variable. The depth sensor measurements were calibrated to yield a stage discharge relationship, using the power function of equation 3:

$$Q = a \times Z^b \tag{3}$$

where Q represents discharge in cms, Z is the stage in m, and a and b are regression coefficients (*Horsburgh et al.*, 2010). Once half-hour estimates of concentration and flow rates were complete, the product of these yielded half-hour estimates of the TP load at each site. These half hour load estimates were summed to develop an annual load more refined than that based on grab samples alone.

Using the daily or half-hour estimates of the nutrient loads, the instantaneous load contributed to each study reach over the corresponding time period was the difference between the loads at up and downstream sites of both study reaches. Summing these values, annual loads from each study watershed were determined. Since nutrient export varied greatly by season, seasonal loads were also calculated from each study watershed.

2.3.4 Export Coefficients

Daily or half-hour reach nutrient load estimates were summed over a specific duration to find the total mass added to the reach. The total load was averaged by the contributing area and the duration to determine the ExC as in the following:

$$ExC = \frac{L_D}{A \times t_D} \tag{4}$$

where ExC is the export coefficient for the contributing watershed area, A, L is the total load

Table 2: Available literature values for mean TN and TP, kg/ha/hr, as summarized by *Lin* (2004).

Land Use	TN	TP
Non-row crops	5.9e-4	1.2e-4
Pasture	9.9e-4	1.7e-4
Rangeland	1.0e-4	9.1e-6
Urban	1.1e-3	2.2e-4

during the selected duration (D), and t is the total duration time for the period of interest. Total and event-based ExCs were compared. For reference, available literature values are reported in Table 2.

CHAPTER 3

RESULTS AND DISCUSSION

3.1 Geographic Information Systems

GIS analysis was used to determine the land uses of each contributing watershed. Land uses in this study were generalized from classifications based on those outlined by the Utah Division of Water Resources (*Utah Division of Water Resources*, 2007). Non-row crops were specifically areas used for growing alfalfa, grain, grass hay, and seeds. This classification also included land which was previously used for small grains but that had been dormant for two or more years. The pasture classification included uncut grazing areas with any irrigation technique. Riparian areas included riverbeds and riparian zones not used for agriculture. Rangeland constituted remaining areas, specifically land which receives only natural precipitation and is not within other water use areas. Table 3 summarizes the land use areas of the two contributing reach watersheds for both the irrigation and non-irrigation season scenarios.

Table 3: Study watersheds' land use areas.

Reach	Land Use	Non-irrigation		Irrigation	
		Fraction	Area, ha	Fraction	Area, ha
North Branch	Non-row crops	0.46	83	0.44	87
	Pasture	0.17	27	0.24	47
	Rangeland	0.01	2.0	0.01	2.0
	Riparian	0.23	36	0.19	38
	Urban	0.13	20	0.12	23
	Total		**160**		**200**
South Branch	Non-row crops	0.08	530	0.08	520
	Pasture	0.01	77	0.01	58
	Rangeland	0.89	5600	0.89	5600
	Riparian	0.01	36	0.01	34
	Urban	0.01	66	0.01	64
	Total		**6300**		**6300**

The total drainage area of the North Branch increased by 40 ha during the irrigation season as open diversions allowed water, which previously had a different flow path, to enter the watershed. Open diversions tended to have an opposite effect on the South Branch, directing water out of this watershed, but only to a small degree.

3.2 Surrogate Measurements

A linear model was used to conduct single stratum analysis of variance (*R Development Core Team*, 2010) for each site with TP concentrations as the dependent variable and turbidity, EC, temperature, and water level as the independent variables. Turbidity was found to be the only dependent variable that showed significance (p=0.05) in estimating TP at all sites. Based on this, a linear regression equation was found between grab sample TP and high-frequency mean turbidity for each site. Figure 11 shows the linear regressions. The residuals from these regressions can be found in Appendix C Figure C.1. Quantiles of residuals reasonably followed a normal distribution. Contrary to reports from other studies (*Christensen et al.*, 2000, 2002; *Rasmussen et al.*, 2005; *Ryberg*, 2006), no surrogate measurements were found to consistently describe describe NO_x-N or SRP when all high-frequency measurements in this study were analyzed at the four sites. As such, NO_x and SRP were not predicted with high-frequency. Using a power function, stage-discharge relationships between flow and high-frequency water level were created as shown in Figure 12 and residual plots are in Appendix C Figure C.2. Figures 13 and 14 contain time series plots of predicted and measured turbidity and flow, respectively, for all the South Fork sites. A summary of the regression coefficients and statistics is found in Table 4.

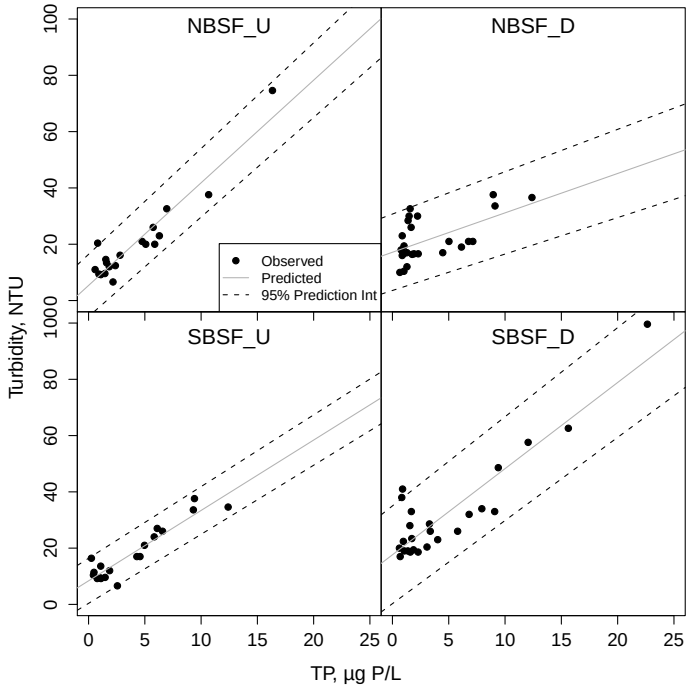

Fig. 11: Linear regressions predicting TP given high-frequency turbidity.

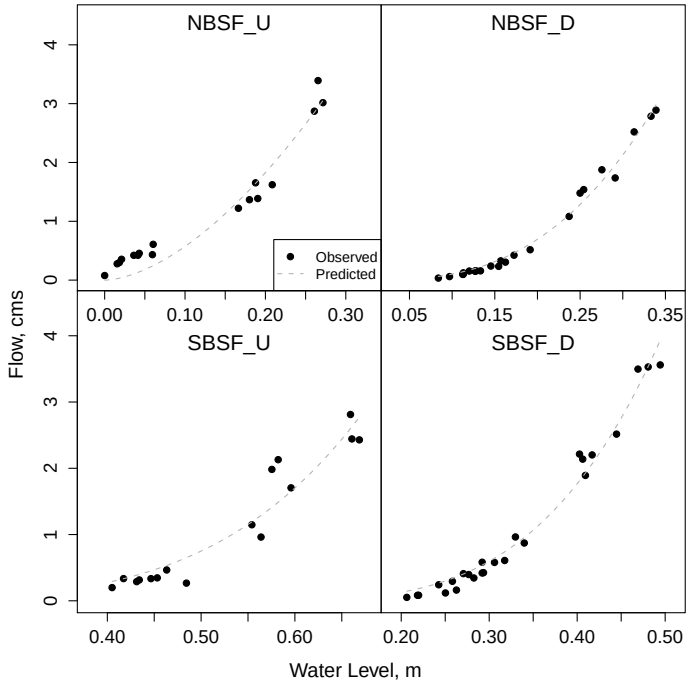

Fig. 12: Power regressions predicting flow given high-frequency water level.

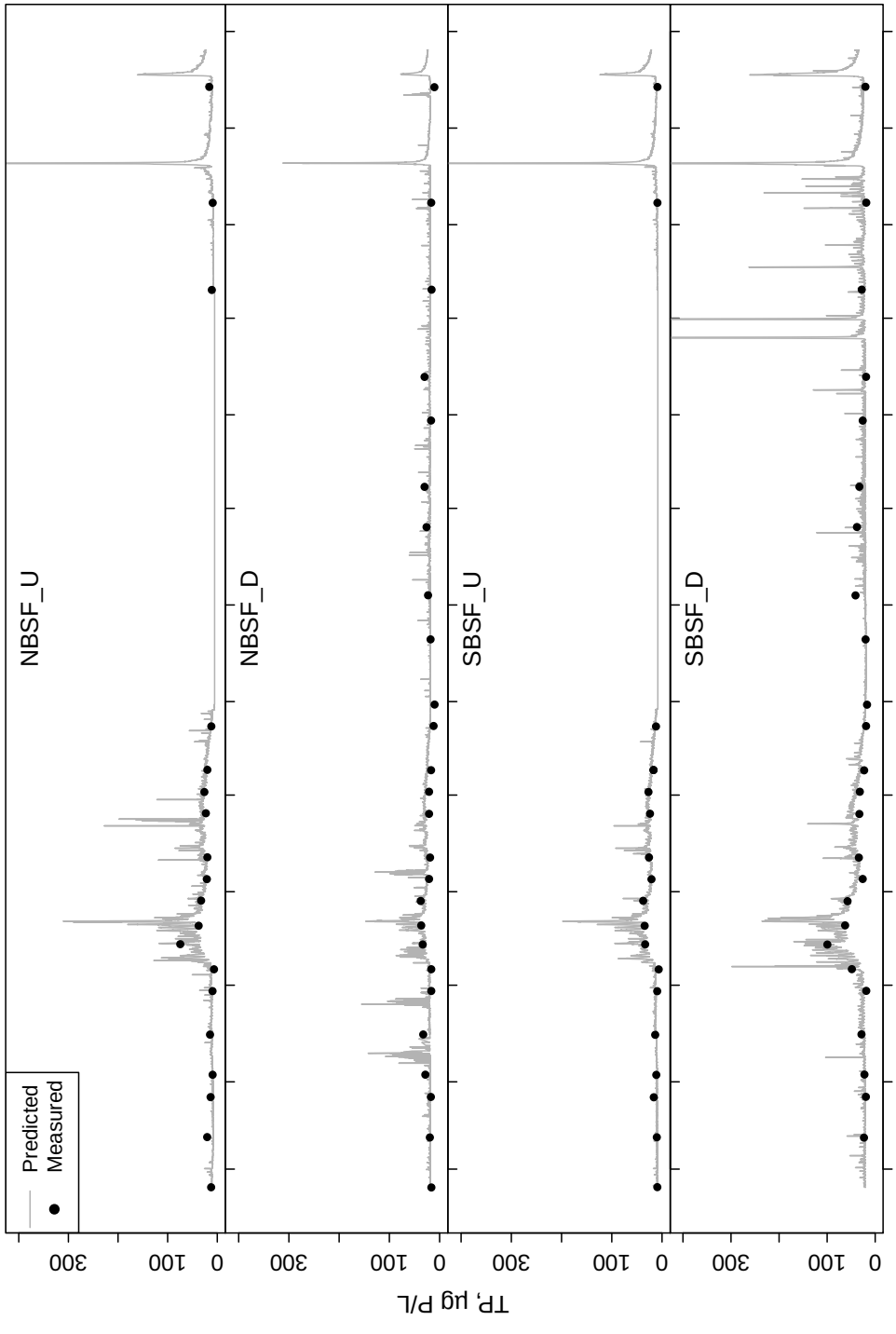

Fig. 13: High-frequency TP concentrations as predicted from turbidity compared with grab sample concentrations as measured.

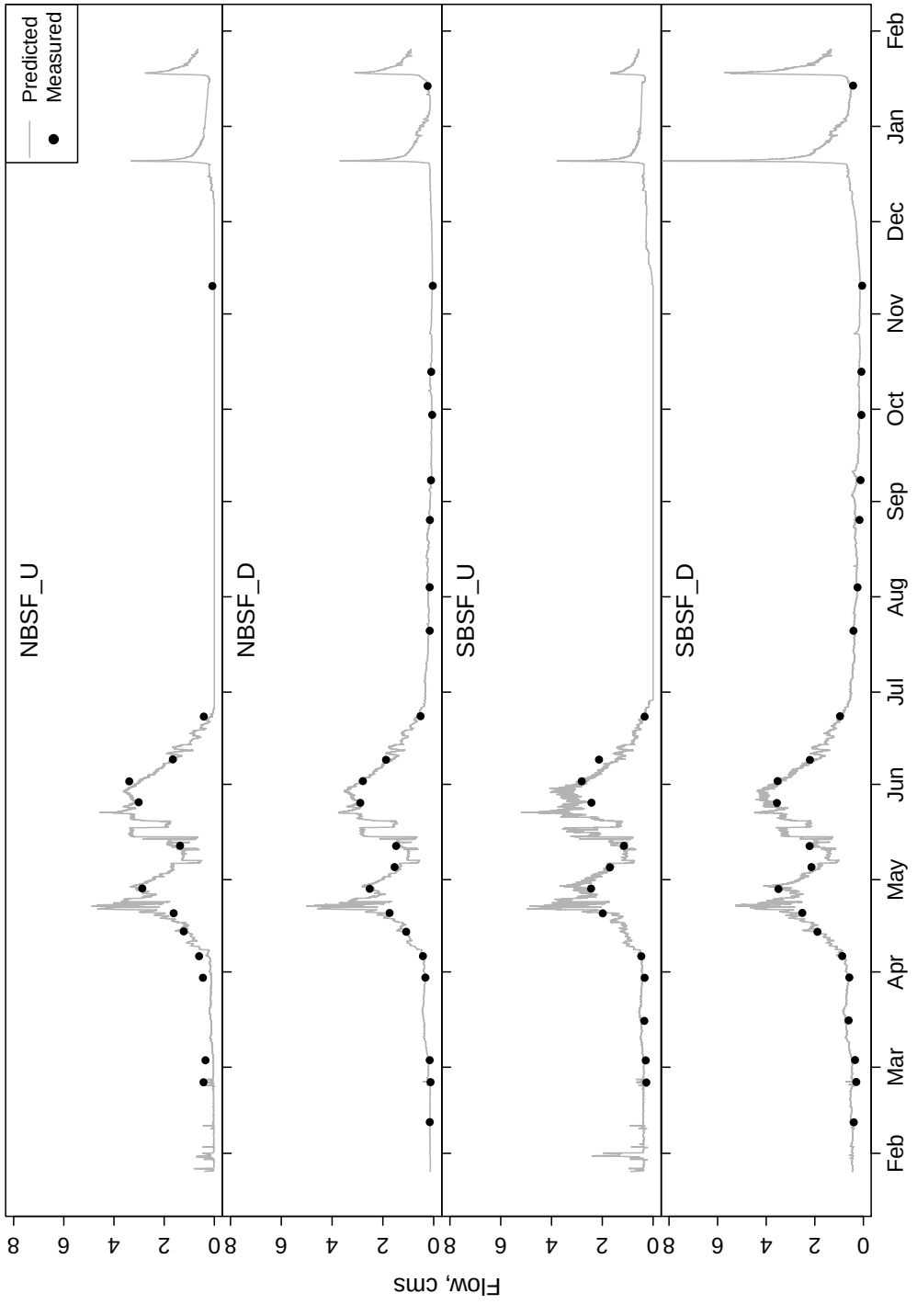

Fig. 14: High-frequency flow as predicted from water level compared with flow rates as measured.

Table 4: Summary of regression coefficients and statistics from surrogate measurements for TP and flow.

Site	Equation	R^2	Residual Std. Error	df
NBSF_U	$TP = 3.65Turb + 5.37$	0.89	5.2	17
	$Flow = 27.0Level^{1.67}$	NA	0.277	15
NBSF_D	$TP = 1.40Turb + 17.1$	0.34	6.5	24
	$Flow = 61.1Level^{2.79}$	NA	0.102	23
SBSF_U	$TP = 2.50Turb + 8.38$	0.86	3.7	17
	$Flow = 16.9Level^{4.49}$	NA	0.300	14
SBSF_D	$TP = 3.06Turb + 17.6$	0.81	8.3	23
	$Flow = 56.2Level^{3.78}$	NA	0.171	23

[1]"NA" denotes no value available for this regression.

Appendix C contains joint confidence regions for the linear and nonlinear regressions in Figures C.3 and C.4. The joint confidence regions are elongated suggesting parameter correlation with the greatest variability in the intercept and parameter *a* (see Equation 3) estimations. It would be difficult to obtain more precise parameter estimates since this would require additional data reflective of extreme events. This was impractical since it would necessitate more frequent sampling to capture high/low flow or turbidity conditions especially given short-duration events and measurement limitations at low levels.

3.3 Data Trends

Initially, all time series parameters were plotted as shown in Figures 15 through 19 according to site and were scaled as necessary in order to examine related and seasonal data trends.

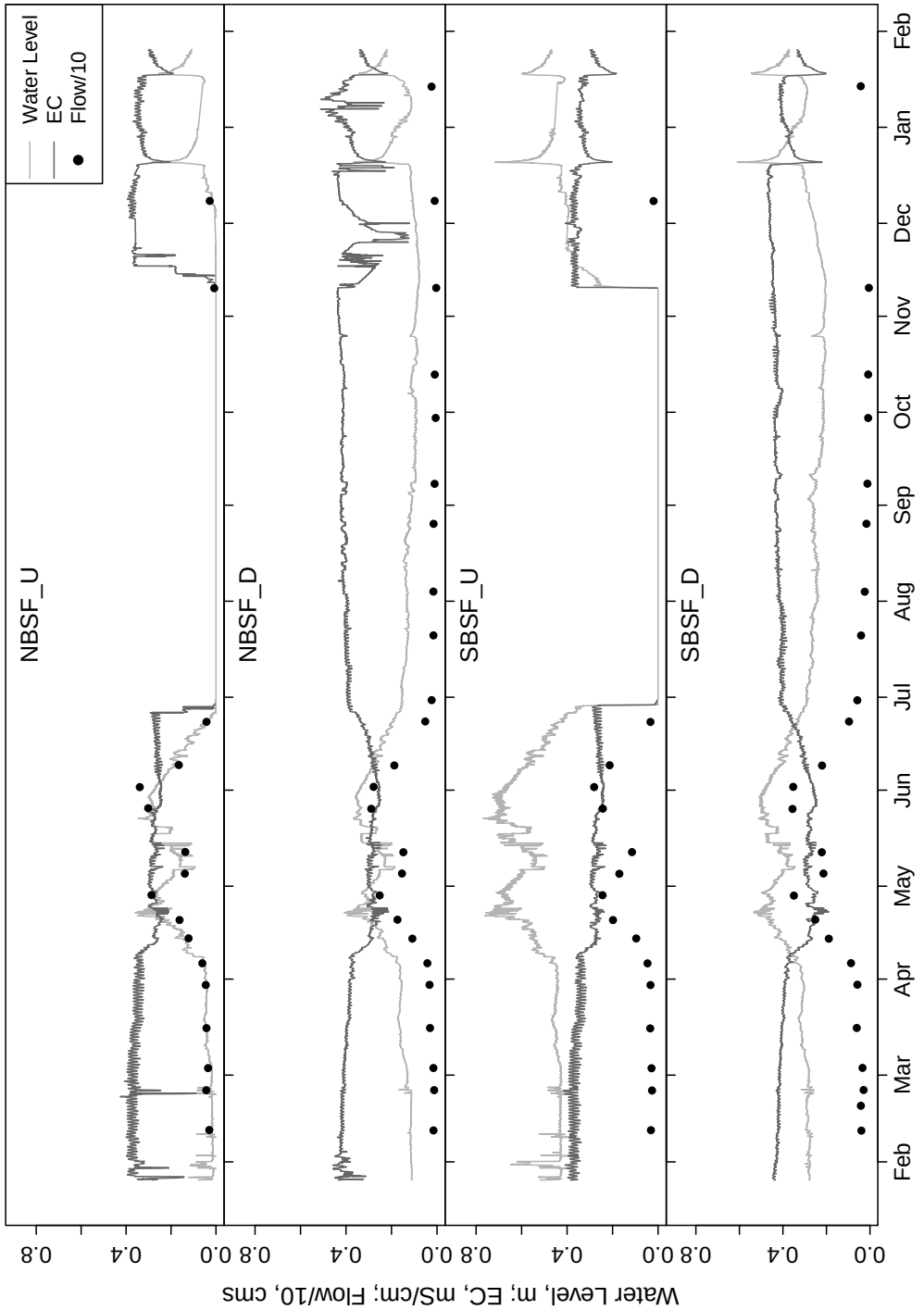

Fig. 15: High-frequency measurements of water level and EC with measured discharge values.

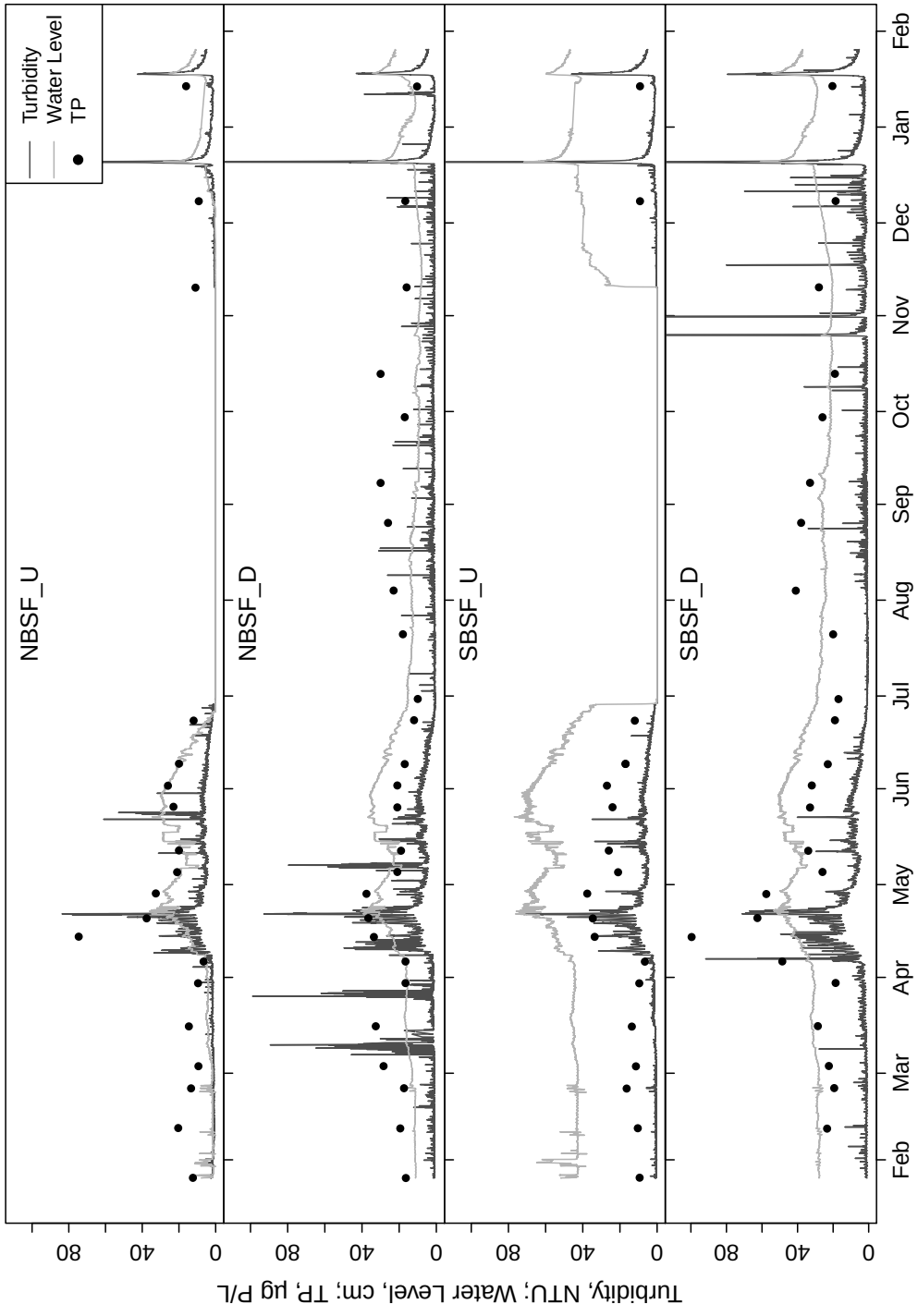

Fig. 16: High-frequency measurements of water level and turbidity with grab sample TP concentrations.

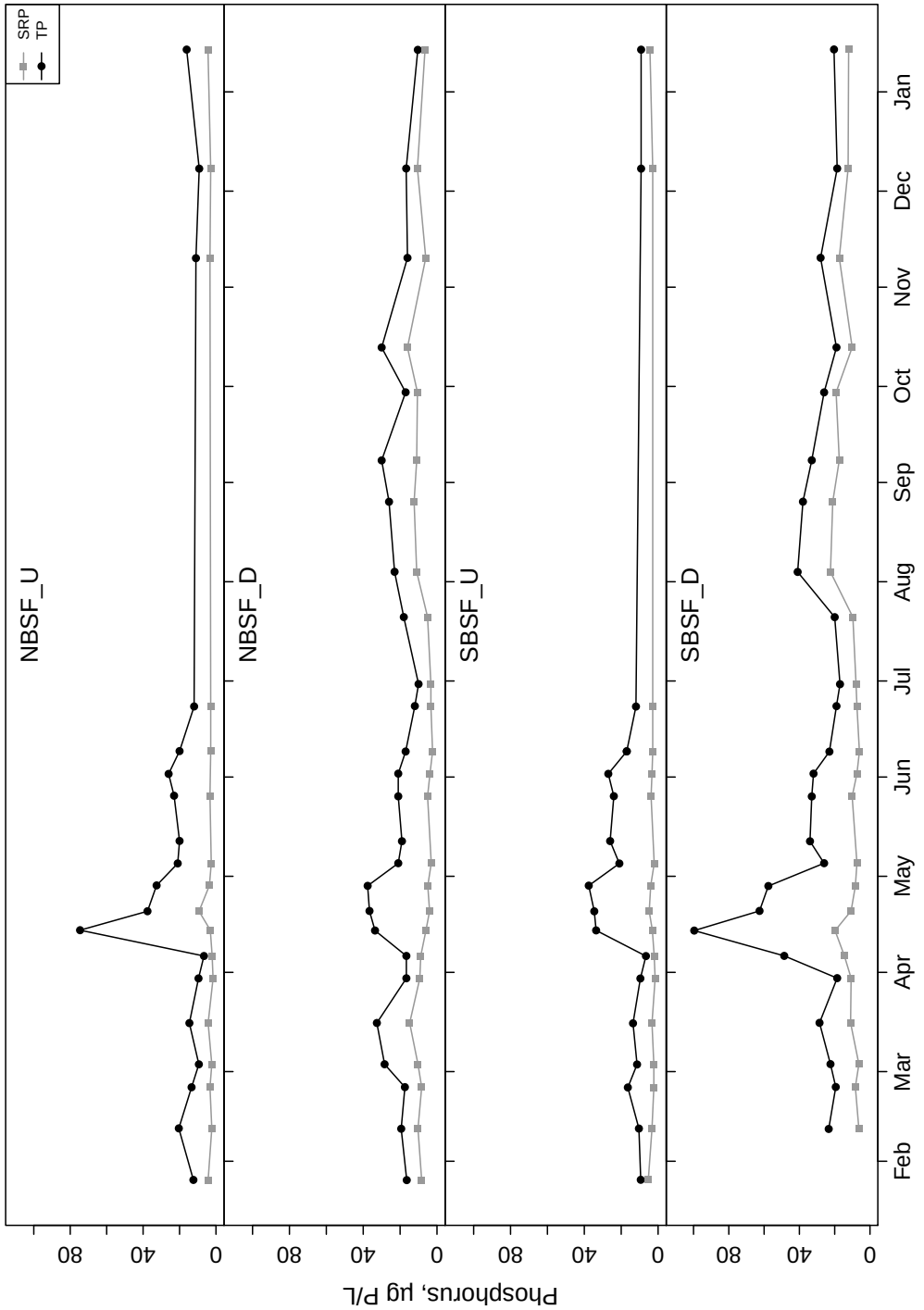

Fig. 17: Grab sample SRP and TP concentrations.

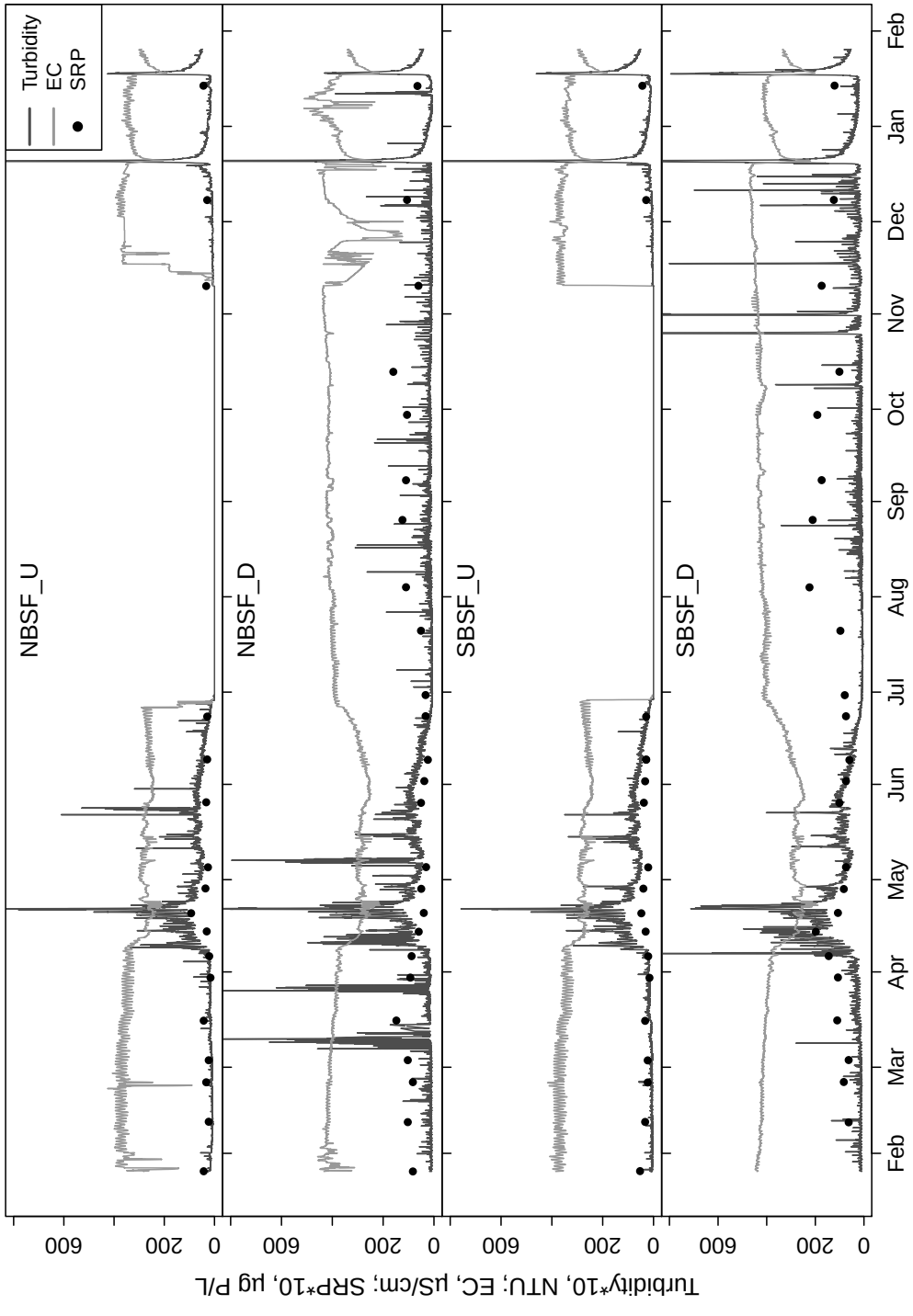

Fig. 18: High-frequency measurements of EC and turbidity with grab sample concentrations of SRP.

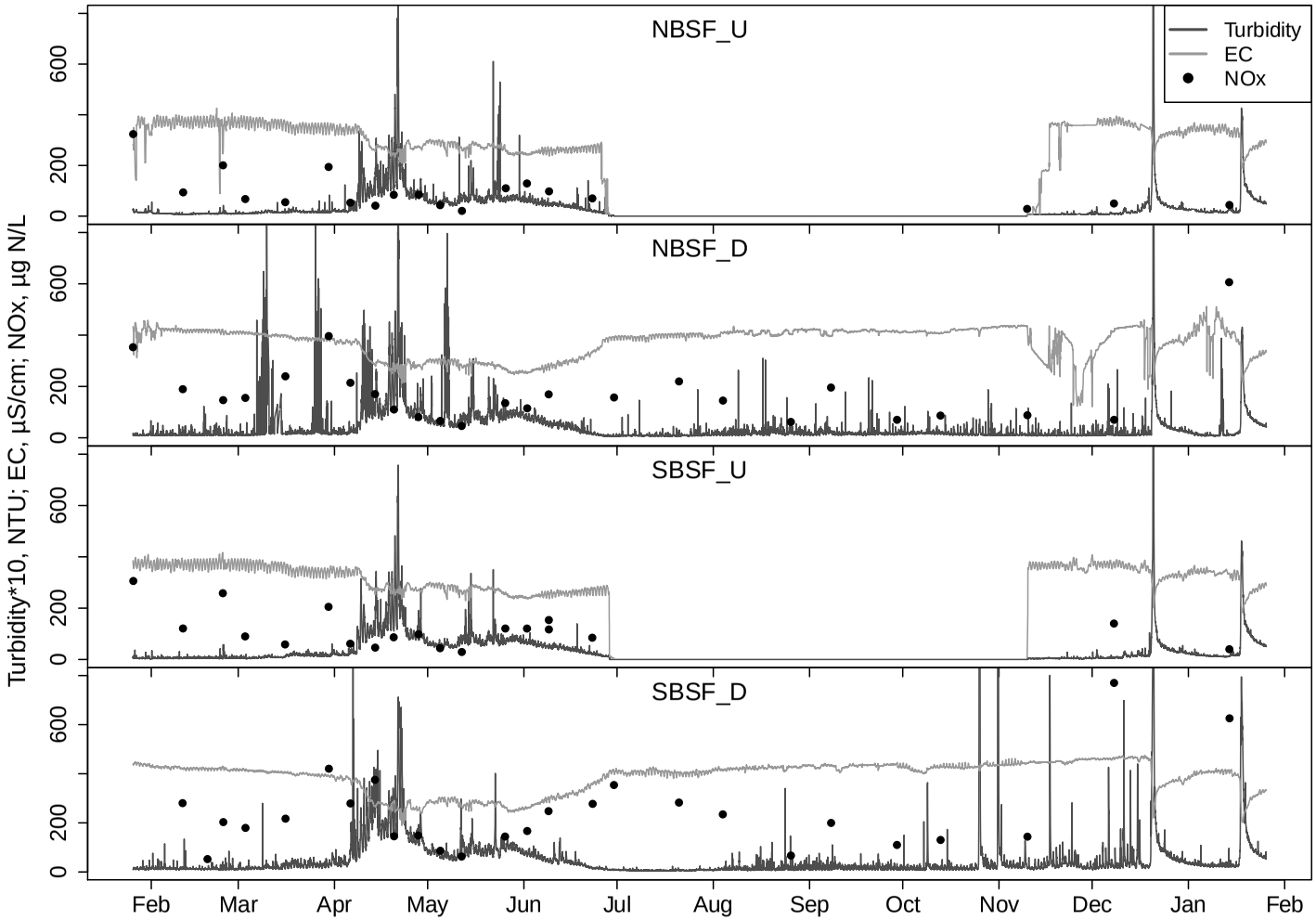

Fig. 19: High-frequency measurements of EC and turbidity with grab sample concentrations of NO_x-N. The outlier at NBSF_D is not shown.

High-frequency water level and manual flow measurements rose simultaneously (Figure 15) to show the two peaks of the spring runoff period from April to late June. It can be seen that each site has its own morphology because of the variable offsets between the water level and flow values. It was necessary to create independent stage-discharge relationships for each site. The upstream sites were dry during the irrigation season from late June to early November. In Figure 20, estimated flow rates showed an inverse relationship with EC at particularly the downstream sites when EC values were truncated at a minimum water level of 0.08 m (the water depth assumed needed to submerge the entire EC sensor). R^2 values at the downstream sites were 0.59 and 0.83 for the North and South Branches, respectively (0.18 and 0.45 at the North and South Branch upstream sites). Figure 20 also shows that the maximum EC values at the downstream sites are greater than the maximum values at the upstream sites and Figure 15 shows how EC levels are higher during the late summer, fall, and winter baseflows. The streams cross the confining layer boundary between the up and downstream sites (Figure 7) and it is likely that they became more influenced by shallow ground water at this point. Surface water inputs from runoff events increased flow rates and decreased the ground water ratio causing EC levels to drop. A significant correlation was not observed at the upstream sites perhaps because flows at these sites are predominantly from surface water inputs year round.

Water temperatures reflected air temperatures with the highest temperatures midsummer and lowest during December and January. There was a particularly cold spell followed by a warming trend in late November. When very cold conditions persisted, the rivers froze completely over at the upstream sites and water level values became inaccurate because flow below the frozen layer continued and during the day, when solar radiation caused melting on the surface, water also flowed over the frozen layers. When below freezing water temperatures were observed to correspond with unusual data values, it was assumed that the conditions impaired the sensors' function and the impaired values were

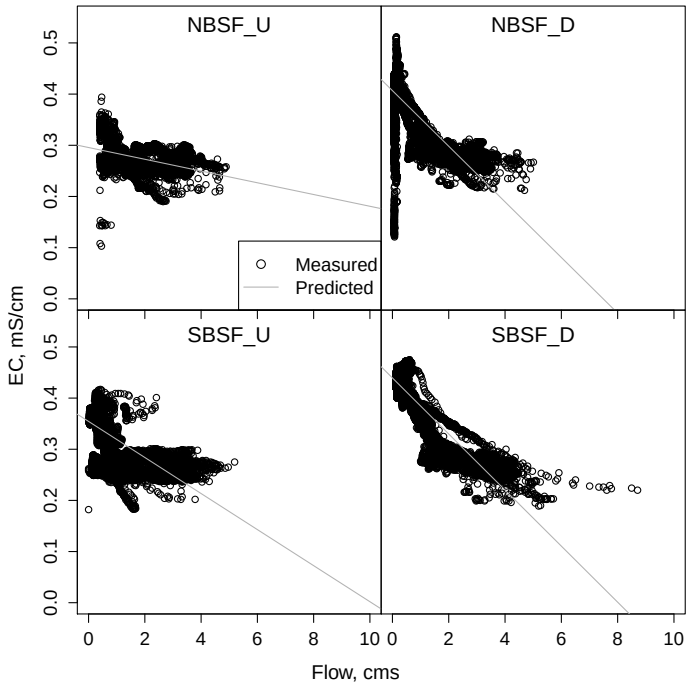

Fig. 20: High-frequency EC as a function of estimated flow rates.

replaced by interpolated values. Some EC measurements were also influenced by dramatically low water temperatures which resulted in conductivity values less than 0.005 mS/cm which could not be corrected for ionization errors and caused these values to be censored.

As would be anticipated, turbidity increases were observed (Figure 16) with the rising limb of the water level peaks at all sites suggesting a flushing of loose particulate matter as newly melted water flowed across and through soils. Notable are the large turbidity spikes in the winter. The events on 19 December 2010 and 17 January 2011 which were observed at all four South Fork sites corresponded with higher than usual antecedent air temperatures above freezing. A warming trend began on 17 December at 7:00AM with temperatures rising from -14°C to 9.6°C peaking on 19 December at 8:00PM and conditions continued above freezing until 10:00AM on 20 December. The January warming trend from -18°C to 9.1°C began at 11:00PM on 11 January and ended 17 January at 4:00AM. Temperatures remained above freezing until 6:00AM on 18 January.

In general, more frequent turbidity spikes were observed during the early spring at NBSF_D than at any of the other three sites. Due to the frequency of data collection, the sensors were able to describe some of the pollutant loading events characteristic of this watershed. Due to its lower elevation, several snow melt events occurred during the early spring and, unlike the large, higher-elevation watersheds represented by the other three South Fork sites, created flushing and erosion events more frequently than simply during the 'spring runoff' period from April to June. The erodibility of these soils may also be greater since the dominant portion of this watershed is impacted by anthropogenic factors such as tilling and landscaping and may contain more fine, residual organic matter. Without high-frequency data collection, these transport events would likely go unnoticed, especially if only spring runoff indicated by sustained increased flow rates from high-elevation melting was examined.

TP concentrations tended to follow turbidity values and the hydrographs (Figure 16), illustrating their association with erosion events. Figure 17 illustrates SRP concentrations were somewhat more constant and sometimes showed minor increases at times simultaneously with TP. An unusually high NO_x-N concentration at NBSF_D (1.9 mg/L on 22 June) appeared to be anomalous and was omitted since it is nearly four times larger than any other NO_x-N values and occurred at a time of low turbidity, flow, and P concentrations. Figures 18 and 19 show SRP and NO_x-N concentrations in relation to EC and turbidity. It appears that NO_x-N was not necessarily transported during the same events as TP. No useful regressions between NO_x-N or SRP with EC or turbidity were observed and transport of these dissolved nutrients did not appear to be associated with periods of high ground water inputs.

Histograms of grab sample concentrations are in Appendix B Figure B.1 for reference. Appendix B also contains histograms of laboratory (pH, SC, and turbidity) and high-frequency measurements following the quality control processing completed using

ODM Tools in Figures B.2 and B.3. The gage height, temperature, and turbidity are all positively skewed and EC measurements are negatively skewed. The turbidity values show the greatest spread of the high-frequency measurements. This is as would be anticipated since runoff conditions would cause rapid, periodic increases of the gage height and turbidity. Temperatures were positively skewed due to the upstream sites (downstream sites showed no outliers) which dried up during the summer and experienced very low flows prior to being completely dry. As noted previously, EC measurements were temperature corrected and very low water temperatures combined with low conductivities produced values which were below the detection limit. These values were interpolated but created the negative skew. Appendix B Figures B.4 through B.7 show box plots of high-frequency measurements by site. Temperature measurements at the downstream sites show no extreme outliers since these sites are more influenced by ground water and have more stable flows and temperatures. The greatest turbidity values were observed at SBSF_D since the South Branch watershed varies dramatically from the North Branch in its topography and size (greater slopes and distances to stream banks).

The median pH value was 8.17 with minimum and maximum values of 6.95 and 8.57, values typical of watersheds high in carbonate minerals. Figure 21 compares grab sample measurements of turbidity with high-frequency mean turbidity. The dashed line depicts a 1:1 relationship with zero intercept that would be expected if measured values were the same. Linear regression on the data (grey line) yielded a slope of 1.4 and R^2 value of 0.95. The fixed volume of grab sample was allowed to settle slightly in order to obtain a stable turbidity measurement. This is opposed to the sensor measurements which captured real-time conditions of all suspended particles. The highest turbidities often occurred with increased flows suggesting that increased velocities would entrain larger particles which are typically associated with less P. A greater mass of large particles would be represented at the same turbidity of a mass of small particles detected at the same turbidity. As such, the high-

frequency turbidity would tend to overestimate the mass of P-enriched colloids. While the grab sample turbidity measurement likely includes only the slowly settling particulates and more accurately represents true turbidity and colloid mass, the available data suggests that the turbidity is overestimated at a constant rate. Should this hold true at higher turbidities, the TP regression should reflect the ratio of unsettleable, phosphorus-sorbing colloids based on the measured TP concentrations.

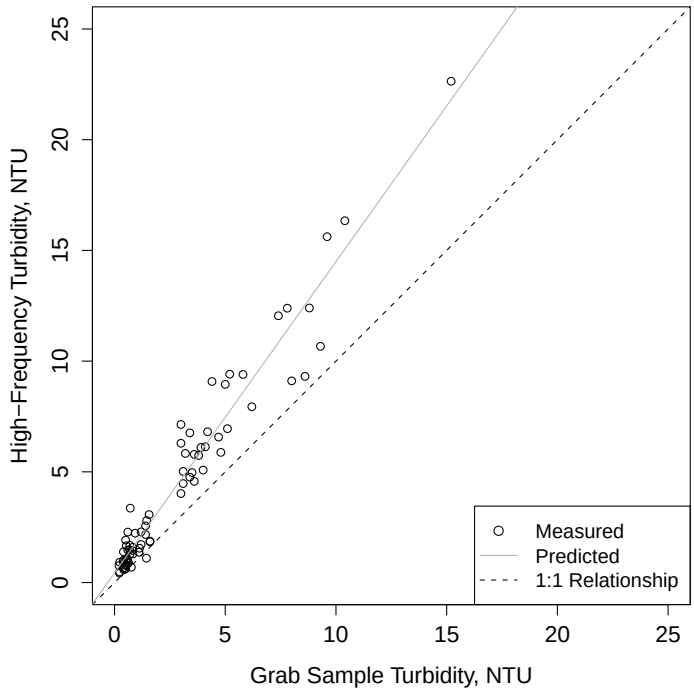

Fig. 21: Grab sample turbidity vs. high-frequency mean turbidity. The dashed line depicts a 1:1 relationship with zero intercept.

3.4 Grab Samples

3.4.1 Replication at Upstream Sites

Table 5 shows the p-values for the Wilcoxon tests comparing the parameter distributions at each site. The p-values were such that the null hypothesis was not rejected and so

grab samples at the upstream sites were not significantly different.

Table 5: Wilcoxon results comparing upstream sites.

Parameter	p-value
NO_x-N	0.20
SRP	0.91
TP	0.85
pH	0.45
SC	0.82
Turbidity	1.0

3.4.2 Differences Across Reaches

Maximum NO_x-N and SRP concentrations at the downstream sites were about two times greater than those at the upstream sites. Maximum TP concentrations were 75, 38, 38, and 100 μg P/L at the NBSF_U, NBSF_D, SBSF_U, and SBSF_D sites, respectively. A similar pattern was observed for turbidities where NBSF_D was less than NBSF_U and SBSF_D was greater than SBSF_U. Table 6 compares the p-values for grab sample comparisons from the North and South Branches.

Comparing the up and downstream sites, TP and turbidity of the North Branch and turbidity of the South Branch were not significantly different across either branch over the one-year study period. A decrease in pH was observed as streams traveled through the valley. For NO_x-N, SRP, TP (South Branch) and SC an increase in concentrations was

Table 6: Wilcoxon results comparing across reach sites.

Parameter	p-value	
	North Branch	South Branch
NO_x-N	0.0041	8.0e-4
SRP	4.0e-5	4.2e-8
TP	0.16	0.0013
pH	7.4e-6	2.0e-6
SC	0.0022	0.0021
Turbidity	0.15	0.68

observed at the downstream sites. Grab sampling, in general, illustrated changes in the parameters across the study reaches when grab sampling was conducted on a weekly to monthly basis. However, high-frequency methods have the potential to illustrate changes caused by short-duration events which were not detected here.

3.4.3 Hydraulic and Nutrient Loads

Daily and annual loads were estimated using the RD method (*Lee*, 2008). During the 12-month study period, the South Fork Ogden River (North and South Branches) contributed an estimated 4.0e+7 m^3 of water to Pineview Reservoir. This volume represented 41% of the total flow of water from the monitored tributaries making the South Fork the dominant tributary to the reservoir. The South Branch South Fork represented 61% of the hydraulic load from the South Fork. Tributary hydraulic loads are summarized in Table 7 alongside nutrient loads. The average annual flow rate of the South Fork was 1.3 cms; however, during the 77 days of spring runoff from 05 April through 20 June the average flow rate was 3.6 cms and the peak flow rate was 7.2 cms.

The combined flow contribution of both upstream sites was 3.1e+7 m^3. Average annual flow rate was 0.98 cms. During the spring months, the average flow rate was 3.0 cms and the maximum flow rate was 6.7 cms. Figure 22 shows the modeled flow rates from both branches with their respective upstream sites.

Observed peaks in the hydrograph which occurred during the spring runoff season from April through June imply the surface water system was hydrologically dominated by inflows generated from snow melt. Figure 22 shows portions of the year during which the North Branch was a losing stream with the upstream site having a higher discharge than the downstream site while the South Branch was a gaining stream most of the year. During the annual period, the North Branch gained 1.7e+5 m^3 (primarily during the irrigation season when upstream sites were dry) and the South Branch gained 9.3e+6 m^3 between

Table 7: Summary of estimated tributary load estimates to Pineview Reservoir based on grab sampling.

Tributary	Flow, m^3/yr	NO_x, kg N/yr	SRP, kg P/yr	TP, kg P/yr
North Fork	3.0e+7	16,000	150	920
Middle Fork	1.8e+7	390	78	470
Spring Creek	9.9e+6	2,400	140	940
North Branch South Fork	1.6e+7	2,400	86	350
South Branch South Fork	2.5e+7	5,600	240	820
Total	**9.9e+7**	**27,000**	**690**	**3,500**

the upstream and downstream sites. Water which flowed at the downstream sites during irrigation season when upstream sites were dry was due to overland flow, irrigation tail water, or ground water recharge from irrigation return flows or precipitation events.

Estimated annual surface water nutrient loads were 8,000 kg NO_x-N, 330 kg SRP, 1,200 kg TP from the South Fork to Pineview Reservoir. These South Fork loads represented 30%, 47%, and 33% of the total NO_x-N, SRP, and TP contributions of all monitored tributaries to Pineview Reservoir and represented the largest load of both SRP and TP. The South Branch South Fork was the dominant contributor to the total South Fork load of all three constituents. Loads to the reservoir are summarized in Table 7 and the total load to the reservoir is shown in Figure 23. Figure 24 compares the dissolved nutrient loads via tributaries according to the TMDL with those estimated in this study using the RD method.

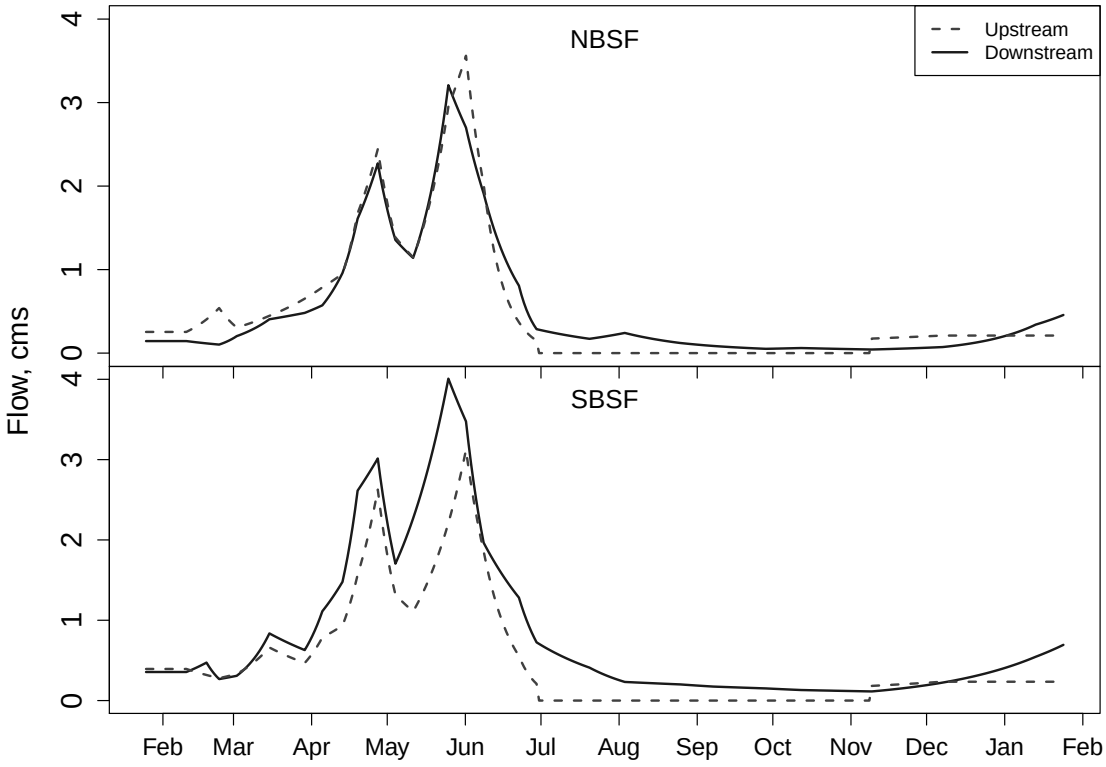

Fig. 22: Daily flow rates estimated from measured rates.

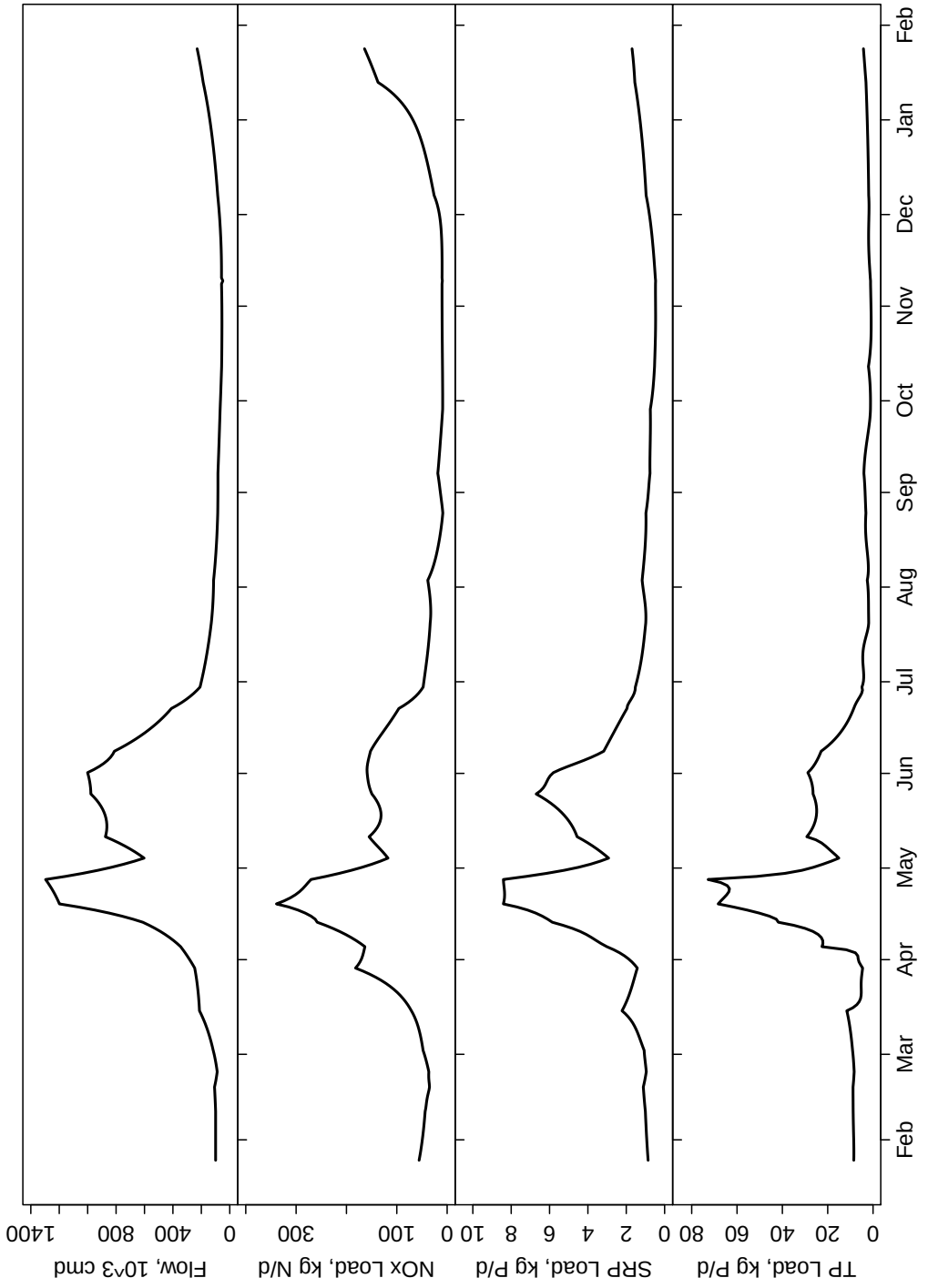

Fig. 23: Estimated daily nutrient loads to Pineview Reservoir based on grab samples.

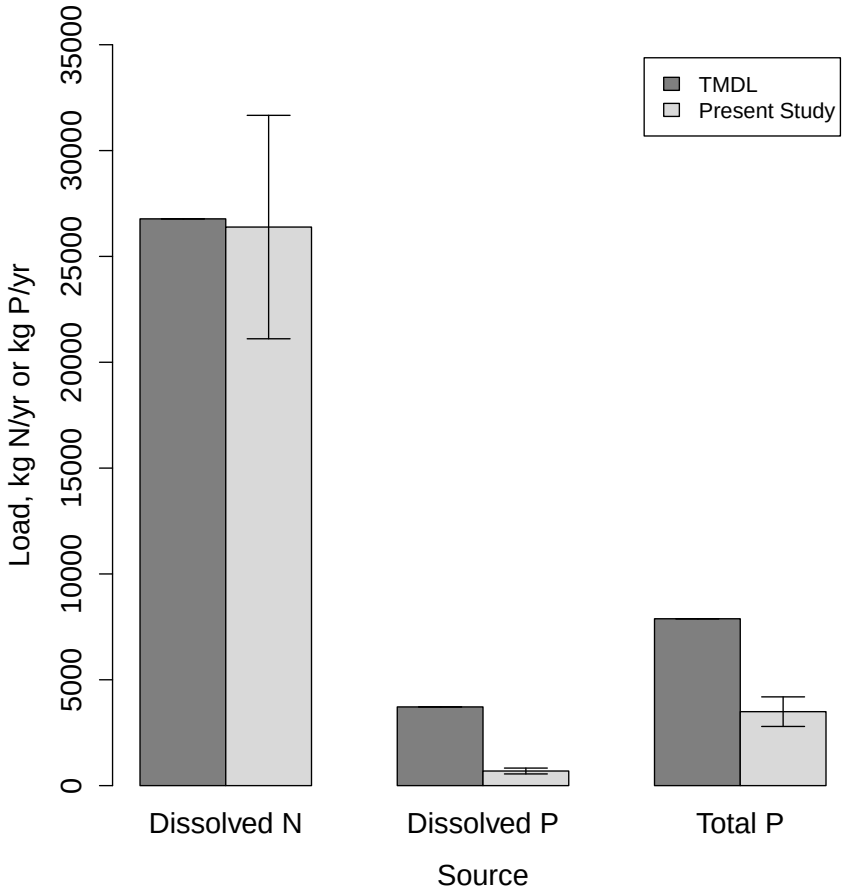

Fig. 24: Comparison of nutrient load estimates from the TMDL and the present study. Error bars for the predicted loads of this study represent $\pm 20\%$ as approximated by *Lee* (2008) using the RD method.

The majority of nutrient transport to the reservoir took place from late March to late June (Figure 23), corresponding to the spring runoff season. This differs from the TMDL prediction (*Tetra Tech Inc.*, 2002) which used the only available climate data (a valley-elevation weather station) to populate the SWAT model and found 75% of surface water loads were transported from January to March. The TMDL (*Tetra Tech Inc.*, 2002) recognized that this timing was earlier than would be expected from a snowfall-dominated watershed but assumed that the total loads would still be valid. This assumption held true for NO_x-N (Figure 24). The SRP load from this study was five times less than what was es-

timated in the TMDL and the TP load was two times less. The TP load in the TMDL (*Tetra Tech Inc.*, 2002) was only available for tributary contributions and was not considered in the final load reductions.

This P load from particulates has the potential to accumulate in the sediments and significantly impact Pineview Reservoir eutrophication since it undergoes anoxia in the hypolimnion during late summer. These reducing conditions cause the dissolution of P from sediments to pore water and into the water column at concentrations based on the diffusional gradient dependent upon hypolimnetic and sediment concentrations. *Worwood* (2011) estimated the annual SRP load from sediments to the reservoir water column in 2009 as approximately 2,800 kg P.

Annual combined loads of 2,900 kg NO_x-N, 99 kg SRP, and 690 kg TP were estimated at the upstream sites of the South Fork. As the North and South Branches flowed through the valley, the North Branch gained 1.7e+5 m^3, 990 kg NO_x-N, and 36 kg SRP but lost 16 kg TP while the South Branch gained 9.3e+6 m^3, 4,100 kg NO_x-N, 190 kg SRP, and 500 kg TP per year. Figures 25 and 26 illustrate the reach gains/losses of flow and nutrient loads based on the differences of modeled daily loads of up and downstream sites.

Seasonal loads at the four study sites on the South Fork are summarized in Figure 27. Seasons correspond to the hydrologic conditions of spring runoff, open irrigation canal diversions (irrigation), and non-spring-runoff with closed diversions (baseflow). *Lee* (2008) reported up to 10% observed error for ten year flow totals and so this variance was used to calculate error bars for flow estimates. Error bars for load estimates, the product of flow and concentration estimates, represent $\pm 20\%$ of the calculated load.

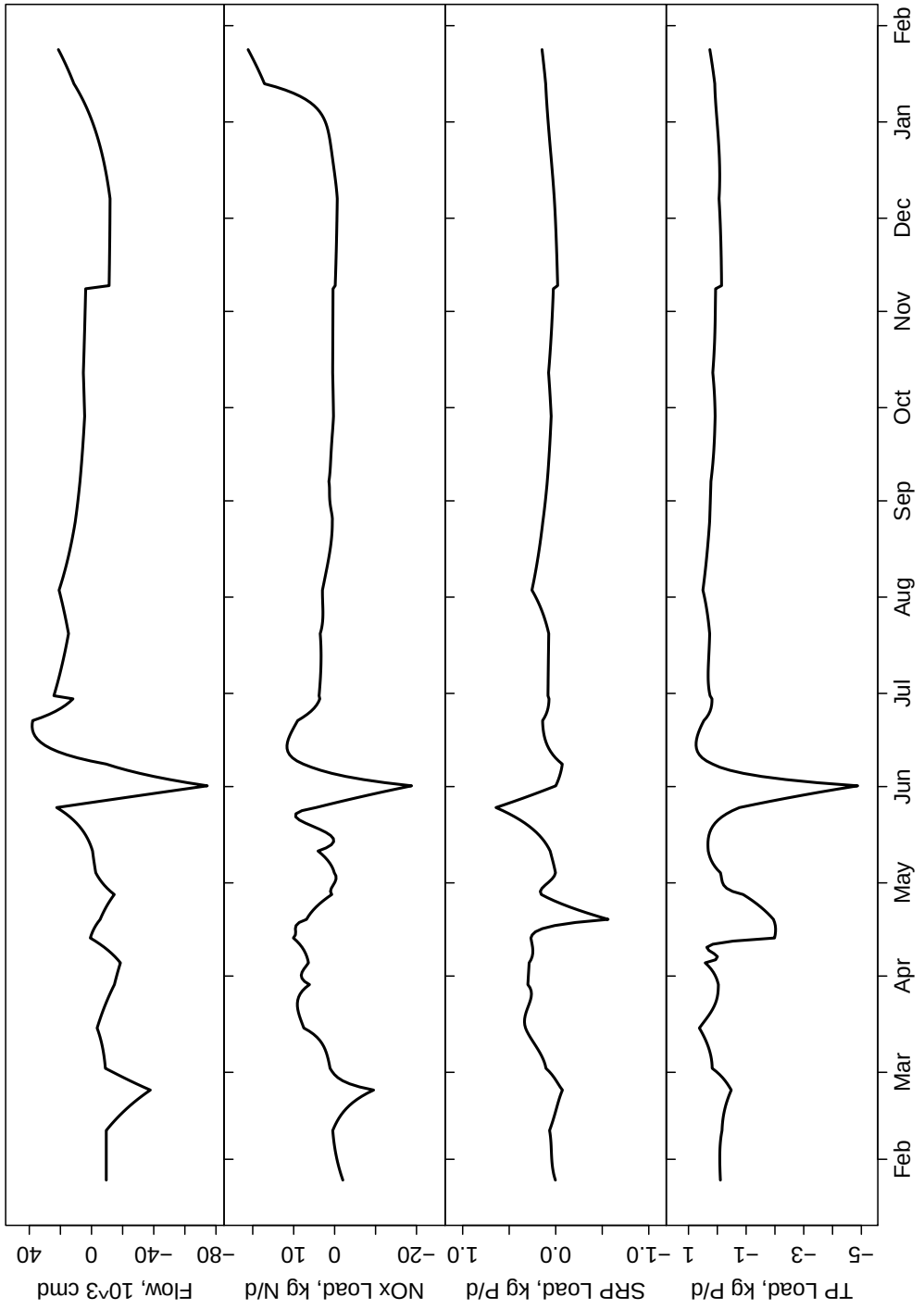

Fig. 25: Estimated reach gains/losses in the North Branch South Fork Ogden River.

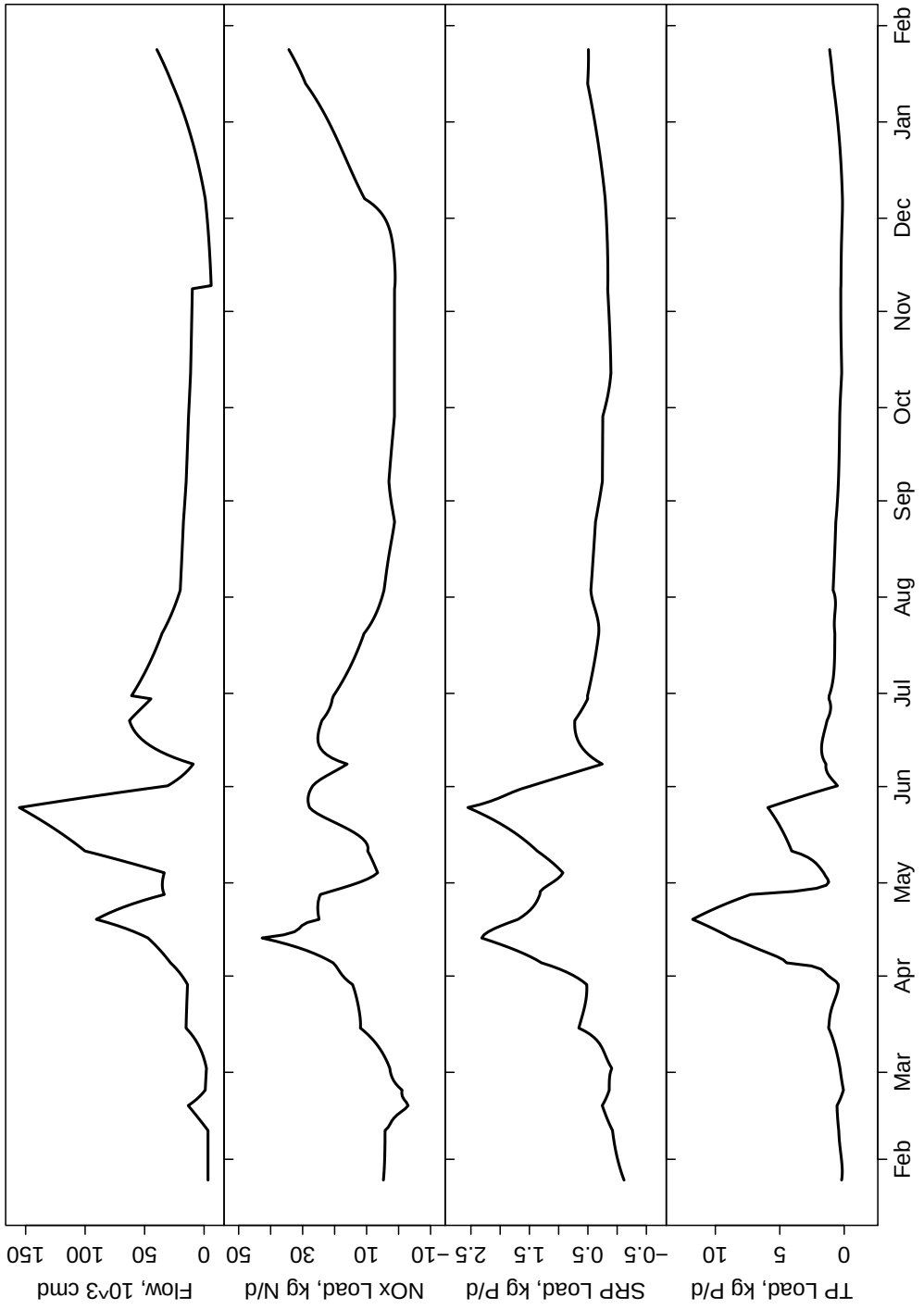

Fig. 26: Estimated reach gains/losses in the South Branch South Fork Ogden River.

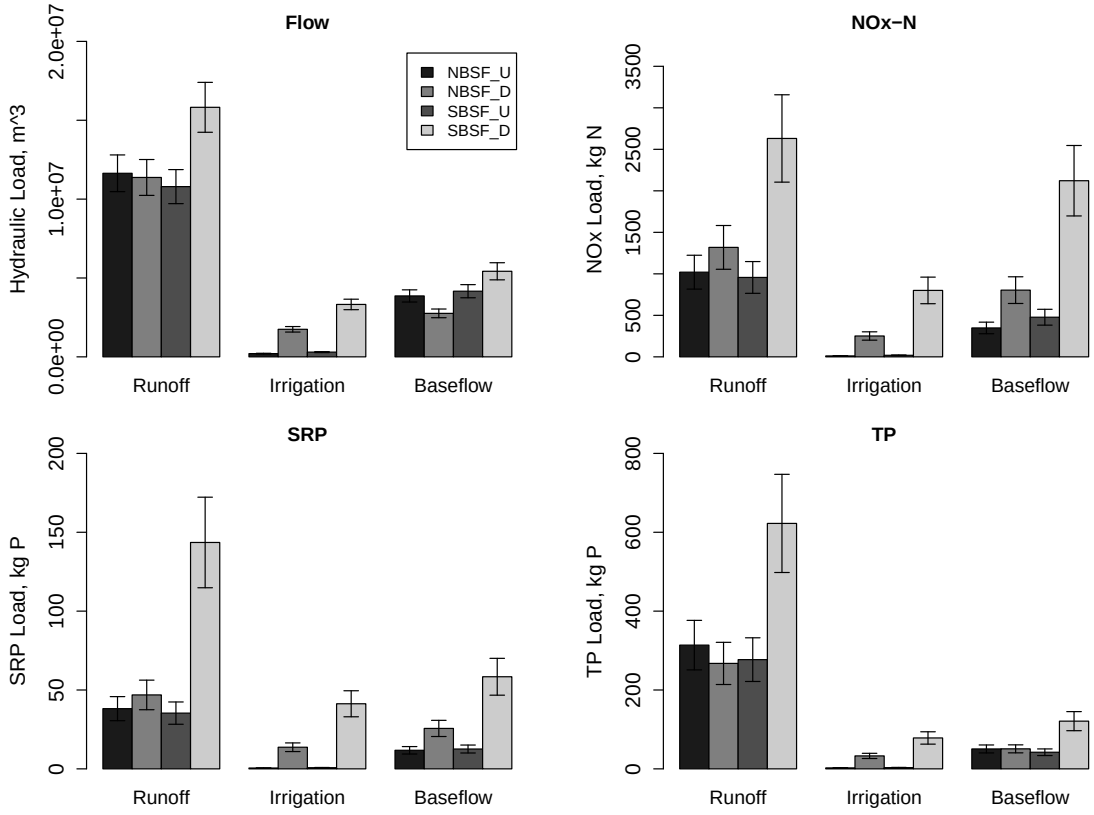

Fig. 27: Estimated seasonal loads from the South Fork Ogden River. Error bars represent $\pm 10\%$ for flow rates and $\pm 20\%$ for nutrient loads (*Lee*, 2008).

Decreases in flow between up and downstream sites on the North Branch (Figure 25) influenced the nutrient load characteristics similarly. When stream beds were dry during the irrigation season, loads at the upstream sites were zero and any loads at the downstream sites would have produced a (positive) reach gain. During March and June when significant flow losses were encountered, decreases in the nutrient loads (particularly NO_x-N and TP) were also observed. In contrast, the South Branch (Figure 26) acted consistently as a gaining reach for flow and nutrient loads. The largest increases of nutrient loads across this study reach mimic the increased flows during spring runoff. However, relative increases in the TP load were most substantial during the first peak in the hydrograph and showed little increase during the second hydrograph peak whereas NO_x-N and SRP had relatively more

substantial increases during the second peak. As the majority of easily erodible particulates were flushed from the system during the first hydrograph peak, few remained to be transported during the second peak, creating the TP transport pattern observed. Dissolved N and P were transported during both events since these species were dissolved by the water passing over and through soils on its way to the streams.

Larger decreases in the TP load compared with the SRP load does not mean that the TP load at any given site is less than the SRP load but signifies a shift in the SRP fraction. This phenomenon is illustrated in Figure 28 which shows the dominance of particulate P during the erosive spring runoff period (low SRP fraction). Particularly at the downstream sites, there is a marked decrease in the SRP fraction mid-April corresponding to the rising limb of the hydrograph. The SRP fraction increased during the low baseflow conditions of late fall and winter. Annually, 28% of the TP load to Pineview Reservoir from the South Fork was SRP.

The South Branch gained in flow and nutrient loads across the study reach every season with greatest gains during the runoff season (Figure 27). The North Branch basically acted as a gaining reach for only NO_x-N and SRP for all seasons. Both reaches increased in hydrologic and nutrient loads during the irrigation season since upstream sites were dry for the majority of this season. It was during this season that discharge from ground water was especially influential since it was the primary source of water at the downstream sites. Flows at this time were generally low with moderate nutrient concentrations possibly influenced by irrigation return flows. Figure 15 showed the higher, stable EC values during this time and Figure 20 showed the correlation between low flows and high EC at the downstream sites. These higher EC values are characteristic of ground water which typically contains higher concentrations of dissolved salts.

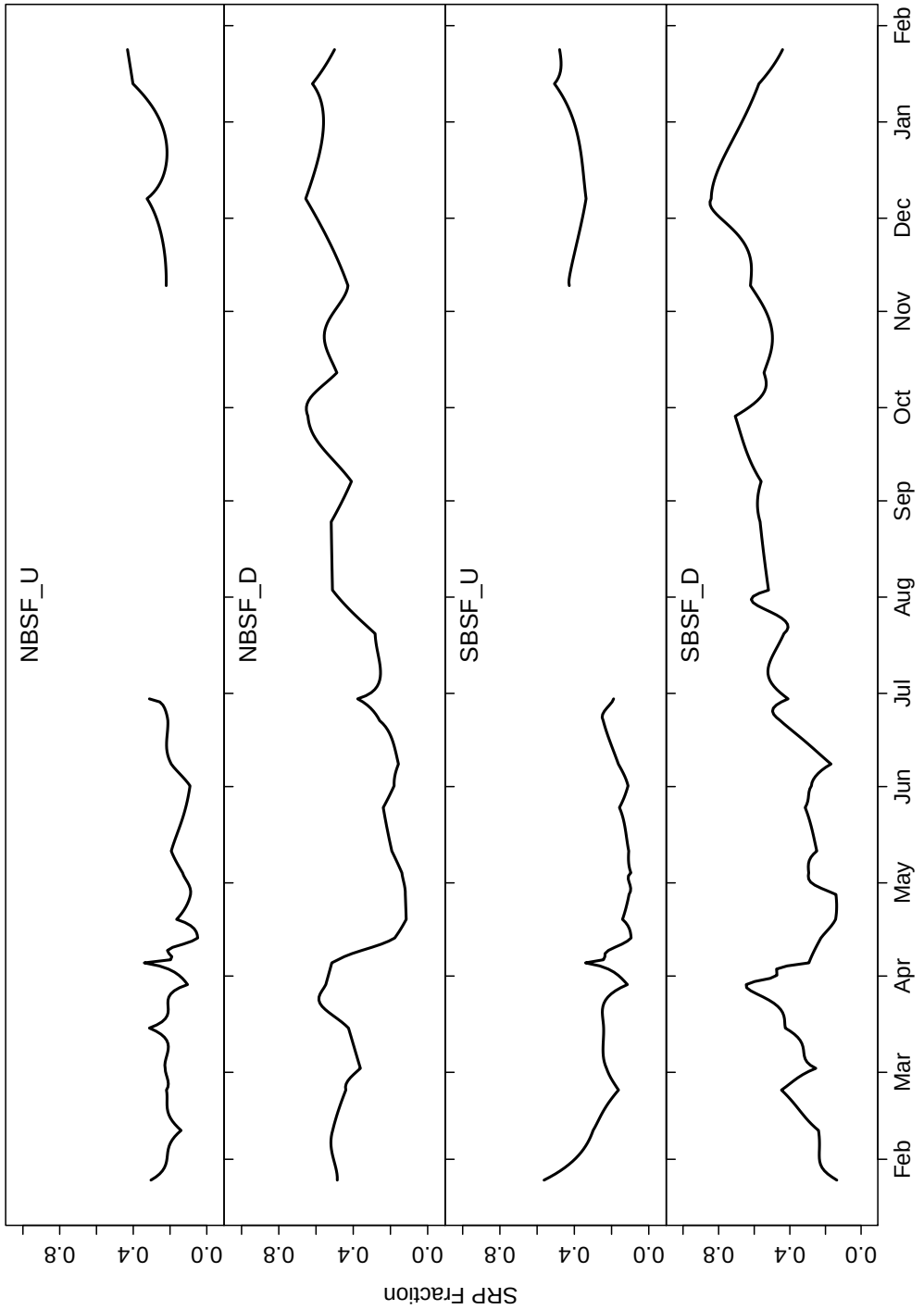

Fig. 28: SRP fraction at the four South Fork sites.

Though these two study reaches flow geographically close to one another and originate from the same headwater, estimates based on grab samples revealed that they exhibit different hydrology and water quality. These differences were most marked during the spring runoff period. Recharge of ground water may account for losses, which are more noticeable in the North Branch. While it is likely that this phenomenon happened to both reaches, it is less obvious in the South Branch which receives water from smaller tributaries originating in its comparatively larger watershed.

3.5 High-Frequency Monitoring

3.5.1 Replication at Upstream Sites

A high degree of autocorrelation (Appendix D Figure D.1) was exhibited by the data. Due to this, the sites could not be compared quantitatively without violating the assumptions of the Wilcoxon test but were compared graphically as found in Appendix D Figures D.2 to D.7. The graphs show the entire study period excluding the irrigation season when the upstream sites were dry.

In general, most measurement values at the two sites overlapped and showed corresponding diurnal and seasonal cycles. For EC, the greatest discrepancies occurred during the colder, winter months from November to January. Water temperatures were typically also the same at both upstream sites. Turbidities at the two sites were similar particularly when at background levels. Variances between the sites were observed during the winter months when the NBSF_U turbidity levels were greater than SBSF_U but fluctuations generally occurred simultaneously. Other notable variations between the sites were usually one to two data points, suggesting that these measurements were influenced by debris or biota momentarily passing the sensors.

3.5.2 Differences Across Reaches

High-frequency measurements at each respective up and downstream site are compared in Appendix D Figures D.8 to D.13 for the North Branch and Figures D.14 to D.19 for the South Branch.

Measurements on the up and downstream sites were not consistently similar. Throughout most of the year, cycles observed in all the measurement parameters corresponded well yet their magnitude and amplitude were frequently different. Downstream temperatures and EC were typically greater than upstream during low flow conditions which was representative of solar warming and the higher ground water/surface water ratio at these times. Figures D.11 and D.17 show this changing ratio as the upstream maximum and minimum temperatures surpassed the downstream temperatures and EC values at the downstream sites steadily increased. More noise is shown in the downstream turbidity measurements than at the upstream, in general, and significantly higher turbidity events (Figures D.9 and D.18) reflective of the study watersheds' influences were evident.

3.5.3 Hydraulic and Nutrient Loads

High-frequency load estimates were created using the surrogate measurements for TP concentrations and flow rates. The annual hydraulic load from the South Fork to Pineview Reservoir as estimated from high-frequency water level was 4.8e+7 m^3. This represents a 20% increase over the RD estimate. The South Branch portion of the total South Fork flow was still 61%. Average annual combined flow rate for the South Fork was 1.5 cms with a peak of 12 cms. The peak flow for the North Branch occurred during the spring runoff but the South Branch maximum flow rate was observed during December. The spring runoff season had an average flow rate of 4.3 cms and a peak flow of 10 cms.

At the upstream sites, the annual hydraulic load was 3.4e+7 m showing a 9.7% increase over the RD estimate. The average flow rate was 1.1 cms annually and 3.9 cms

Table 8: Summary of South Fork loads using surrogate measurements at high frequencies.

Site	Flow, m^3/yr	TP, kg P/yr
North Branch South Fork East	1.6e+7	660
North Branch South Fork	1.9e+7	590
South Branch South Fork East	1.8e+7	540
South Branch South Fork	2.9e+7	1,500

during runoff. The peak flow was 9.8 cms which occurred during spring runoff in May.

Spring runoff peaks were notable (Figure 14) and were the most sustained events delivering a large hydraulic load. Additionally, short-duration peaks, probably snow melt events, were observed from late December to early February at all sites. The magnitude of such maximum flow rates exceeded the spring runoff maximum at SBSF_D.

The total combined annual TP loads using surrogate measurements to predict high-frequency loads were 1,300 and 2,100 kg TP at the up and downstream sites, respectively. This was an increase of 88% and 75% over the RD estimates from grab samples. Annual loads using high-frequency surrogate measurement techniques are summarized in Table 8.

Across the study reaches, the North Branch increased its hydraulic load by 3.0e+6 m^3 and decreased TP load by 70 kg TP and the South Branch increased by 1.1e+7 m^3 and 1000 kg TP. These differences are more polar than was estimated using the RD method based on grab sampling alone. Figures 29 and 30 illustrate the instantaneous load gains/losses (volume or mass) per half-hour based on the sensor measurement time scale.

Seasonal loads are shown in Figure 31. Error bars illustrate the error in the inverse prediction of TP from turbidity. Since the maximum median difference by season between the two upstream sites' turbidity measurements was only 0.46 NTU which resulted in up to ± 2.0 μg/L and the 95% prediction intervals from the TP/turbidity regressions showed as much as ± 18 μg/L, it was assumed that the final variance would not be much different than the largest variance (*Berthouex and Brown*, 2002). For sake of simplicity and because no

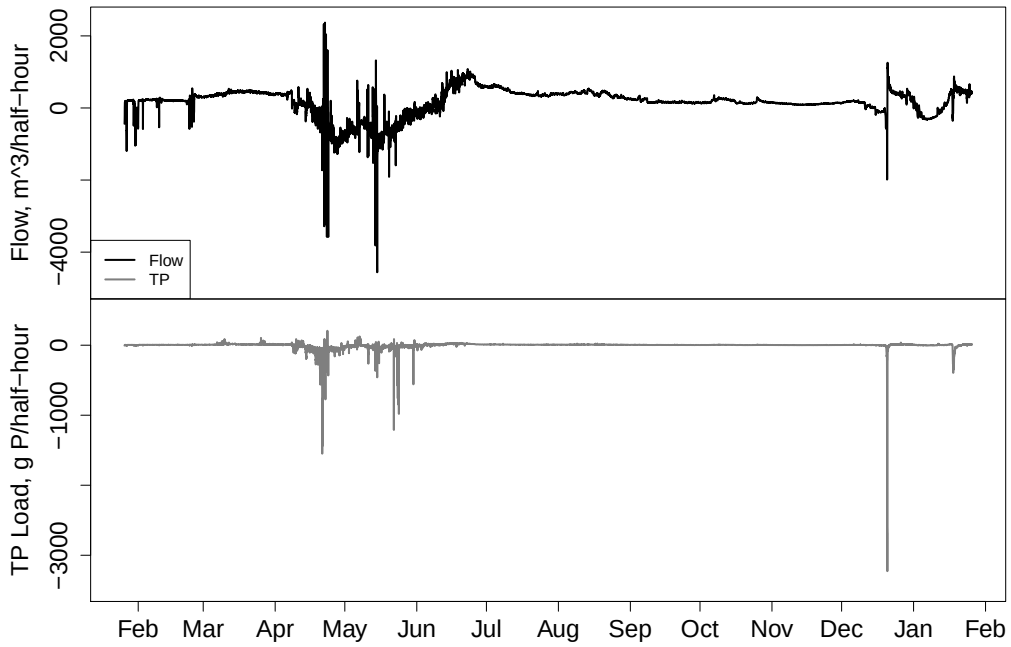

Fig. 29: High-frequency estimates of reach gains/losses at the North Branch South Fork Ogden River.

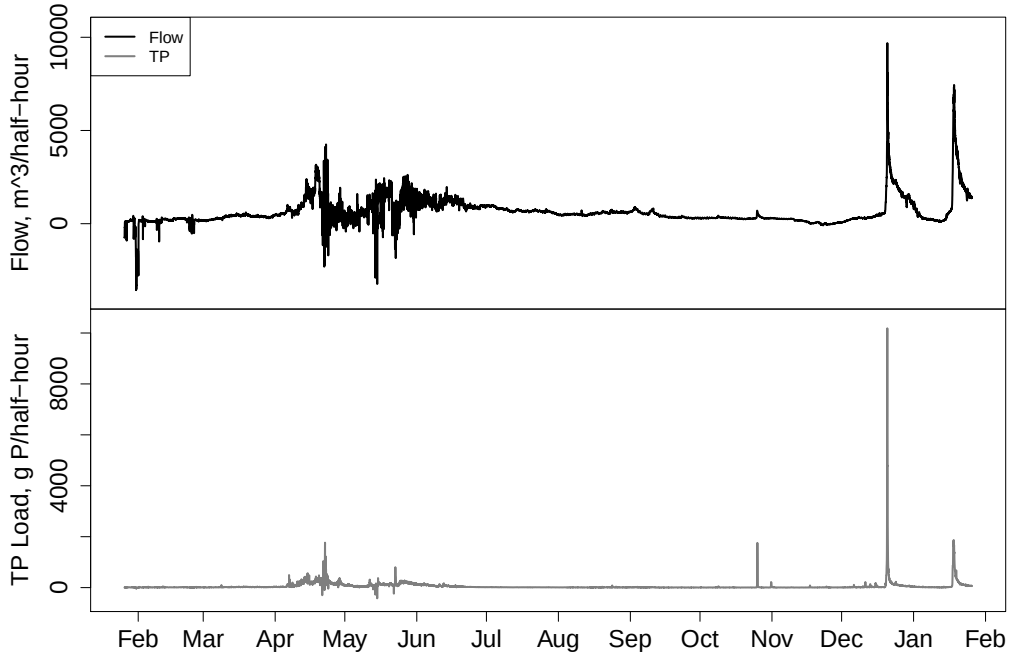

Fig. 30: High-frequency estimates of reach gains/losses at the South Branch South Fork Ogden River.

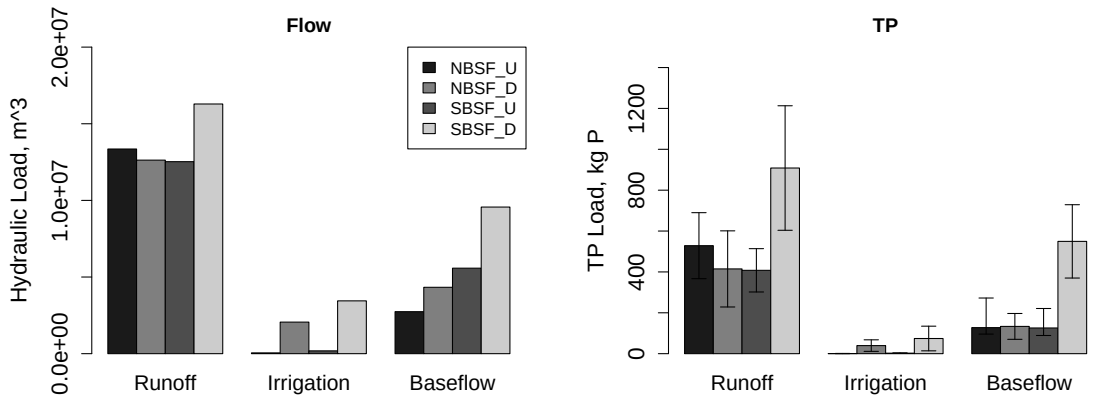

Fig. 31: Seasonal high-frequency loads from the South Fork Ogden River. Error bars represent the estimated 95% confidence region.

exact measurement replicates exist, variance of flow rates was ignored.

At the North Branch (Figure 29), losses of TP were observed when increases and decreases in flow were observed. Hydraulic load fluctuations also occurred across the South Branch (30) but gains in TP were predominantly observed. Travel times through the study reaches varied from 0.5 to 10 hours and some fluctuations may be an artifact of the approach used to find the instantaneous reach loads; however, summing the reach loads for time periods greater than the travel time should minimize the effect of this. High-frequency estimates of hydraulic and TP loads from the North Branch varied more from RD load estimates than did those from the South Branch.

The losing characteristic of the North Fork is also illustrated in Figure 31 where the mean losses during the runoff season outweighed the gains of the irrigation season (when upstream sites were dry and recharge was via ground water) and baseflow season. When CIs are considered, there were little, if any, reach gains across the North Branch as there were for the South Branch.

The study reaches cross the confining layer boundary as the reservoir is approached (Figure 7) but upstream from the confining layer surface water recharges the aquifer. In agreement with the seepage identified by *Avery* (1994), this ground water recharge is as-

sumed to account for the decreased hydraulic loads. This phenomenon could help explain the decreased TP loads. It is possible that if NO_x-N and SRP could be monitored with high-frequency as TP is, their loads would also decrease across this reach. Also interesting to note is that when the South Branch was increasing in hydraulic and TP loads across the study reach, the North Branch was often decreasing in TP load and decreasing and then increasing in flow. These periods usually coincided with high flows which perhaps created a greater seepage potential. When flows were greater, the cross-sectional area of the streams increased and more water interacted with the hyporheic zone. When the North Branch, which travels on the valley floor, reached the confining layer boundary, some water contained in the hyporheic zone probably entered the confined aquifer. The South Branch received loads from the small tributaries originating from higher elevations and greater slopes within its watershed which would mask its ground water loss properties and keep sediments entrained.

3.6 Export Coefficients

This study originally planned to use the network of water quality nodes supplying surrogate measurements to allow for multiple land-use-based ExCs to be determined empirically via multiple linear regression. However, due to the losing nature of the system, absolute export coefficients per land use area could not be determined as the load contributions to ground water are unknown and some resulting ExCs were negative. However, assuming the ground water loss rate was constant for both branches and transport within the tributaries was conservative, contributions per area per time can be compared for reach gain events on the two study reaches. Short events with high turbidity were isolated and examined along with seasonal and annual ExCs obtained from the gaining South Branch watershed.

Using RD estimated daily loads, the South Branch watershed had ExCs as summarized

Table 9: Export rates from the South Branch watershed based on loads estimated from grab sampling.

Nutrient	Runoff	Irrigation	Baseflow	Annual
NO_x, g N/ha/hr	0.14	0.042	0.066	0.075
SRP, g P/ha/hr	0.0093	0.0022	0.0018	0.0035
TP, g P/ha/hr	0.030	0.0041	0.0032	0.0091

Table 10: TP export rates from the South Branch watershed based on loads estimated via high-frequency monitoring.

Nutrient	Runoff	Irrigation	Baseflow	Annual
TP, g P/ha/hr	0.043	0.0039	0.017	0.018

in Table 9. From high-frequency monitoring, ExCs for the South Branch are found in Table 10. Runoff season for the South Branch watershed had the greatest seasonal rates of any nutrient for either method.

In comparison to the rangeland literature values reported by *Lin* (2004), the annual high-frequency TP export estimates from the South Fork were nearly 2,000 times greater and those from the RD estimates were 1,000 times greater. This is interesting that the occurrence of snow melt, and in some areas with high slopes, presumably caused greater erosion and had such an impact on ExCs when compared to those from traditional rainfall-dominated study watersheds. The dissolved NO_x-N estimate is 750 times the TN literature value suggesting that not only P is affected by erosive transport events.

Using high-frequency measurements, early, low-elevation snow melt events were identified from Figure 13 from peaks in turbidity which were prior to the peaks corresponding to the spring runoff hydrograph. These occurred beginning 08 and 25 March 2010, lasting 55.5 and 38.0 hours, respectively, and were observed at the NBSF_D site only. The SBSF_D site did exhibit a small increase in turbidity during the 08 March event which lasted only four hours. These turbidity spikes at NBSF_D were thought to be indicative of low-elevation snow melt since none were observed at the upstream sites (predominantly

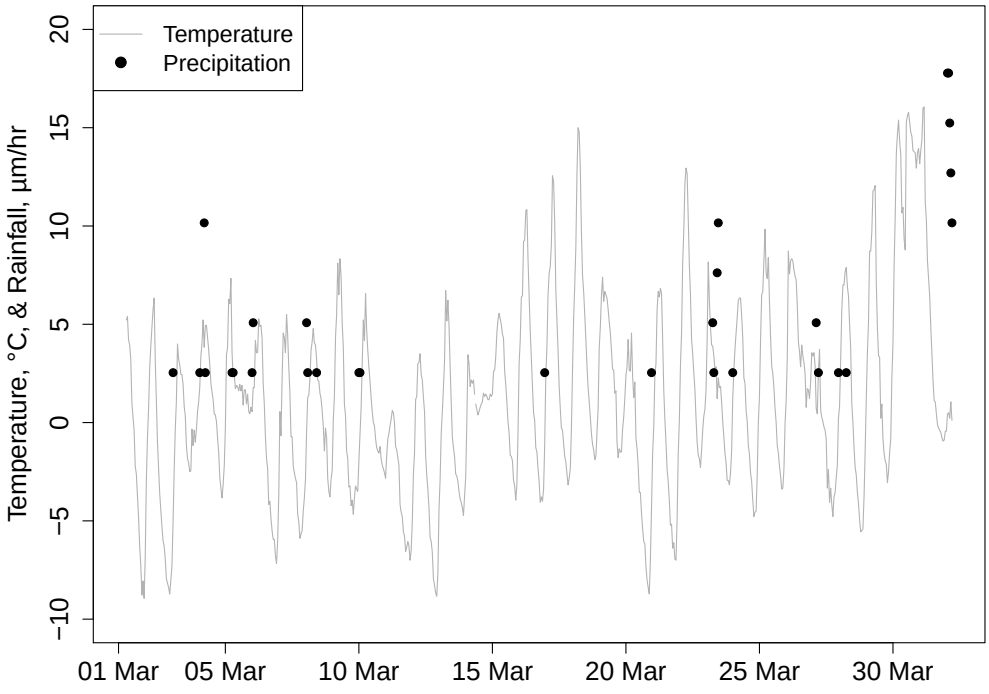

Fig. 32: Hourly air temperatures and precipitation totals for March 2010.

higher-elevation drainage areas with 98% rangeland) or at the SBSF_D site which watershed is 87% rangeland. These events coincided with precipitation events and above freezing daytime temperatures. The highest temperature for the 08 March event was 8.3°C and for the 25 March event it was 9.8°C, which occurred the day previous. Figure 32 shows the hourly air temperatures and precipitation totals during the month of March 2010.

These events contributed total loads of 3.3 and 1.9 kg TP which, when averaged by the duration and the total watershed area, were 0.38 and 0.32 g TP/ha/hr representing valley lands (1% rangeland negligable). In contrast, during the same periods the South Branch watershed contributed total loads of 2.2 and 1.7 kg TP or 0.0062 and 0.0071 g TP/ha/hr. Considering the 11% non-rangeland area of the South Branch and using the export coefficients estimated from the North Branch for such lands, just the non-rangeland area of the South Branch should have exported total loads of 15 and 8.6 kg TP. This disparity could be caused by the slightly different land use fractions of non-rangeland in each watershed

whereby the soils of the North Branch watershed have undergone more anthropogenic disturbances. Another factor could be that soils high in decomposing organic matter from the North Branch watershed were also subject to and broken down by more freeze-thaw cycles. These factors would have made the soils of the North Branch more easily erodible and the selective transport of clay materials caused higher P enrichment ratios (*Lal and Stewart*, 1994). Another cause of the high load from the North Branch during spring melt events could be the influence of precipitation if this occurred as rain at the low elevations characteristic of the North Branch watershed and as snow at higher elevations characteristic of the South Branch watershed. Soils saturated by melting snow could have been disturbed by raindrops and greater volumes of flowing water caused an increase in the energy of the flowing water making it more able to detach and transport particles from the soil surface or streambank.

Some of the greatest turbidity spikes at all the sites occurred on 19 December 2010 and 17 January 2011 lasting 38.5 and 34.0 hours (Figure 13). With turbidity increases observed at all sites (the greatest turbidity at SBSF_D) coinciding with warming temperature trends (Figure 33), this suggested that snow melt happened watershed-wide, particularly originating in the higher elevations. On 19 December at 5:00 temperatures rose above freezing and did not drop below freezing until 20 December 17:00. For the January event, temperatures above freezing began 14 January 7:00 and remained so until 18 January 13:00. While these events did not yield the anticipated TP reach gain on the North Branch, the total gains across the South Branch were 130 and 66 kg TP or 0.53 and 0.31 g TP/ha/hr for the 19 December and 17 January events, respectively. These melt events exhibited erosive transport potentials similar to those which occur during spring runoff only on a shorter duration. The rising limb of the hydrograph, regardless of its total duration, was seen to correspond with relatively high turbidity. This is similar to first flush patterns in storm water which have been observed in urban watersheds (*Li et al.*, 2005, 2007). Flushed particulates here

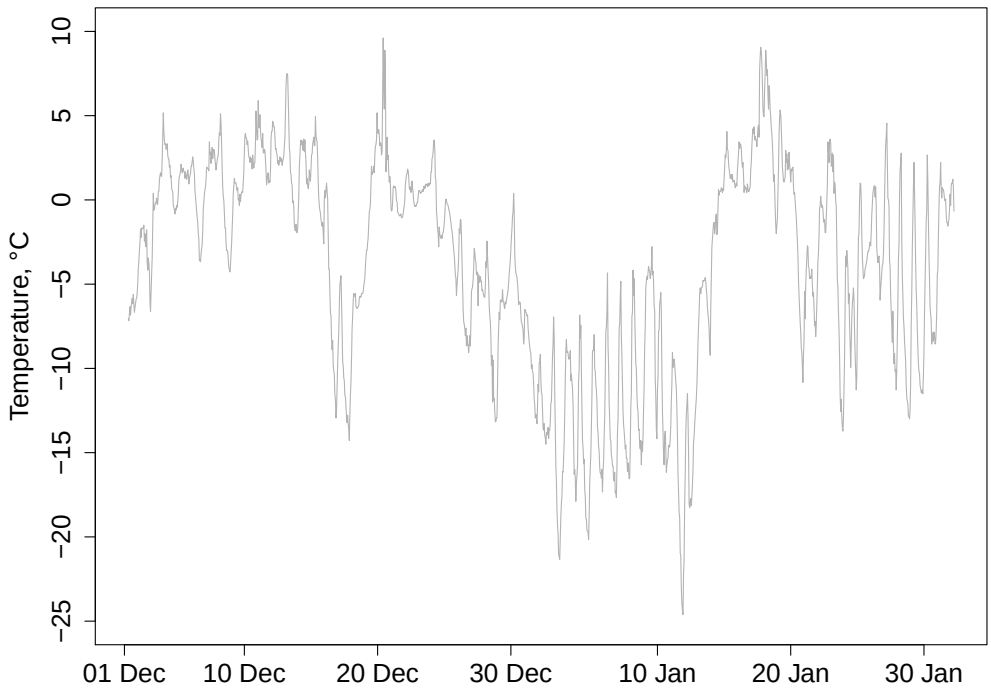

Fig. 33: Hourly air temperatures for December 2010 and January 2011.

were likely composed of erodible clay and decomposing organic matter which had accumulated under snow. The transport of these particulates required a certain energy threshold in order to detach them from the soil surface (*Pierzynski et al.*, 1993). They were flushed by the onset of snow melt flowing down-slope across the soil surface which had an energy value equal to or greater than that required to displace the particles. As water from melted snow continued to flow toward streams its energy content was not great enough to displace the remaining particulates. Soluble nutrients were also dissolved and transported by the flowing water.

Without the aid of high-frequency turbidity, it was difficult to distinguish melt events from Figures 29 and 30. However, for comparison, the nutrient loads estimated on a daily basis by the RD method were examined during the same time periods. The three daily loads from 08 through 10 March had positive North Branch reach gains for all nutrient loads. All nutrient loads were gaining across the North Branch from 25 to 26 March except the TP

load on 26 March so the duration was only considered as one day for this event. Each spring event, respectively, contributed 0.71 g NO_x-N/ha/hr, 0.055 g SRP/ha/hr, and 0.084 g TP/ha/hr and 2.3 g NO_x-N/ha/hr, 0.070 g SRP/ha/hr, and 2.3e-4 g TP/ha/hr. All values were typically greater than runoff and annual estimates and these TP ExCs were one to three orders of magnitude less than corresponding high-frequency estimates. Winter events showed positive reach gains at the South Branch using RD daily load estimates throughout their three and two day durations. Export rates for these events were, respectively, 0.11 g NO_x-N/ha/hr, 0.0019 g SRP/ha/hr, and 0.0018 g TP/ha/hr and 0.21 g NO_x-N/ha/hr, 0.0032 g SRP/ha/hr, and 0.0063 g TP/ha/hr. These winter event estimates are two orders of magnitude less than those estimated using high-frequency surrogate measurements for TP but give some idea of the rates for NO_x-N and SRP. This gives reason to believe that ExCs for NO_x-N and SRP are also under predicted for short events when the daily time step from the RD method is used and that these events also transport disproportionately high loads of NO_x-N and SRP.

The high-frequency TP ExC was nearly two times greater than the annual average ExC from RD estimates. While the durations of some melt events were short, their cumulative exports created substantial loads from nonpoint sources. For example, according to the high-frequency estimates, short event ExCs were 17 to 29 times greater than the annual TP average and 7.2 to 12 times greater than the runoff season average. Since the short event TP ExCs from the RD estimates were one to three orders of magnitude less than those from high-frequency estimates and several ExCs from short events were greater than annual and seasonal averages, short event ExCs for NO_x-N and SRP could be disproportionately high as well considering the RD method's limitation to detect short-duration events.

CHAPTER 4

ENGINEERING SIGNIFICANCE

In order for water quality modeling reflecting nonpoint sources to be accurate, nutrient export rates from nonpoint sources need to be accurate. Where nutrient export rates from snowfall-dominated watersheds are concerned, there is a deficit since most literature values are based in rainfall-dominated watersheds. These do not accurately represent the geographic, topographic, and climatic conditions which are typical of snowfall-dominated watersheds and reservoirs of intermediate latitudes in mountainous areas. Also, these watersheds tend to have highly mixed land uses due to mankind's need for nearby water sources. These watersheds are often characterized, as was seen in this study, by short-duration, nutrient transport events. Since watershed processes can occur on times scales less than one day, this must also be considered in the description and calculation of ExCs.

This study has shown that high-frequency surrogate measurements have the potential to depict short-duration transport events which occur within a watershed. High-frequency loads can be estimated and seasonal and annual averages determined with greater confidence than by using grab samples alone. With the aid of GIS techniques, mixed land use areas which runoff into the study reaches can be calculated and nutrient export of a given duration can be land area based.

Significant loads were transported during the spring runoff season; however, an important advantage of high-frequency monitoring was in determining short-duration loads. This nutrient flushing from the system contributed substantial loads which corresponded to the rising limbs of the hydrograph. These short-duration loads caused by snow melt events were seen to contribute disproportionately high loads from both the valley floor and upper elevations. With the use of high-frequency monitoring to enable inclusion of short-duration events in ExCs, more real-time conditions were represented and an increase above

the annual ExC from grab sampling alone resulted.

Identifying hydrologic events in this watershed, including short-duration events, that result in runoff across the variety of land uses may be more important to selecting and implementing effective nutrient control actions than ascribing export coefficients to exact land uses. This is a significant realization for water quality managers since focusing on timing of loads for management practices could prove beneficial in determining best management practices. For example, application of fertilizers following the growing season, on frozen ground, or on snow makes nutrients more easily transportable since they have not been incorporated into the underlying soil layers and surface soils are more easily erodible (*Pierzynski et al.*, 1993). Winter and early spring melt and erosion events observed in the North Branch watershed would have a significant potential to transport P from fields that received such post-growing season fertilization. Management strategies to remediate this would be to avoid over-fertilization and to incorporate fertilizers into the soil just prior to the growing season so that P has less time on the soil surface and can be readily assimilated by plants (*Pierzynski et al.*, 1993). It would also be beneficial to reduce the amount of crop residue left on fields since this affects P availability and would reduce a source of organic P (*Lal and Stewart*, 1994).

Particulate loading of TP to Pineview and other reservoirs in the area is of more importance than might be expected since reducing conditions occur in the sediments and allow the dissolution of P into the water column. High turbidities were observed during winter melt events and spring runoff at all sites in this study indicating that significant erosion events occurred. These erosion events were identified as significant contributors of TP but such process have also been shown to transport sediment-bound organic N as well as dissolved species of N and P (*Pierzynski et al.*, 1993). Management techniques to reduce the transport of particulate species of nutrients might also prove beneficial to reduce dissolved nutrients. Management strategies for surface waters of the Pineview Reservoir watershed

should, in general, focus on erosion prevention. Two key factors in this are improving soil structure to resist erosion and reducing the runoff velocity (*Troeh et al.*, 1980).

The presence of native vegetation in the catchment and filter strips surrounding streams has been shown to reduce the transport of particulates by stabilizing soil (*Lal and Stewart*, 1994; *Valentin et al.*, 2005; *Fu et al.*, 2011). In the Loess Plateau of China, croplands with slopes from 8°to 35°were re-established as forests or grasslands and showed 28% to 35% decrease in soil loss rates (*Fu et al.*, 2011). While it was reported that originally 60% to 90% of eroded soil in this area originated from rills and gullies, following vegitation of slopes the soil loss rate was less than 1/1500 of previous rates (*Fu et al.*, 2011). Grazing should be managed and have stocking rates that allow natural grasses to regenerate (*Troeh et al.*, 1980). Runoff and erosion of bare soils have been reduced by implementing biodegradable soil erosion control blankets such as those from a mulch-compost mix for 4% slopes or mulch for higher slopes (*Bhattarai et al.*, 2011). This approach might be useful for construction sites, bare fields, or previously eroded zones bordering stream banks until native vegitation can be re-established.

In pastures or rangeland areas, terraces could be used with a berm surrounding the downstream side of the terrace to intercept overland flow and allow water to infiltrate the soil (*Troeh et al.*, 1980). Using these berms constructed perpendicular to the slope to stop and collect runoff, *Fiener et al.* (2005) investigated dry detention basins with maximum holding volume of 490 m^3 constructed at the pour point of the fields. The basins, here with maximum retaining wall height of 1.7 m, were equipped with a perforated standpipe for normal draining to a grass waterway or toe slope and an emergency outflow pipe (*Fiener et al.*, 2005). These structures can be built and dredged of sediment as necessary using on-farm equipment and are designed to dry within 4 days of submergence to prevent crop damage (longer submergence times were observed following winter due to snow melt and frozen ground) (*Fiener et al.*, 2005). The ponds were particularly benficial in that they pre-

vented gully formation (*Fiener et al.*, 2005). While other on-site erosion control methods significantly reduced the amount of sediment delivered to the ponds, 54% to 85% of the sediment was trapped by the ponds prior to and following implementation of other prevention methods. Nutrient trapping was slightly less and ranged from 35% to 75% due to the nutrient enrichment of fine, slower settling particles (*Fiener et al.*, 2005). These methods would likely be most useful in lower-sloping elevations, such as the North Branch watershed, and could be most readily implemented in areas currently influced by anthropogenic uses.

Bank stabilization, such as riprap rock, would be beneficial in limiting streambank erosion (*Troeh et al.*, 1980) which occurs particularly during high flows. Such features have been installed in some sections of the river channels but sections without protective structures are highly susceptible to erosion during high flows and have created braided streambeds. Riprap is useful since it can easily fit with river contours and is most effective when the sizes of the rock reflect the maximum stream velocity (*Iowa Department of Natural Resources*, 2006).

Ultimately, much of the erosion originates from elevations beyond the inhabited valley floor and is possibly due to natural processes. Management strategies should include locals in solution development and should be livlihood-based in order to increase implementation rates (*Mwanukuzi*, 2011; *Lwenya and Yongo*, 2010). A careful consideration of the cost-benefit ratio should be taken before implementation of erosion reduction strategies.

CHAPTER 5

CONCLUSIONS

GIS with minimal data requirements was found to be an effective tool in determining sub-watersheds and their mixed land use components. Grab samples at the upstream sites were not found to be significantly different. High-frequency measurements at the upstream sites were considered similar and differences observed were due to stream morphometry and installation restraints. Across the study reaches, most downstream grab sample parameters were significantly different than the upstream samples. Also, considerable variability was observed between the up and downstream high-frequency measurements. These differences were as anticipated due to the respective watershed characteristics. This study showed that differences in the measured parameters must be due to actual changes in water quality. Annual ExCs in this study were up to 2,000 times greater than literature values for rainfall-dominated watersheds. This suggests that melt events and mountainous topography are characteristics which distinguish ExCs based on snowfall-dominated watersheds from those dominated by rainfall. Data from four independent sites were necessary to determine the ExCs associated with four land uses and since the North Branch yielded nutrient losses, all positive ExCs could not be calculated. Using high-frequency surrogate measurements allowed calculated surface water loads to include short-duration loading events but in this study area it is necessary that losses to ground water also be quantified.

CHAPTER 6

PROPOSED FUTURE WORK

High-frequency surrogate measurements of turbidity and water level were used to predict TP concentrations and flow rates which resulted in refined load estimates for TP. Yet, there remains a need for estimates of NO_x-N and SRP concentrations with the same frequency. As was shown by load estimates of TP from high-frequency compared to RD estimates from grab samples, short-duration transport events contributed significant loads. In order for accurate load estimates of NO_x-N and SRP to be made, short-duration events which transport these constituents also need to be included. Since no strong relationships were observed with the available sensor measurements, other predictor variables need to be investigated.

As was encountered by this study, losses to ground water are unknown and need to be quantified in order to complete mass balances and determine nonpoint source contributions from runoff. Could a more complete mass balance for the surface water system be created, it is possible that ExCs based on land use could be determined. When reach gains are positive such that an increase in the watershed size at a given node shows an increase in the load at that node, it could be possible that multiple linear regression equations could be solved to yield ExCs for varying land uses. This would require the number of land uses of concern be less than or equal to the number of water quality nodes.

Similar studies using upstream-downstream bracketing techniques could also be preformed on other tributaries to Pineview Reservoir. This would also necessitate that ground water interactions with these tributaries are quantified. Such studies could validate the results in this study to see if similar processes occur throughout the Pineview watershed and the region. Once accurate ExCs which reflect the influence of the local climate and topography on short-duration transport events are known, the creation of future development

scenarios would enable watershed managers to direct land development and best management practices. These should also be compared to event-based ExCs so that management practices can be applied efficiently to protect Pineview Reservoir water quality.

REFERENCES

Ahl, R. S., S. W. Woods, and H. R. Zuuring (2008), Hydrologic calibration and validation of SWAT in a snow-dominated Rocky Mountain watershed, Montana, USA, *J. Am. Water Resour. Assoc.*, *44*(6), 1411–1430.

APHA (1995a), 4500-NH_3 Nitrogen (Ammonia), in *Standard Methods for the Examination of Water and Wastewater*, edited by A. Eaton D., L. Clesceri S., and A. E. Greenberg, pp. 4–82, 19th ed., American Public Health Association, Washington, DC.

APHA (1995b), 4500-NO_3 Nitrogen (Nitrate), in *Standard Methods for the Examination of Water and Wastewater*, edited by A. Eaton D., L. Clesceri S., and A. E. Greenberg, pp. 4–91, 19th ed., American Public Health Association, Washington, DC.

APHA (1995c), 4500-P Phosphorus, in *Standard Methods for the Examination of Water and Wastewater*, edited by A. Eaton D., L. Clesceri S., and A. E. Greenberg, pp. 4–115, 19th ed., American Public Health Association, Washington, DC.

Avery, C. (1994), *Ground-Water Hydrology of Ogden Valley and Surrounding Area, Eastern Weber County, Utah, and Simulation of Ground-Water Flow in the Valley-Fill Aquifer System*, 84 pp., State of Utah Department of Natural Resources.

Beaulac, M. N., and K. H. Reckhow (1982), An examination of land-use–nutrient export relationships, *Water Resour. Bull.*, *18*(6), 1013–1024.

Berthouex, P. M., and L. C. Brown (2002), Precision of calculated values, in *Statistics for Environmental Engineers*, pp. 87–95, 2 ed., CRC Press, Boca Raton, FL.

Bhattarai, R., P. K. Kalita, S. Yatsu, H. R. Howard, and N. G. Svendsen (2011), Evaluation of compost blankets for erosion control from disturbed lands, *J. Environ. Manage.*, *92*(3), 803–812, doi:10.1016/j.jenvman.2010.10.028.

Campbell Scientific (2009), CS547a conductivity and temperature probe and A547 interface, *Tech. Rep.*, Campbell Scientific Inc., Logan, UT, Available from: http://www.campbellsci.com/documents/manuals/cs547a.pdf.

Campbell Scientific (2010), CR800/CR850 measurement and control system, *Tech. Rep.*, Campbell Scientific Inc., Logan, UT, Available from: http://www.campbellsci.com/documents/manuals/cr800-cr850.pdf.

Chapra, S. C. (1997), Rivers and streams, in *Surface Water-Quality Modeling*, chap. 14, pp. 238–242, 1 ed., Waveland Press, Inc., Long Grove, IL.

Christensen, V. G., X. Jian, and A. C. Ziegler (2000), Regression analysis and real-time water-quality monitoring to estimate constituent concentrations, loads, and yields in the Little Arkansas River, south-central Kansas, 1995-99, *Tech. Rep.*, U.S. Geological Survey, Lawrence, KS, Water-Resources Investigations Report 00-412 Available from: http://ks.water.usgs.gov/pubs/reports/wrir.00-4126.html.

Christensen, V. G., P. P. Rasmussen, and A. C. Ziegler (2002), Real-time water quality monitoring and regression analysis to estimate nutrient and bacteria concentrations in Kansas streams, *Tech. Rep.*, U.S. Geological Survey, Lawrence, KS, Available from: http://ks.water.usgs.gov/pubs/reports/vgc.0610.html.

Conley, D. J., H. W. Paerl, R. W. Howarth, D. F. Boesch, S. P. Seitzinger, K. E. Havens, C. Lancelot, and G. E. Likens (2009), Controlling eutrophication: Nitrogen and phosphorus, *Science*, *323*, 1014–1016.

Dodds, W. K. (2002), *Freshwater Ecology*, 569 pp., Academic Press, San Diego, CA.

ESRI (2009), World imagery, Accessed 25 Oct 2010 from: http://www.arcgis.com/home/item.html?id=10df2279f9684e4a9f6a7f08febac2a9.

ESRI (2011), Index of ftp://RiverHydraulics@ftp.esri.com/ArcHydro/Setup10, Accessed 27 Apr 2011 from: ftp://ftp.esri.com/ArcHydro/Setup10.

Federal Water Pollution Control Act 33 U.S.C. (1972), 1251 et seq., Available from: http://epw.senate.gov/water.pdf.

Fiener, P., K. Auerswald, and S. Weigand (2005), Managing erosion and water quality in agricultural watersheds by small detention ponds, *Agric., Ecosyst. and Environ.*, *110*, 132–142, doi:10.1016/j.agee.2005.03.012.

Fu, B., Y. Liu, L. Yihe, C. He, Y. Zeng, and B. Wu (2011), Assessing the soil erosion control service of ecosystems change in the Loess Plateau of China, *Ecological Complexity*, doi: 10.1016/j.ecocom.2011.07.003.

Gilliom, R. J., and D. R. Helsel (1986), Estimation of distributional parameters for censored trace level water-quality data. 1. Estimation techniques, *Water Resour. Res.*, *22*(2), 135–146.

Helsel, D. R. (2005), More than obvious: Better methods for interpreting nondetect data, *Environ. Sci. Technol.*, *39*(20), 419a–423a.

Horizon Systems Corporation (2006), Great Basin (Hydrologic Region 16) NHD Flowline, Accessed 17 Oct 2008 from: http://www.horizon-systems.com/nhdplus/HSC-wth16.php.

Horsburgh, J. S., D. G. Tarboton, D. R. Maidment, and I. Zaslavsky (2008), A relational model for environmental and water resources data, *Water Resour. Res.*, *44*(5), W05,406.

Horsburgh, J. S., A. S. Jones, D. K. Stevens, D. G. Tarboton, and N. O. Mesner (2010), A sensor network for high frequency estimation of water quality constituent fluxes using surrogates, *Environ. Modelling & Software*, *25*(9), 1031–1044.

Horsburgh, J. S., D. G. Tarboton, D. R. Maidment, and I. Zaslavsky (2011), Components of an environmental observatory information system, *Comput. Geosci.*, *37*(2), 207–218.

Iowa Department of Natural Resources (2006), How to Control Streambank Erosion, *Tech. Rep.*, U.S. Department of Agriculture and U.S. Environmental Protection Agency, Kansas City, Kansas, accessed 18 Nov 2011 from: www.iowadnr.gov.

Lal, R., and B. A. Stewart (1994), *Soil Processes and Water Quality*, 398 pp., CRC Press, Inc., Boca Raton, FL.

Lee, J.-H. (2008), Rank-date distribution method (R-D method) for daily time-series bayesian networks and total maximum daily load estimation, Ph.D., pp. 83–112, Utah State University, Logan, UT.

Lewis, W. M., and W. A. Wurtsbaugh (2008), Control of lacustrine phytoplankton by nutrients: Erosion of the phosphorus paradigm, *Int. Rev. Hydrobiol.*, *93*(4-5), 446–465, doi:10.1002/iroh.200811065.

Li, L.-q., C.-q. Yin, Q.-c. He, and L.-l. Kong (2007), First flush of storm runoff pollution from an urban atchment in China, *J. Environ. Sci.*, *25*(3), 295–299.

Li, Y., S.-L. Lau, M. Kayhanian, and M. K. Stenstrom (2005), Particle size distribution in highway runoff, *J. Environ. Engineer.*, *131*(9), 1267–1276, doi:10.1061/(ASCE) 0733-9372(2005)131:9(1267).

Lin, J. (2004), Review of published export coefficient and event mean concentration (EMC) data, *Tech. Rep.*, Wetlands Regulatory Assistance Program, ERDC TN-WRAP-04-3.

Lowe, M., J. Wallace, L. E. Spangler, and C. J. Allen (1999), The hydrogeology of Ogden Valley, Weber County, Utah, and recommended waste-water management practices to

protect ground-water quality, in *Geology of Northern Utah and Vicinity*, pp. 313–336, Carr Printing Company, Bountiful, UT.

Lwenya, C., and E. Yongo (2010), Human aspects of siltation of Lake Baringo: Causes, impacts and interventions, *Aquat. Ecosyst. Health Manage.*, *13*(4), 437–441, doi:10.1080/14634988.2010.524497.

Masters, G. M., and W. P. Ela (2008), Water pollution, in *Introduction to Environmental Engineering and Science*, chap. 5, pp. 173–280, 3 ed., Pearson Education, Inc., Upper Saddle River, NJ.

Mwanukuzi, P. K. (2011), Impact of non-livelihood-based land management on land resources: The case of upland watersheds in Uporoto Mountains, South West Tanzania, *The Geographical J.*, *177*(1), 27–34, doi:10.1111/j.1475-4959.2010.00362.x.

Pierzynski, G. M., J. T. Sims, and G. F. Vance (1993), *Soils and Environmental Quality*, 313 pp., CRC Press, Inc., Boca Raton, FL.

R Development Core Team (2010), *R: A Language and Environment for Statistical Computing*, R Foundation for Statistical Computing, Vienna, Austria, Available from: http://www.R-project.org, ISBN 3-900051-07-0.

Rasmussen, T. J., A. C. Ziegler, and P. P. Rasmussen (2005), Estimation of constituent concentrations, densities, loads, and yields in lower Kansas River, northeast Kansas, using regression models and continuous water-quality monitoring, January 2000 through December 2003, *Tech. Rep.*, U.S. Geological Survey, Reston, VA, Scientific Investigations Report 2005-5165 Available from: http://pubs.usgs.gov/sir/2005/5165/pdf/SIR20055165.pdf.

Ryberg, K. R. (2006), Continuous water-quality monitoring and regression analysis to estimate constituent concentrations and loads in the Red River of

the North, Fargo, North Dakota, 2003-05, *Tech. Rep.*, U.S. Geological Survey, Reston, VA, Scientific Investigations Report 2006-5241 Available from: http://pubs.usgs.gov/sir/2006/5241/pdf/sir2006-5241.pdf.

Seal Analytical (2006), Nitrate-N + Nitrite-N in drinking and surface waters, and domestic and industrial wastes, AQ2 Method No: EPA-127-A Rev. 5, *Tech. Rep.*, Seal Analytical, Ltd., Available from: http://www.seal-analytical.com/Methods/DiscreteMethods-/AQ2EPAMethodspage2/tabid/77/Default.aspx.

Seal Analytical (2009), Ammonia-N in drinking and surface waters, and domestic and industrial wastes, AQ2 Method No: EPA-103-A Rev. 6, *Tech. Rep.*, Seal Analytical, Ltd., Available from: http://www.seal-analytical.com/Methods/DiscreteMethods-/AQ2EPAMethodspage1/tabid/76/Default.aspx.

Shrestha, S., F. Kazama, and L. T. H. Newham (2008), A framework for estimating pollutant export coefficients from long-term in-stream water quality monitoring data, *Environ. Modelling & Software*, *23*, 182–194.

Sivertun, A., and L. Prange (2003), Non-point source critical area analysis in the Gisselo watershed using GIS, *Environ. Modelling & Software*, *18*(10), 887–898.

Tang, C. G., and C. Q. Liu (2008), Nonpoint source pollution assessment of Wujiang River watershed in Guizhou Province, SW China, *Environ. Modeling & Assessment*, *13*(1), 155–167.

Tetra Tech Inc. (2002), Pineview Reservoir TMDL, *Tech. Rep.*, Utah Department of Environmental Quality; Division of Water Quality, Salt Lake City, Utah.

Thornton, K. W., B. L. Kimmel, and F. E. Payne (1990), *Reservoir Limnology: Ecological Perspectives*, 246 pp., John Wiley & Sons, New York City, NY.

Troeh, F. R., J. A. Hobbs, and R. L. Donahue (1980), *Soil and Water Conservation for Productivity and Environmental Protection*, 718 pp., Prentice-Hall, Inc., Englewood Cliffs, NJ.

UDEQ Division of Water Quality (2008), Draft version of Utah's 2008 integrated report part 3–303(d) list of impaired waters, *Tech. Rep.*, Utah Department of Environmental Quality; Division of Water Quality, Salt Lake City, Utah, Available from: http://www.waterquality.utah.gov/WQAssess/2008IR.htm.

UNEP (2010), Lakes and reservoirs similarities, differences and importance, *Tech. Rep.*, United Nations Environment Programme; Division of Technology, Industry and Economics, Available from: http://www.unep.or.jp/ietc/publications/short_series/lakereservoirs-1/index.asp.

U.S. Census Bureau (2009), Population finder: Huntsville, UT, Accessed 13 Jul 2011 from: http://factfinder.census.gov/servlet/SAFFPopulation?_event=Search&_name=Huntsville+&_state=04000US49&_county=Huntsville&_cityTown=Huntsville&_zip=&_sse=on&_lang=en&pctxt=fph.

U.S. Census Bureau (2010), American fact finder, Accessed 23 Sept 2011 from: http://factfinder2.census.gov/faces/tableservices/jsf/pages/productview.xhtml?src=bkmk.

U.S. EPA (1978), Phosphorus, all forms (colorimetric, ascorbic acid, two reagent), Accessed 10 Jun 2008 from: http://www.epa.gov/waterscience/methods/method/files/365_3.pdf.

U.S. Geological Survey (2010), USGS surface-water monthly statistics for the nation, Accessed 26 Nov 2010 from: http://www.waterdata.usgs.gov.

Utah Division of Water Resources (2007), WaterRelatedLandUse, Accessed 04 Mar 2011 from: http://gis.utah.gov/sgid-vector-download/utah-sgid-vector-gis-data-layer-download-index?fc=WaterRelatedLandUs.

Utah GIS Portal (2008), webe_ned10, Accessed 08 Mar 2008 from http://gis.utah.gov-/elevation-terrain-data/national-elevation-dataset-ned.

Valentin, C., J. Poesen, and Y. Li (2005), Gully erosion: Impacts , factors and control, *Catena*, *63*, 132–153, doi:10.1016/j.catena.2005.06.001.

Weber County (2008), Ogden Valley General Plan, Accessed 13 Jul 2010 from: http://www.co.weber.ut.us/mediawiki/index.php/Ogden_Valley_General_Plan.

Worwood, B. K. (2011), Analysis of the Import, Export, and Bioavailability of Nitrogen and Phosphorus within Pineview Reservoir, M.S. thesis, pp. 74–77, Utah State University, Logan, UT.

WRCC (2009), Western US Climate Historical Summaries: Huntsville Monastery, Utah (424135), Accessed 14 Jul 2010 from: http://www.wrcc.dri.edu/cgi-bin/cliMAIN.pl?ut4135.

APPENDICES

APPENDIX A

CENSORED DATA AND GRAB SAMPLING VALUES

Table A.1: Example calculations from high-frequency electrical conductivity measurements showing data censoring and corrections.

Date Time	Temperature, °C	Conductivity, mS/cm	EC, mS/cm	$EC_{censoring}$, mS/cm	EC_{stored}, mS/cm
11/26/2010 2:00	0.340	0.021078	0.039117	0.039	0.039
11/26/2010 2:30	0.311	-1.317347	-2.447164	0.005	0.038
11/26/2010 3:00	0.283	-1.317972	-2.450709	0.005	0.037
11/26/2010 3:30	0.216	-1.318239	-2.45693	0.005	0.035
11/26/2010 4:00	0.141	-1.318329	-2.463537	0.005	0.034
11/26/2010 4:30	0.131	-1.318329	-2.464398	0.005	0.033
11/26/2010 5:00	0.102	-1.318329	-2.466899	0.005	0.031
11/26/2010 5:30	0.053	-1.318329	-2.471136	0.005	0.030
11/26/2010 6:00	-0.024	-1.318418	-2.477991	0.005	0.029
11/26/2010 6:30	-0.060	-1.318418	-2.48113	0.005	0.028
11/26/2010 7:00	-0.098	-1.318418	-2.484453	0.005	0.026
11/26/2010 7:30	-0.156	-1.318507	-2.489709	0.005	0.025
11/26/2010 8:00	-0.185	-1.318507	-2.492261	0.005	0.024
11/26/2010 8:30	-0.176	-1.318507	-2.491468	0.005	0.023
11/26/2010 9:00	-0.068	-1.318507	-2.481996	0.005	0.021
11/26/2010 9:30	-0.010	-1.318507	-2.476939	0.005	0.020
11/26/2010 10:00	0.112	-1.318418	-2.466202	0.005	0.019
11/26/2010 10:30	0.323	-1.318329	-2.447968	0.005	0.017
11/26/2010 11:00	0.574	-1.318329	-2.426817	0.005	0.016
11/26/2010 11:30	0.794	-1.317972	-2.407924	0.005	0.015
11/26/2010 12:00	1.050	-1.316097	-2.383651	0.005	0.014
11/26/2010 12:30	1.283	0.002465	0.004429	0.005	0.012
11/26/2010 13:00	1.550	0.006155	0.010962	0.011	0.011

Table A.2: NO_x-N grab sample concentrations with imputed values.

Site	Date	Data Value, mg/L	Censored	Imputed Value, mg/L
Middle Fork	1/25/2010	0.1689	N	
Middle Fork	2/23/2010	0.0268	Y	0.0337
Middle Fork	3/2/2010	0.0476	N	
Middle Fork	3/15/2010	0.0774	N	
Middle Fork	3/29/2010	0.1533	N	
Middle Fork	4/5/2010	0.0045	Y	0.0066
Middle Fork	4/13/2010	0.0065	Y	0.0082
Middle Fork	4/19/2010	0.0653	N	
Middle Fork	4/27/2010	0.0071	Y	0.0097
Middle Fork	5/4/2010	0.0108	Y	0.0191
Middle Fork	5/11/2010	0.0001	Y	0.003
Middle Fork	5/25/2010	0.0017	Y	0.0049
Middle Fork	6/1/2010	0.0113	Y	0.0214
Middle Fork	6/8/2010	0.0183	Y	0.0260
Middle Fork	6/22/2010	0.0093	Y	0.0131
Middle Fork	6/29/2010	0.0365	N	
Middle Fork	7/20/2010	0.0636	N	
Middle Fork	8/3/2010	0.0080	Y	0.0114
Middle Fork	8/25/2010	0.1188	N	
Middle Fork	9/7/2010	0.0366	N	
Middle Fork	10/12/2010	0.0236	Y	0.0300
Middle Fork	11/9/2010	0.0174	Y	0.0240
Middle Fork	12/7/2010	0.0100	Y	0.0150
Middle Fork	2/8/2011	0.0104	Y	0.0169
NBSF D	1/25/2010	0.3530	N	
NBSF D	2/10/2010	0.1894	N	
NBSF D	2/23/2010	0.1467	N	
NBSF D	3/2/2010	0.1555	N	
NBSF D	3/15/2010	0.2395	N	
NBSF D	3/29/2010	0.3964	N	
NBSF D	4/5/2010	0.2143	N	
NBSF D	4/13/2010	0.1703	N	
NBSF D	4/19/2010	0.1102	N	
NBSF D	4/27/2010	0.0805	N	
NBSF D	5/4/2010	0.0657	N	
NBSF D	5/11/2010	0.0460	N	
NBSF D	5/25/2010	0.1349	N	
NBSF D	6/1/2010	0.1149	N	
NBSF D	6/8/2010	0.1693	N	
NBSF D	6/22/2010	1.878	N	
NBSF D	6/29/2010	0.1571	N	
NBSF D	7/20/2010	0.2197	N	
NBSF D	8/3/2010	0.1450	N	
NBSF D	8/25/2010	0.0618	N	
NBSF D	9/7/2010	0.1957	N	
NBSF D	9/28/2010	0.0700	N	
NBSF D	10/12/2010	0.0866	N	

Table A.2: (continued)

Site	Date	Data Value, mg/L	Censored	Imputed Value, mg/L
NBSF D	11/9/2010	0.0879	N	
NBSF D	12/7/2010	0.0700	N	
NBSF D	1/13/2011	0.6063	N	
NBSF D	2/8/2011	0.5252	N	
NBSF U	1/25/2010	0.3238	N	
NBSF U	2/10/2010	0.0940	N	
NBSF U	2/23/2010	0.2007	N	
NBSF U	3/2/2010	0.0676	N	
NBSF U	3/15/2010	0.0551	N	
NBSF U	3/29/2010	0.1942	N	
NBSF U	4/5/2010	0.0532	N	
NBSF U	4/13/2010	0.0415	N	
NBSF U	4/19/2010	0.0842	N	
NBSF U	4/27/2010	0.0848	N	
NBSF U	5/4/2010	0.0434	N	
NBSF U	5/11/2010	0.0184	Y	0.0209
NBSF U	5/25/2010	0.1101	N	
NBSF U	6/1/2010	0.1291	N	
NBSF U	6/8/2010	0.0979	N	
NBSF U	6/22/2010	0.0702	N	
NBSF U	11/9/2010	0.0252	Y	0.0287
NBSF U	12/7/2010	0.0500	N	
NBSF U	1/13/2011	0.0442	N	
NBSF U	2/8/2011	0.0948	N	
North Fork	1/25/2010	1.042	N	
North Fork	2/23/2010	0.8128	N	
North Fork	3/2/2010	0.8835	N	
North Fork	3/15/2010	0.6034	N	
North Fork	3/29/2010	1.313	N	
North Fork	4/5/2010	0.9828	N	
North Fork	4/13/2010	0.7219	N	
North Fork	4/19/2010	0.5524	N	
North Fork	4/27/2010	0.4838	N	
North Fork	5/4/2010	0.5225	N	
North Fork	5/11/2010	0.4316	N	
North Fork	5/25/2010	0.3457	N	
North Fork	6/1/2010	0.2985	N	
North Fork	6/8/2010	0.2692	N	
North Fork	6/22/2010	0.3480	N	
North Fork	6/29/2010	0.3031	N	
North Fork	7/20/2010	0.5647	N	
North Fork	8/3/2010	0.6291	N	
North Fork	8/25/2010	0.1380	N	
North Fork	9/7/2010	0.3700	N	
North Fork	10/12/2010	0.1221	N	
North Fork	12/7/2010	0.2900	N	
North Fork	1/13/2011	1.081	N	

Table A.2: (continued)

Site	Date	Data Value, mg/L	Censored	Imputed Value, mg/L
North Fork	2/8/2011	1.539	N	
SBSF D	1/25/2010	0.4718	N	
SBSF D	2/10/2010	0.2803	N	
SBSF D	2/18/2010	0.0524	N	
SBSF D	2/23/2010	0.2031	N	
SBSF D	3/2/2010	0.1795	N	
SBSF D	3/15/2010	0.2171	N	
SBSF D	3/29/2010	0.4205	N	
SBSF D	4/5/2010	0.2791	N	
SBSF D	4/13/2010	0.3753	N	
SBSF D	4/19/2010	0.1452	N	
SBSF D	4/27/2010	0.1485	N	
SBSF D	5/4/2010	0.0863	N	
SBSF D	5/11/2010	0.0628	N	
SBSF D	5/25/2010	0.1442	N	
SBSF D	6/1/2010	0.1668	N	
SBSF D	6/8/2010	0.2477	N	
SBSF D	6/22/2010	0.2774	N	
SBSF D	6/29/2010	0.3541	N	
SBSF D	7/20/2010	0.2826	N	
SBSF D	8/3/2010	0.2346	N	
SBSF D	8/25/2010	0.0669	N	
SBSF D	9/7/2010	0.1997	N	
SBSF D	9/28/2010	0.1100	N	
SBSF D	10/12/2010	0.1304	N	
SBSF D	11/9/2010	0.1437	N	
SBSF D	12/7/2010	0.7700	N	
SBSF D	1/13/2011	0.6258	N	
SBSF D	2/8/2011	0.5078	N	
SBSF U	1/25/2010	0.3059	N	
SBSF U	2/10/2010	0.1209	N	
SBSF U	2/23/2010	0.2582	N	
SBSF U	3/2/2010	0.0899	N	
SBSF U	3/15/2010	0.0587	N	
SBSF U	3/29/2010	0.2052	N	
SBSF U	4/5/2010	0.0615	N	
SBSF U	4/13/2010	0.0462	N	
SBSF U	4/19/2010	0.0865	N	
SBSF U	4/27/2010	0.0982	N	
SBSF U	5/4/2010	0.0439	N	
SBSF U	5/11/2010	0.0233	Y	0.0292
SBSF U	5/25/2010	0.1207	N	
SBSF U	6/1/2010	0.1206	N	
SBSF U	6/8/2010	0.1537	N	
SBSF U	6/8/2010	0.1170	N	
SBSF U	6/22/2010	0.0848	N	
SBSF U	12/7/2010	0.1400	N	

Table A.2: (continued)

Site	Date	Data Value, mg/L	Censored	Imputed Value, mg/L
SBSF U	1/13/2011	0.0400	N	
SBSF U	2/8/2011	0.1041	N	
Spring Creek	3/15/2010	0.3715	N	
Spring Creek	3/29/2010	0.5539	N	
Spring Creek	4/5/2010	0.3809	N	
Spring Creek	4/13/2010	0.2937	N	
Spring Creek	4/19/2010	0.2876	N	
Spring Creek	4/27/2010	0.4952	N	
Spring Creek	5/4/2010	0.3578	N	
Spring Creek	5/11/2010	0.3632	N	
Spring Creek	5/25/2010	0.2073	N	
Spring Creek	6/1/2010	0.1654	N	
Spring Creek	6/8/2010	0.1602	N	
Spring Creek	6/22/2010	0.1644	N	
Spring Creek	6/29/2010	0.0521	N	
Spring Creek	7/20/2010	0.1108	N	
Spring Creek	8/3/2010	0.1122	N	
Spring Creek	8/25/2010	0.0575	N	
Spring Creek	9/7/2010	0.1987	N	
Spring Creek	9/28/2010	0.1300	N	
Spring Creek	10/12/2010	0.2211	N	
Spring Creek	11/9/2010	0.4241	N	
Spring Creek	12/7/2010	0.1100	N	
Spring Creek	2/8/2011	0.7580	N	

Table A.3: SRP grab sample concentrations with imputed values.

Site	Date	Data Value, μg/L	Censored	Imputed Value, μg/L
Middle Fork	1/25/2010	4.30	N	
Middle Fork	2/23/2010	4.30	N	
Middle Fork	3/2/2010	3.30	N	
Middle Fork	3/15/2010	5.20	N	
Middle Fork	3/29/2010	3.60	N	
Middle Fork	4/5/2010	3.10	N	
Middle Fork	4/13/2010	5.00	N	
Middle Fork	4/19/2010	6.90	N	
Middle Fork	4/27/2010	5.50	N	
Middle Fork	5/4/2010	4.00	N	
Middle Fork	5/25/2010	4.70	N	
Middle Fork	6/1/2010	2.90	N	
Middle Fork	6/8/2010	2.90	N	
Middle Fork	6/22/2010	2.90	N	
Middle Fork	6/29/2010	5.10	N	
Middle Fork	7/20/2010	4.20	N	
Middle Fork	8/3/2010	4.20	N	
Middle Fork	8/25/2010	3.80	N	
Middle Fork	9/7/2010	3.80	N	
Middle Fork	10/12/2010	3.30	N	
Middle Fork	11/9/2010	3.80	N	
Middle Fork	12/7/2010	3.30	N	
Middle Fork	2/8/2011	5.60	N	
NBSF D	1/25/2010	8.30	N	
NBSF D	2/10/2010	10.3	N	
NBSF D	2/23/2010	8.30	N	
NBSF D	3/2/2010	10.3	N	
NBSF D	3/15/2010	14.8	N	
NBSF D	3/29/2010	9.30	N	
NBSF D	4/5/2010	8.80	N	
NBSF D	4/13/2010	6.00	N	
NBSF D	4/19/2010	4.00	N	
NBSF D	4/27/2010	5.00	N	
NBSF D	5/4/2010	3.10	N	
NBSF D	5/25/2010	5.10	N	
NBSF D	6/1/2010	3.80	N	
NBSF D	6/8/2010	2.40	N	
NBSF D	6/22/2010	3.30	N	
NBSF D	6/29/2010	3.30	N	
NBSF D	7/20/2010	5.10	N	
NBSF D	8/3/2010	11.0	N	
NBSF D	8/25/2010	12.4	N	
NBSF D	9/7/2010	11.0	N	
NBSF D	9/28/2010	10.6	N	
NBSF D	10/12/2010	16.0	N	
NBSF D	11/9/2010	6.10	N	
NBSF D	12/7/2010	10.6	N	

Table A.3: (continued)

Site	Date	Data Value, μg/L	Censored	Imputed Value, μg/L
NBSF D	1/13/2011	6.50	N	
NBSF D	2/8/2011	5.90	N	
NBSF U	1/25/2010	4.30	N	
NBSF U	2/10/2010	2.30	N	
NBSF U	2/23/2010	3.30	N	
NBSF U	3/2/2010	2.30	N	
NBSF U	3/15/2010	4.30	N	
NBSF U	3/29/2010	1.70	Y	1.60
NBSF U	4/5/2010	2.10	N	
NBSF U	4/13/2010	3.10	N	
NBSF U	4/19/2010	9.30	N	
NBSF U	4/27/2010	3.60	N	
NBSF U	5/4/2010	2.60	N	
NBSF U	5/25/2010	3.30	N	
NBSF U	6/8/2010	2.90	N	
NBSF U	6/22/2010	2.90	N	
NBSF U	11/9/2010	3.30	N	
NBSF U	12/7/2010	2.90	N	
NBSF U	1/13/2011	4.40	N	
NBSF U	2/8/2011	5.30	N	
North Fork	1/25/2010	4.30	N	
North Fork	2/23/2010	4.30	N	
North Fork	3/2/2010	3.30	N	
North Fork	3/15/2010	3.30	N	
North Fork	3/29/2010	2.10	N	
North Fork	4/5/2010	2.10	N	
North Fork	4/13/2010	6.40	N	
North Fork	4/19/2010	6.40	N	
North Fork	4/27/2010	6.90	N	
North Fork	5/4/2010	3.60	N	
North Fork	5/25/2010	6.00	N	
North Fork	6/1/2010	7.00	N	
North Fork	6/8/2010	3.80	N	
North Fork	6/22/2010	2.90	N	
North Fork	6/29/2010	4.70	N	
North Fork	7/20/2010	5.60	N	
North Fork	8/3/2010	5.10	N	
North Fork	8/25/2010	3.30	N	
North Fork	9/7/2010	2.90	N	
North Fork	10/12/2010	6.50	N	
North Fork	12/7/2010	5.10	N	
North Fork	1/13/2011	4.40	N	
North Fork	2/8/2011	5.00	N	
SBSF D	1/25/2010	1.30	Y	2.00
SBSF D	2/10/2010	6.30	N	
SBSF D	2/23/2010	8.30	N	
SBSF D	3/2/2010	6.30	N	

Table A.3: (continued)

Site	Date	Data Value, μg/L	Censored	Imputed Value, μg/L
SBSF D	3/15/2010	11.0	N	
SBSF D	3/29/2010	10.7	N	
SBSF D	4/5/2010	14.5	N	
SBSF D	4/13/2010	19.8	N	
SBSF D	4/19/2010	10.7	N	
SBSF D	4/27/2010	8.30	N	
SBSF D	5/4/2010	7.40	N	
SBSF D	5/25/2010	10.1	N	
SBSF D	6/1/2010	7.40	N	
SBSF D	6/8/2010	6.00	N	
SBSF D	6/22/2010	7.40	N	
SBSF D	6/29/2010	7.90	N	
SBSF D	7/20/2010	9.70	N	
SBSF D	8/3/2010	22.4	N	
SBSF D	8/25/2010	21.1	N	
SBSF D	9/7/2010	17.4	N	
SBSF D	9/28/2010	19.2	N	
SBSF D	10/12/2010	10.1	N	
SBSF D	11/9/2010	17.4	N	
SBSF D	12/7/2010	12.4	N	
SBSF D	1/13/2011	12.1	N	
SBSF D	2/8/2011	8.30	N	
SBSF U	1/25/2010	5.30	N	
SBSF U	2/10/2010	3.30	N	
SBSF U	2/23/2010	2.30	N	
SBSF U	3/2/2010	2.30	N	
SBSF U	3/15/2010	3.30	N	
SBSF U	3/29/2010	1.70	Y	1.60
SBSF U	4/5/2010	2.10	N	
SBSF U	4/13/2010	3.10	N	
SBSF U	4/19/2010	4.80	N	
SBSF U	4/27/2010	4.00	N	
SBSF U	5/4/2010	2.10	N	
SBSF U	5/25/2010	3.80	N	
SBSF U	6/1/2010	3.30	N	
SBSF U	6/8/2010	2.90	N	
SBSF U	6/22/2010	2.90	N	
SBSF U	12/7/2010	2.90	N	
SBSF U	1/13/2011	4.40	N	
SBSF U	2/8/2011	6.80	N	
Spring Creek	3/15/2010	19.5	N	
Spring Creek	3/29/2010	10.7	N	
Spring Creek	4/5/2010	20.7	N	
Spring Creek	4/13/2010	16.9	N	
Spring Creek	4/19/2010	11.7	N	
Spring Creek	4/27/2010	7.40	N	
Spring Creek	5/4/2010	10.2	N	

Table A.3: (continued)

Site	Date	Data Value, μg/L	Censored	Imputed Value, μg/L
Spring Creek	5/25/2010	11.5	N	
Spring Creek	6/1/2010	11.5	N	
Spring Creek	6/8/2010	11.0	N	
Spring Creek	6/22/2010	8.30	N	
Spring Creek	6/29/2010	15.6	N	
Spring Creek	7/20/2010	10.1	N	
Spring Creek	8/3/2010	8.80	N	
Spring Creek	8/25/2010	13.3	N	
Spring Creek	9/7/2010	9.70	N	
Spring Creek	9/28/2010	12.0	N	
Spring Creek	10/12/2010	10.1	N	
Spring Creek	11/9/2010	13.3	N	
Spring Creek	12/7/2010	22.0	N	
Spring Creek	2/8/2011	15.6	N	

Table A.4: TP grab sample concentrations.

Site	Date	Data Value, μg/L
Middle Fork	1/25/2010	20.4
Middle Fork	2/23/2010	10.4
Middle Fork	3/2/2010	8.40
Middle Fork	3/15/2010	16.6
Middle Fork	3/29/2010	14.6
Middle Fork	4/5/2010	12.6
Middle Fork	4/13/2010	46.6
Middle Fork	4/19/2010	51.6
Middle Fork	4/27/2010	38.6
Middle Fork	5/4/2010	27.0
Middle Fork	5/11/2010	21.0
Middle Fork	5/25/2010	23.0
Middle Fork	6/1/2010	21.0
Middle Fork	6/8/2010	21.0
Middle Fork	6/22/2010	12.0
Middle Fork	6/29/2010	11.0
Middle Fork	7/20/2010	11.0
Middle Fork	8/3/2010	12.0
Middle Fork	8/25/2010	10.0
Middle Fork	9/7/2010	12.0
Middle Fork	10/12/2010	13.0
Middle Fork	11/9/2010	10.0
Middle Fork	12/7/2010	4.80
Middle Fork	2/8/2011	19.8
NBSF D	1/25/2010	16.4
NBSF D	2/10/2010	19.4
NBSF D	2/23/2010	17.4
NBSF D	3/2/2010	28.4
NBSF D	3/15/2010	32.6
NBSF D	3/29/2010	16.6
NBSF D	4/5/2010	16.6
NBSF D	4/13/2010	33.6
NBSF D	4/19/2010	36.6
NBSF D	4/27/2010	37.6
NBSF D	5/4/2010	21.0
NBSF D	5/11/2010	19.0
NBSF D	5/25/2010	21.0
NBSF D	6/1/2010	21.0
NBSF D	6/8/2010	17.0
NBSF D	6/22/2010	12.0
NBSF D	6/29/2010	10.0
NBSF D	7/20/2010	18.0
NBSF D	8/3/2010	23.0
NBSF D	8/25/2010	26.0
NBSF D	9/7/2010	30.0
NBSF D	9/28/2010	17.0
NBSF D	10/12/2010	30.0

Table A.4: (continued)

Site	Date	Data Value, μg/L
NBSF D	11/9/2010	16.0
NBSF D	12/7/2010	16.7
NBSF D	1/13/2011	10.4
NBSF D	2/8/2011	14.2
NBSF U	1/25/2010	12.4
NBSF U	2/10/2010	20.4
NBSF U	2/23/2010	13.4
NBSF U	3/2/2010	9.40
NBSF U	3/15/2010	14.6
NBSF U	3/29/2010	9.60
NBSF U	4/5/2010	6.60
NBSF U	4/13/2010	74.6
NBSF U	4/19/2010	37.6
NBSF U	4/27/2010	32.6
NBSF U	5/4/2010	21.0
NBSF U	5/11/2010	20.0
NBSF U	5/25/2010	23.0
NBSF U	6/1/2010	26.0
NBSF U	6/8/2010	20.0
NBSF U	6/22/2010	12.0
NBSF U	11/9/2010	11.0
NBSF U	12/7/2010	9.20
NBSF U	1/13/2011	16.1
NBSF U	2/8/2011	17.9
North Fork	2/23/2010	11.4
North Fork	3/2/2010	11.4
North Fork	3/15/2010	12.6
North Fork	3/29/2010	16.6
North Fork	4/5/2010	14.6
North Fork	4/13/2010	71.6
North Fork	4/19/2010	58.6
North Fork	4/27/2010	42.6
North Fork	5/4/2010	21.0
North Fork	5/11/2010	41.0
North Fork	5/25/2010	31.0
North Fork	6/1/2010	35.0
North Fork	6/8/2010	33.0
North Fork	6/22/2010	17.0
North Fork	6/29/2010	12.0
North Fork	7/20/2010	10.0
North Fork	8/3/2010	11.0
North Fork	8/25/2010	8.00
North Fork	9/7/2010	32.0
North Fork	10/12/2010	14.0
North Fork	12/7/2010	8.60
North Fork	1/13/2011	7.90
North Fork	2/8/2011	12.9

Table A.4: (continued)

Site	Date	Data Value, μg/L
SBSF D	1/25/2010	17.4
SBSF D	2/10/2010	23.4
SBSF D	2/23/2010	19.4
SBSF D	3/2/2010	22.4
SBSF D	3/15/2010	28.6
SBSF D	3/29/2010	18.6
SBSF D	4/5/2010	48.6
SBSF D	4/13/2010	99.6
SBSF D	4/19/2010	62.6
SBSF D	4/27/2010	57.6
SBSF D	5/4/2010	26.0
SBSF D	5/11/2010	34.0
SBSF D	5/25/2010	33.0
SBSF D	6/1/2010	32.0
SBSF D	6/8/2010	23.0
SBSF D	6/22/2010	19.0
SBSF D	6/29/2010	17.0
SBSF D	7/20/2010	20.0
SBSF D	8/3/2010	41.0
SBSF D	8/25/2010	38.0
SBSF D	9/7/2010	33.0
SBSF D	9/28/2010	26.0
SBSF D	10/12/2010	19.0
SBSF D	11/9/2010	28.0
SBSF D	12/7/2010	18.6
SBSF D	1/13/2011	20.4
SBSF D	2/8/2011	21.1
SBSF U	1/25/2010	9.40
SBSF U	2/10/2010	10.4
SBSF U	2/23/2010	16.4
SBSF U	3/2/2010	11.4
SBSF U	3/15/2010	13.6
SBSF U	3/29/2010	9.60
SBSF U	4/5/2010	6.60
SBSF U	4/13/2010	33.6
SBSF U	4/19/2010	34.6
SBSF U	4/27/2010	37.6
SBSF U	5/4/2010	21.0
SBSF U	5/11/2010	26.0
SBSF U	5/25/2010	24.0
SBSF U	6/1/2010	27.0
SBSF U	6/8/2010	17.0
SBSF U	6/22/2010	12.0
SBSF U	12/7/2010	9.20
SBSF U	1/13/2011	9.20
SBSF U	2/8/2011	13.6
Spring Creek	3/15/2010	169

Table A.4: (continued)

Site	Date	Data Value, μg/L
Spring Creek	3/29/2010	45.6
Spring Creek	4/5/2010	256
Spring Creek	4/13/2010	159
Spring Creek	4/19/2010	57.6
Spring Creek	4/27/2010	630
Spring Creek	5/4/2010	39.0
Spring Creek	5/11/2010	124
Spring Creek	5/25/2010	75.0
Spring Creek	6/1/2010	71.0
Spring Creek	6/8/2010	51.0
Spring Creek	6/22/2010	47.0
Spring Creek	6/29/2010	106
Spring Creek	7/20/2010	37.0
Spring Creek	8/3/2010	33.0
Spring Creek	8/25/2010	64.0
Spring Creek	9/7/2010	63.0
Spring Creek	9/28/2010	37.0
Spring Creek	10/12/2010	31.0
Spring Creek	11/9/2010	40.0
Spring Creek	12/7/2010	91.7
Spring Creek	2/8/2011	82.3

Table A.5: Measured flow rates.

Site	Date	Data Value, cfs
Middle Fork	2/23/2010	0.23
Middle Fork	3/2/2010	0.7
Middle Fork	3/15/2010	2.07
Middle Fork	3/29/2010	6.07
Middle Fork	4/5/2010	6.27
Middle Fork	4/13/2010	44.27
Middle Fork	4/19/2010	137.02
Middle Fork	4/27/2010	144.12
Middle Fork	5/4/2010	76.46
Middle Fork	5/11/2010	107.99
Middle Fork	5/25/2010	85.39
Middle Fork	6/1/2010	90.97
Middle Fork	6/8/2010	36.76
Middle Fork	6/22/2010	13.16
Middle Fork	6/29/2010	2.34
Middle Fork	7/20/2010	1.15
Middle Fork	8/3/2010	0.58
Middle Fork	8/25/2010	0.95
Middle Fork	9/7/2010	0.67
Middle Fork	9/28/2010	0.67
Middle Fork	10/12/2010	0.34
Middle Fork	11/9/2010	1.62
Middle Fork	12/7/2010	0.31
Middle Fork	2/8/2011	16.46
NBSF D	2/10/2010	5.45
NBSF D	2/23/2010	4.38
NBSF D	3/2/2010	5.56
NBSF D	3/15/2010	10.79
NBSF D	3/29/2010	11.56
NBSF D	4/5/2010	14.96
NBSF D	4/13/2010	38.25
NBSF D	4/19/2010	61.34
NBSF D	4/27/2010	88.99
NBSF D	5/4/2010	54.35
NBSF D	5/11/2010	52.23
NBSF D	5/25/2010	102.06
NBSF D	6/1/2010	98.39
NBSF D	6/8/2010	66.25
NBSF D	6/22/2010	18.23
NBSF D	6/29/2010	8.27
NBSF D	7/20/2010	5.51
NBSF D	8/3/2010	5.58
NBSF D	8/25/2010	5.32
NBSF D	9/7/2010	3.68
NBSF D	9/28/2010	2.12
NBSF D	10/12/2010	3.41
NBSF D	11/9/2010	1.23

Table A.5: (continued)

Site	Date	Data Value, cfs
NBSF D	12/7/2010	3.56
NBSF D	1/13/2011	8.45
NBSF D	2/8/2011	15.68
NBSF U	2/10/2010	10.55
NBSF U	2/23/2010	15.29
NBSF U	3/2/2010	12.52
NBSF U	3/15/2010	14.93
NBSF U	3/29/2010	16.09
NBSF U	4/5/2010	21.49
NBSF U	4/13/2010	43.13
NBSF U	4/19/2010	57.27
NBSF U	4/27/2010	101.42
NBSF U	5/4/2010	48.99
NBSF U	5/11/2010	48.29
NBSF U	5/25/2010	106.54
NBSF U	6/1/2010	119.79
NBSF U	6/8/2010	58.41
NBSF U	6/22/2010	14.9
NBSF U	6/30/2010	0
NBSF U	11/8/2010	0
NBSF U	11/9/2010	2.76
NBSF U	12/7/2010	9.81
NBSF U	1/13/2011	ICE
North Fork	2/23/2010	1.61
North Fork	3/2/2010	2.47
North Fork	3/15/2010	6.9
North Fork	3/29/2010	32.98
North Fork	4/5/2010	43.13
North Fork	4/13/2010	127.17
North Fork	4/19/2010	188.09
North Fork	4/27/2010	154.75
North Fork	5/4/2010	97.86
North Fork	5/11/2010	134.73
North Fork	5/25/2010	68.16
North Fork	6/1/2010	111.38
North Fork	6/8/2010	146.66
North Fork	6/22/2010	49.33
North Fork	6/29/2010	11.9
North Fork	7/20/2010	2.1
North Fork	8/3/2010	3.06
North Fork	8/25/2010	0.92
North Fork	9/7/2010	0.92
North Fork	9/28/2010	0.46
North Fork	10/12/2010	0.23
North Fork	11/9/2010	0
North Fork	12/7/2010	3.03
North Fork	1/13/2011	20.1

Table A.5: (continued)

Site	Date	Data Value, cfs
North Fork	2/8/2011	32.38
SBSF D	2/10/2010	13.99
SBSF D	2/18/2010	14.82
SBSF D	2/23/2010	10.39
SBSF D	3/2/2010	12.17
SBSF D	3/15/2010	21.48
SBSF D	3/29/2010	20.46
SBSF D	4/5/2010	30.79
SBSF D	4/13/2010	66.82
SBSF D	4/19/2010	88.85
SBSF D	4/27/2010	123.5
SBSF D	5/4/2010	75.5
SBSF D	5/11/2010	78.19
SBSF D	5/25/2010	125.72
SBSF D	6/1/2010	124.63
SBSF D	6/8/2010	77.76
SBSF D	6/22/2010	34.03
SBSF D	6/29/2010	20.56
SBSF D	7/20/2010	14.48
SBSF D	8/3/2010	8.54
SBSF D	8/25/2010	5.73
SBSF D	9/7/2010	4.18
SBSF D	9/28/2010	2.95
SBSF D	10/12/2010	2.93
SBSF D	11/9/2010	1.84
SBSF D	1/13/2011	15
SBSF D	2/8/2011	27.19
SBSF U	2/10/2010	11.12
SBSF U	2/23/2010	9.42
SBSF U	3/2/2010	10.21
SBSF U	3/15/2010	12.23
SBSF U	3/29/2010	11.81
SBSF U	4/5/2010	16.43
SBSF U	4/13/2010	33.97
SBSF U	4/19/2010	70.03
SBSF U	4/27/2010	86.27
SBSF U	5/4/2010	60.21
SBSF U	5/11/2010	40.52
SBSF U	5/25/2010	85.78
SBSF U	6/1/2010	99.3
SBSF U	6/8/2010	75.21
SBSF U	6/22/2010	11.83
SBSF U	6/30/2010	0
SBSF U	11/8/2010	0
SBSF U	11/9/2010	0
SBSF U	12/7/2010	7.04
SBSF U	1/13/2011	ICE

Table A.5: (continued)

Site	Date	Data Value, cfs
Spring Creek	3/15/2010	12.3
Spring Creek	3/29/2010	6.24
Spring Creek	4/5/2010	16.46
Spring Creek	4/13/2010	14.51
Spring Creek	4/19/2010	10.22
Spring Creek	4/27/2010	11.59
Spring Creek	5/4/2010	6.81
Spring Creek	5/11/2010	9.56
Spring Creek	5/25/2010	11.94
Spring Creek	6/1/2010	17.27
Spring Creek	6/8/2010	13.02
Spring Creek	6/22/2010	15.67
Spring Creek	6/29/2010	12.66
Spring Creek	7/20/2010	14.89
Spring Creek	8/3/2010	11.24
Spring Creek	8/25/2010	11.59
Spring Creek	9/7/2010	14.51
Spring Creek	9/28/2010	11.94
Spring Creek	11/9/2010	5.43
Spring Creek	12/7/2010	7.68
Spring Creek	2/8/2011	8.6

APPENDIX B

DISTRIBUTIONS

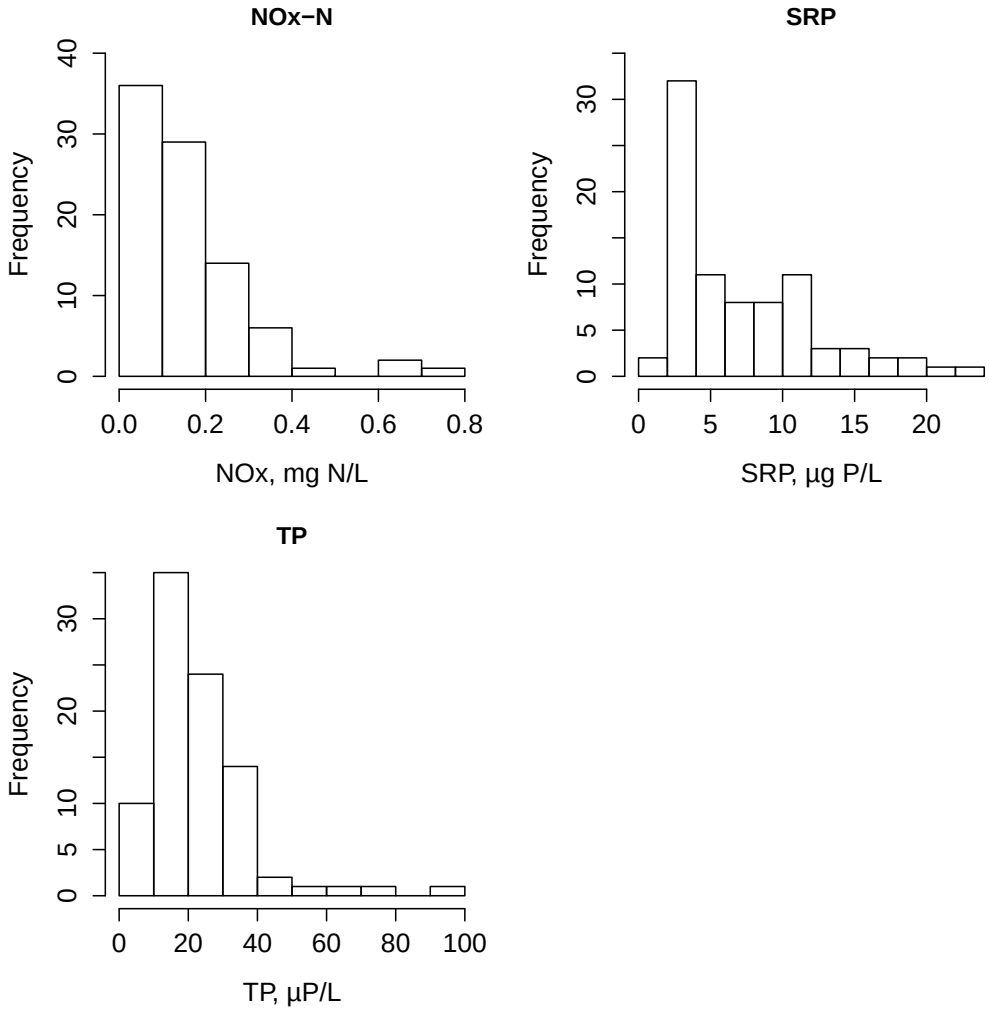

Fig. B.1: Histograms of grab samples at all South Fork sites.

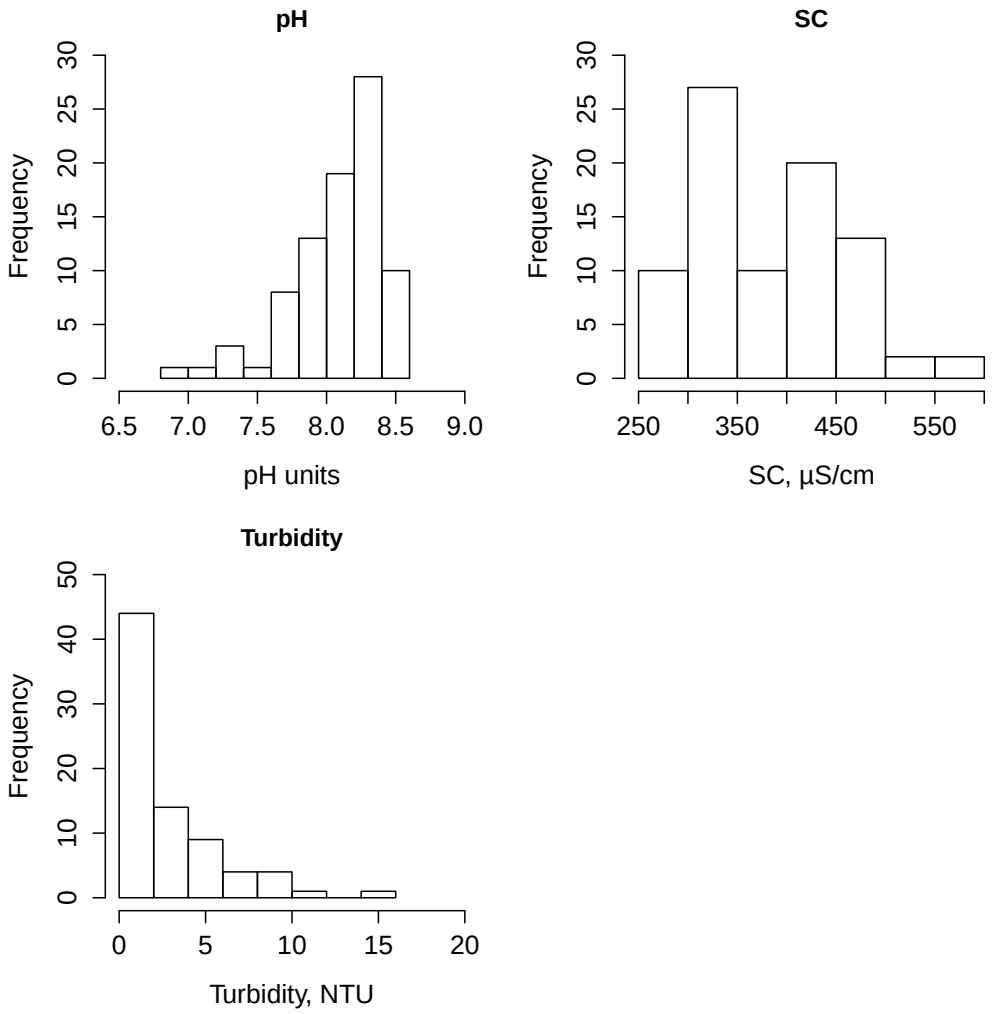

Fig. B.2: Histograms of laboratory measurements at all South Fork sites.

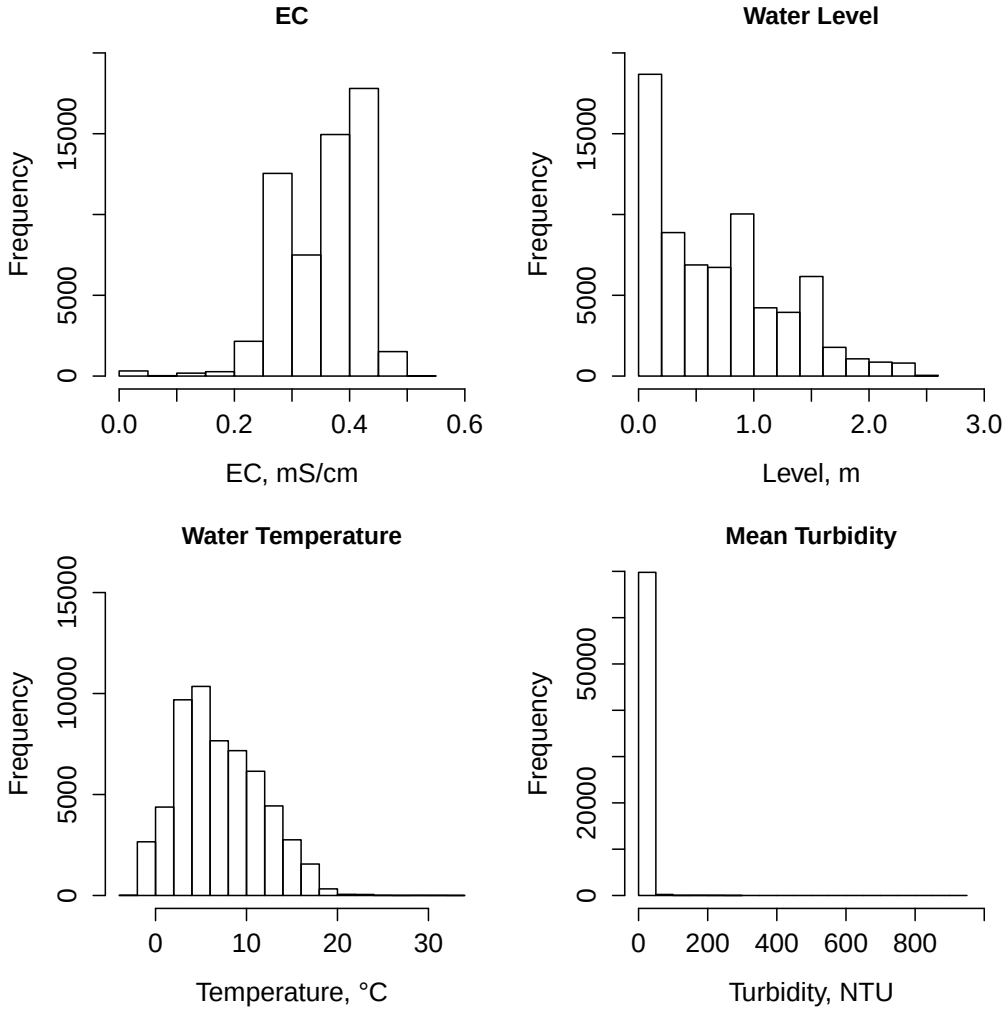

Fig. B.3: Histograms of high-frequency measurements at all South Fork sites after quality control efforts using ODM Tools.

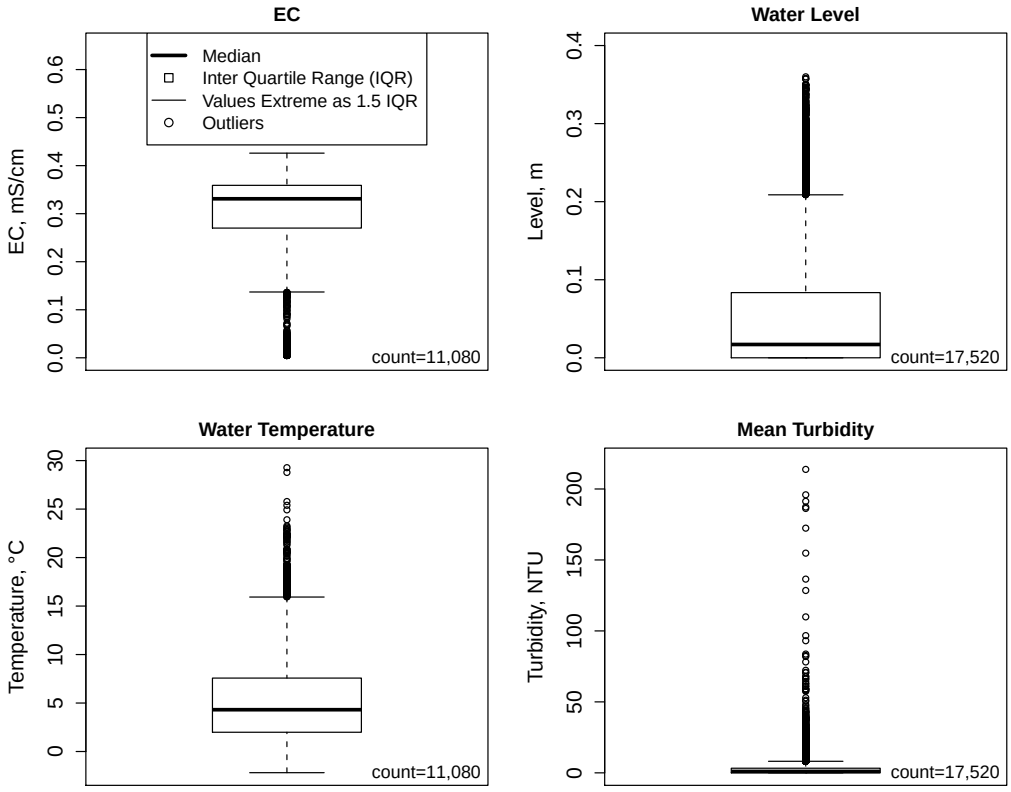

Fig. B.4: Box plots of high-frequency measurements at NBSF_U.

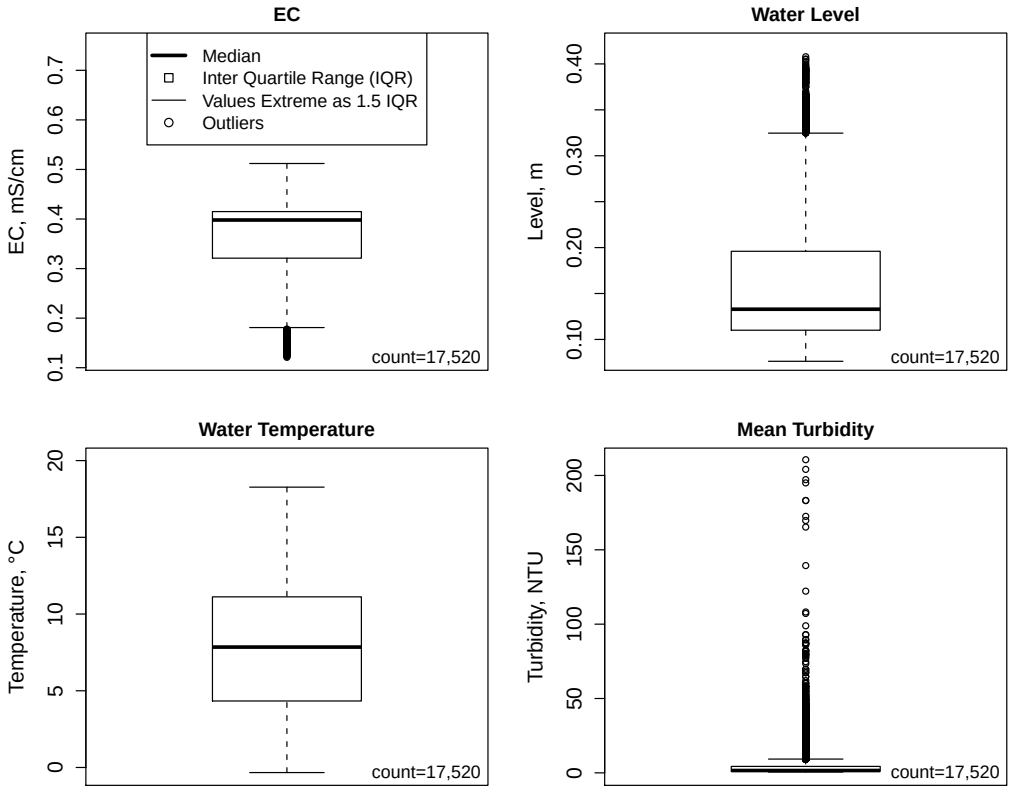

Fig. B.5: Box plots of high-frequency measurements at NBSF_D.

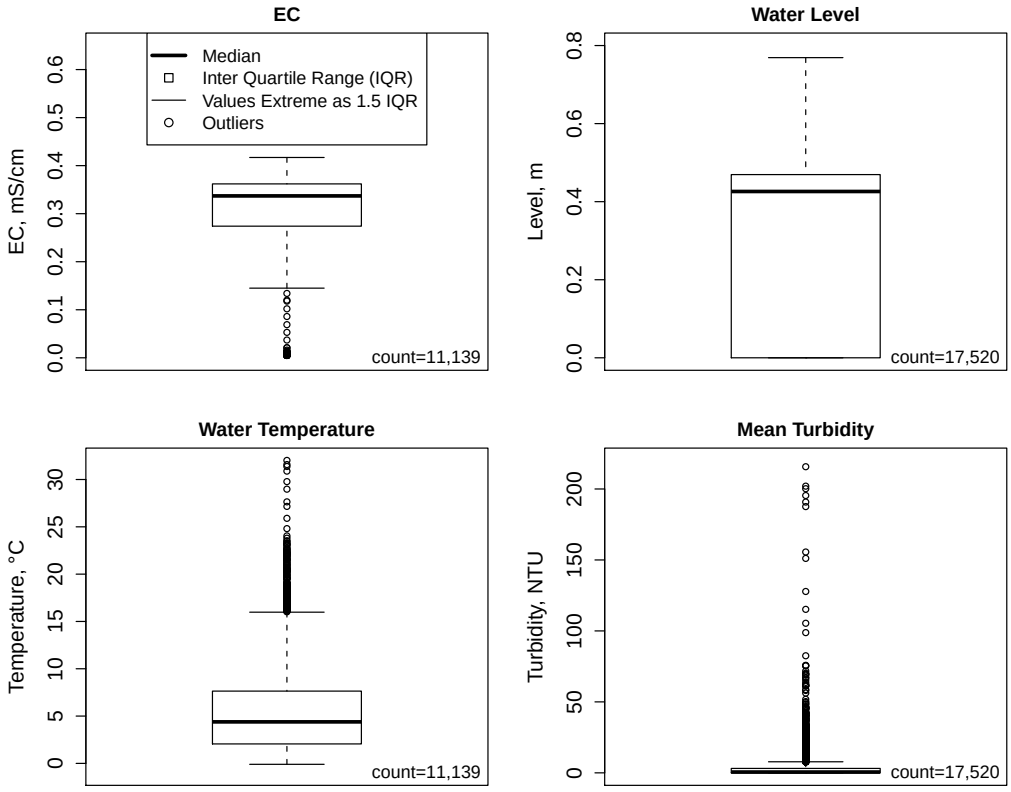

Fig. B.6: Box plots of high-frequency measurements at SBSF_U.

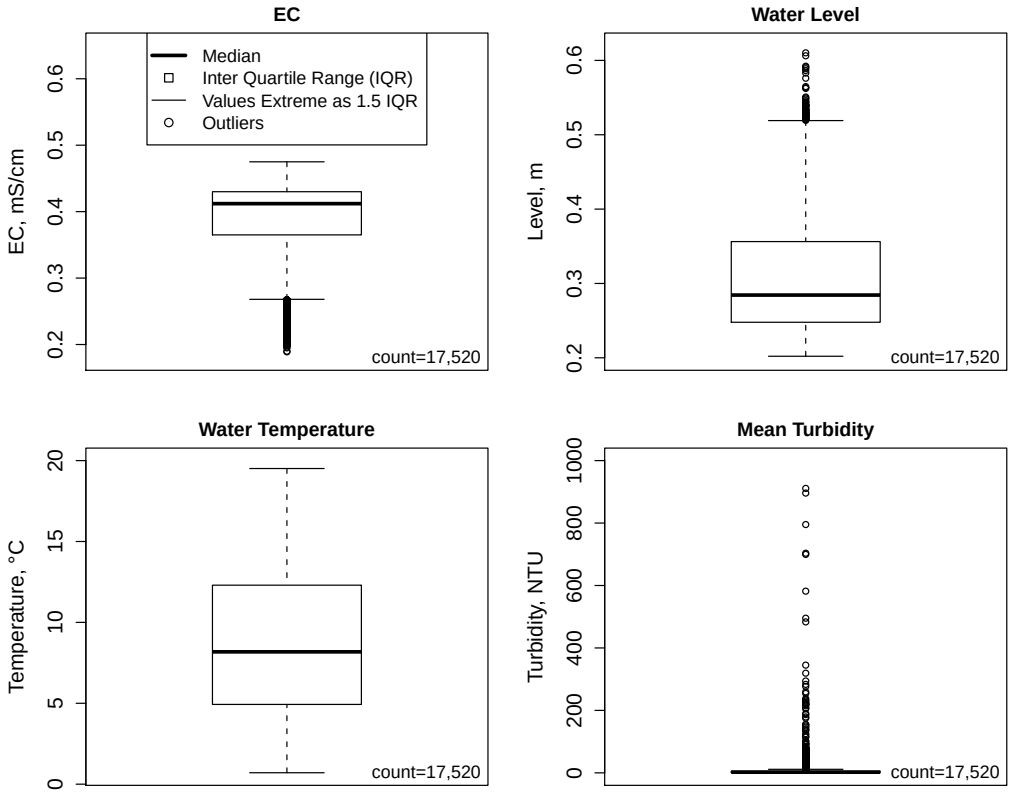

Fig. B.7: Box plots of high-frequency measurements at SBSF_D.

APPENDIX C

REGRESSION STATISTICS

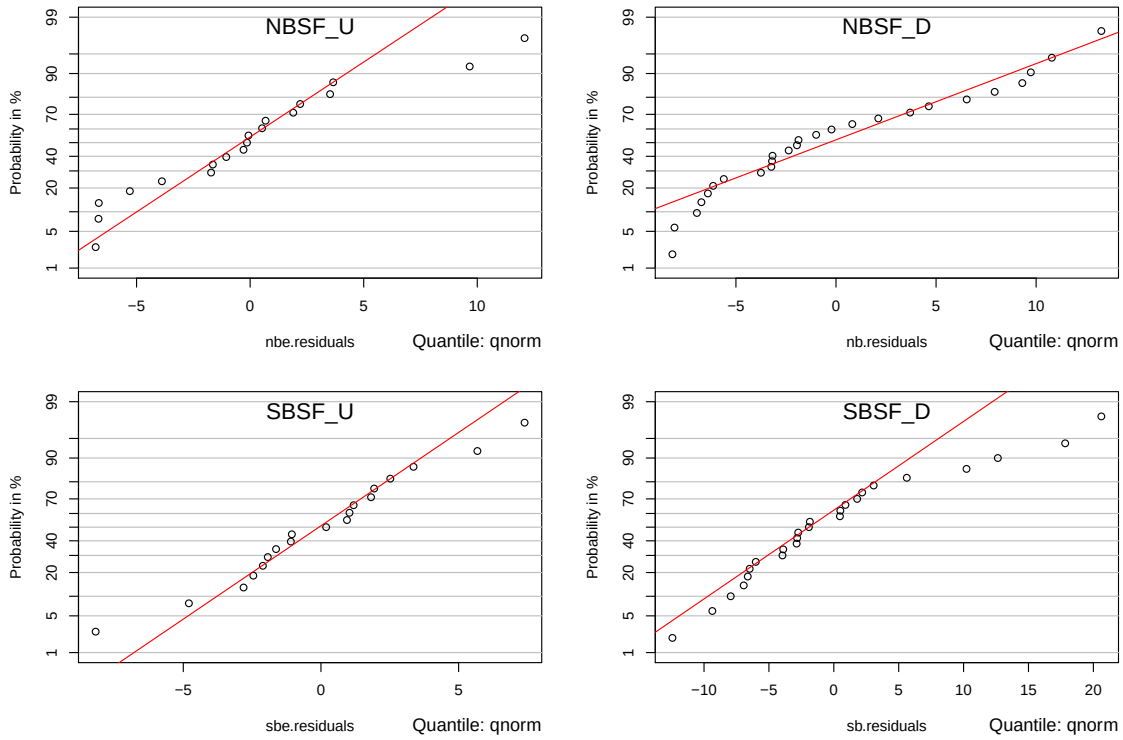

Fig. C.1: Residuals' quantiles from linear regressions predicting TP-P given high-frequency turbidity. The line designates a normal distribution.

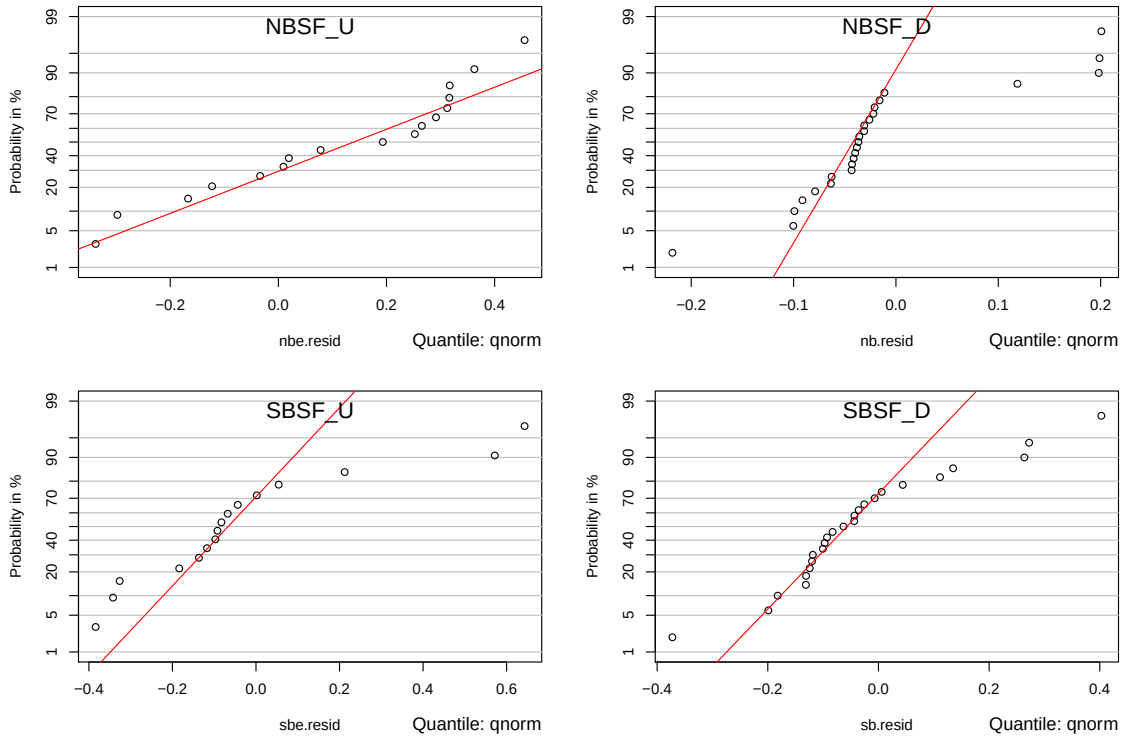

Fig. C.2: Residuals' quantiles from power regressions predicting flow given high-frequency water level. The line designates a normal distribution.

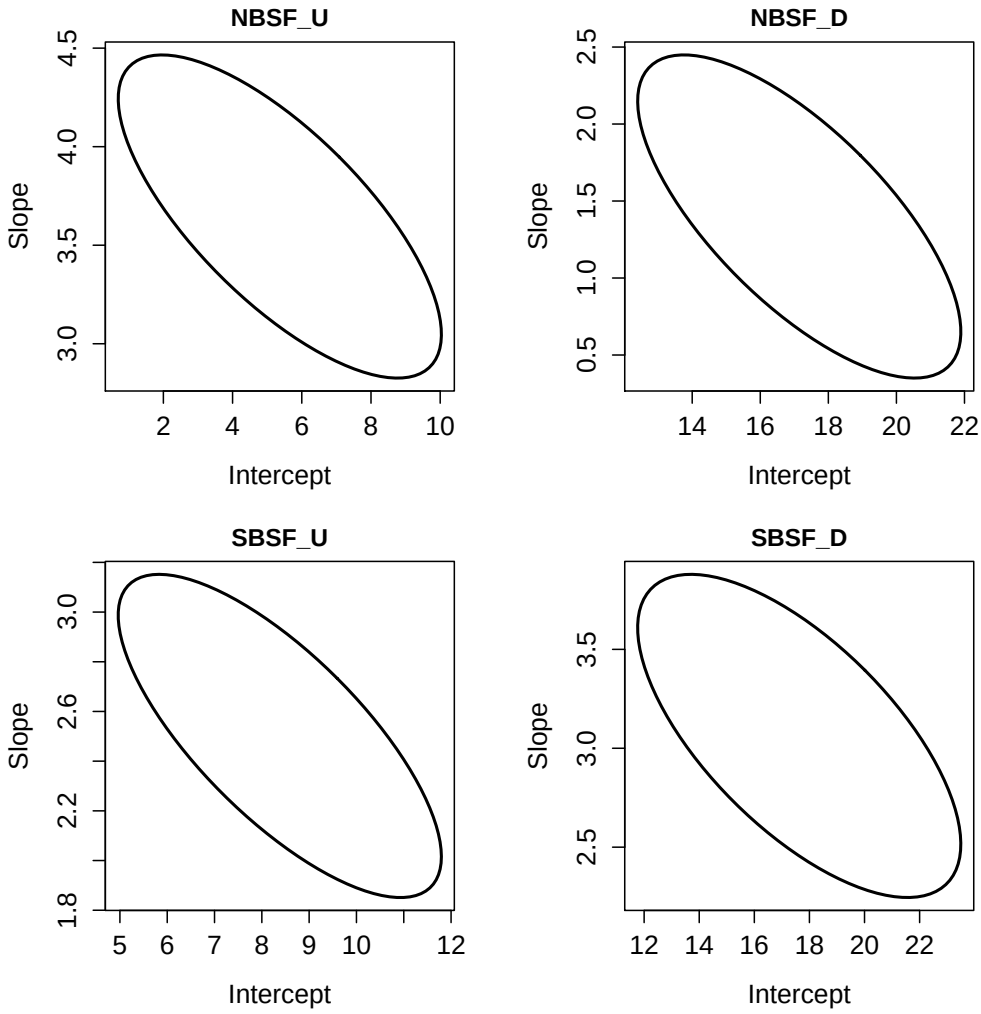

Fig. C.3: Joint confidence regions of the linear regression coefficients from turbidity-TP relationships.

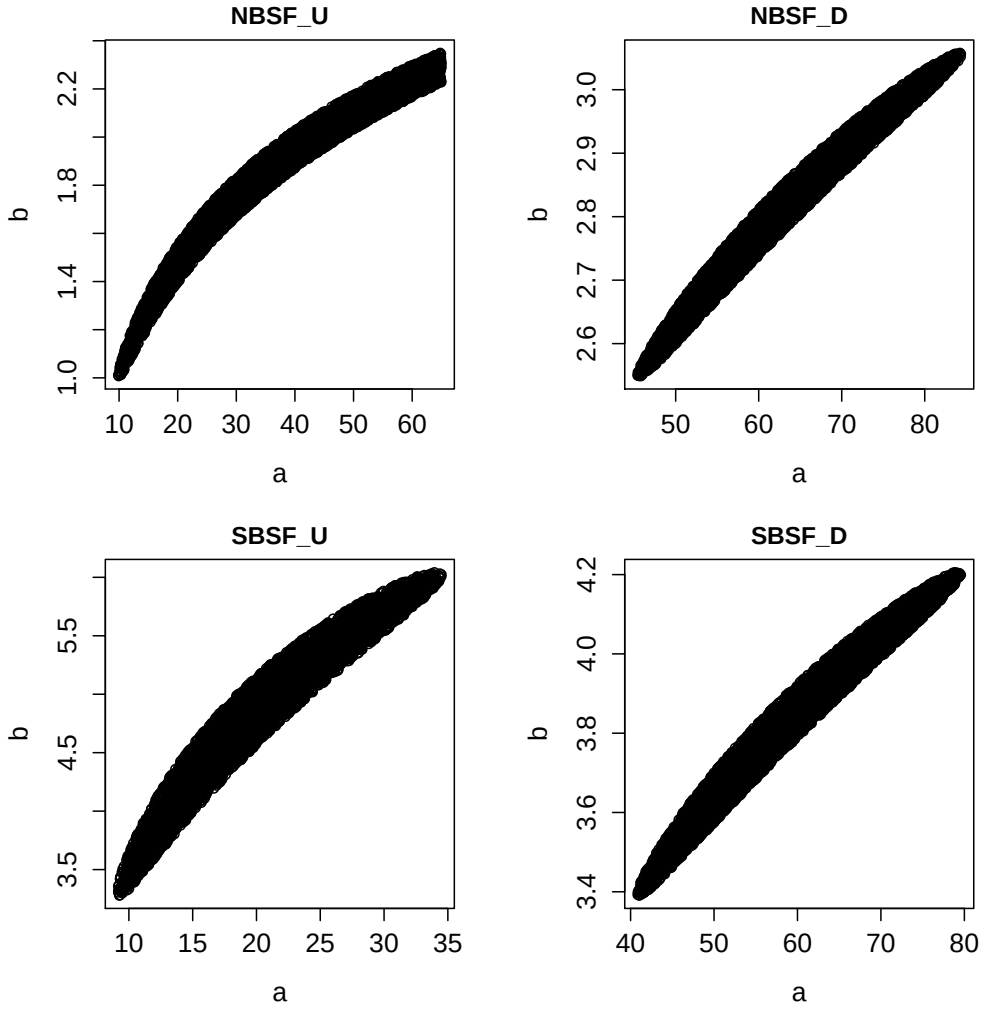

Fig. C.4: Joint confidence regions of the nonlinear regression coefficients from stage-discharge relationships.

APPENDIX D

HIGH-FREQUENCY MEASUREMENT COMPARISONS

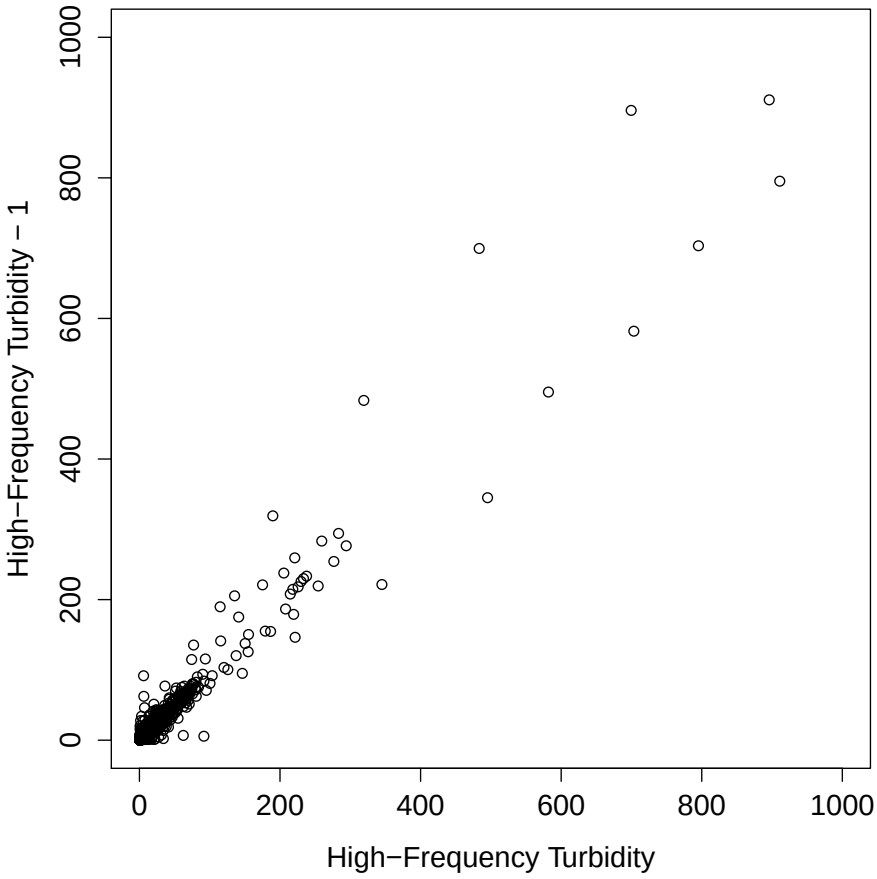

Fig. D.1: High-frequency mean turbidity values against their previous measurement at SBSF_D.

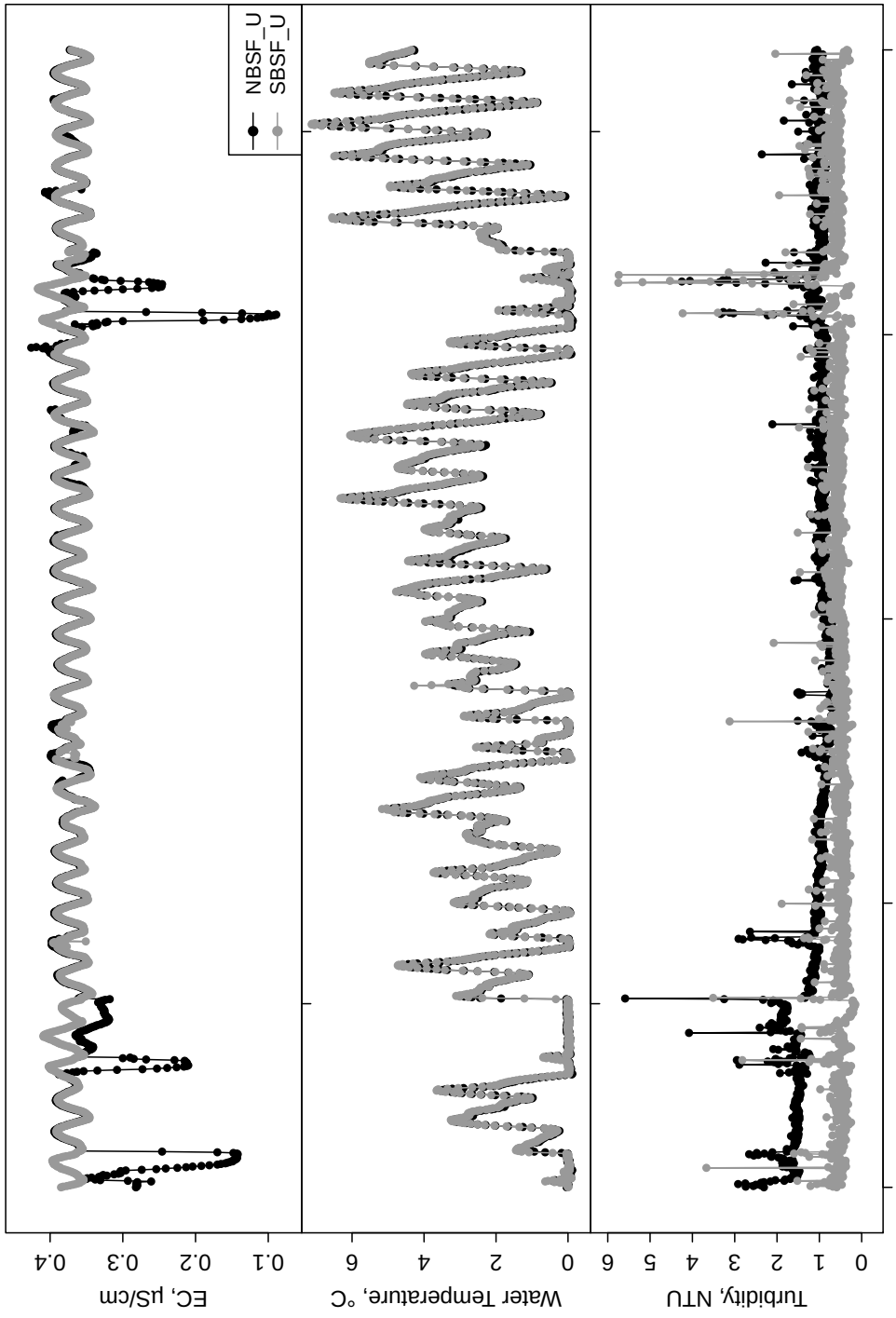

Fig. D.2: Comparison of high-frequency measurements at the upstream sites from 25 January to 03 March 2010.

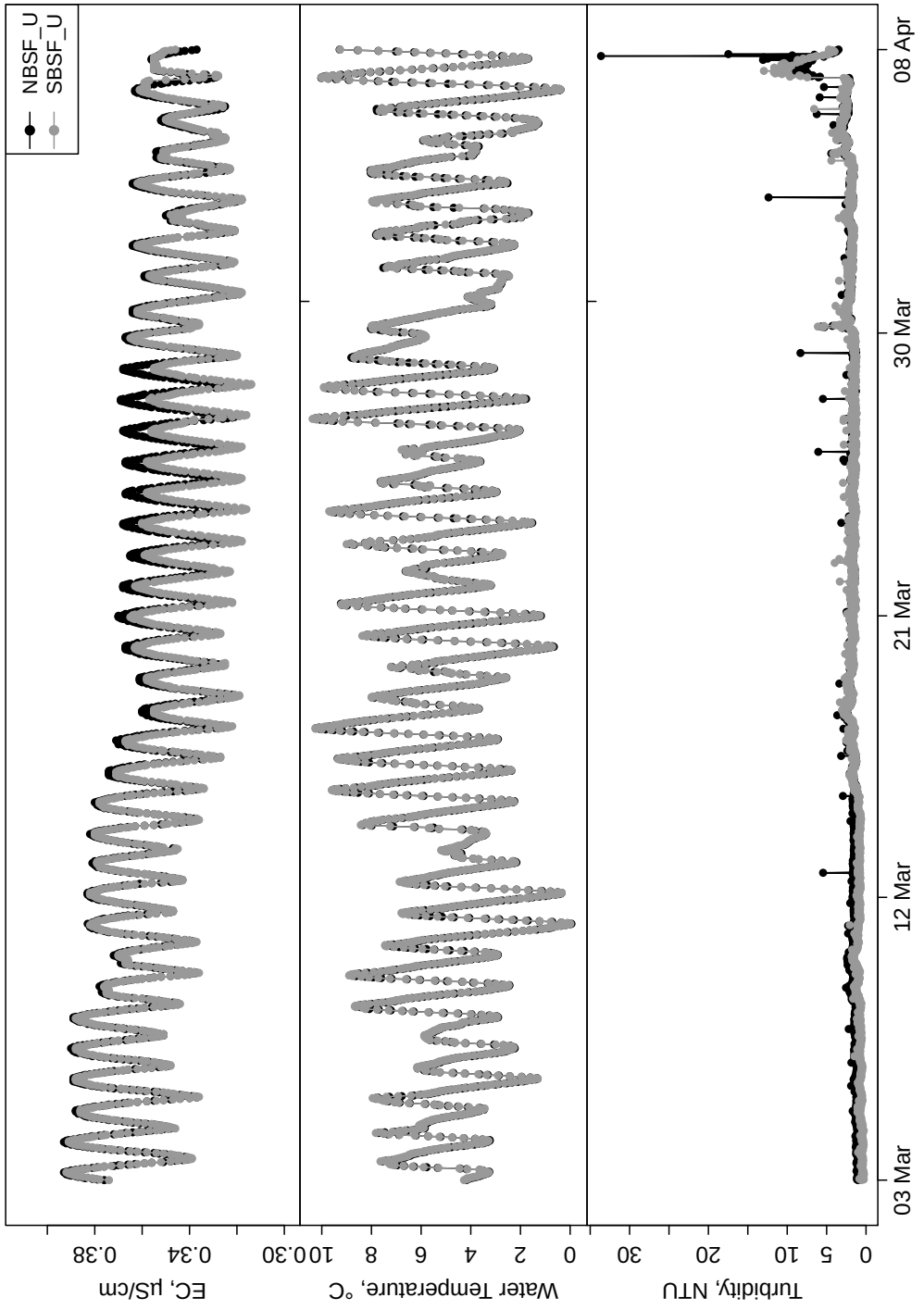

Fig. D.3: Comparison of high-frequency measurements at the upstream sites from 03 March to 08 April 2010.

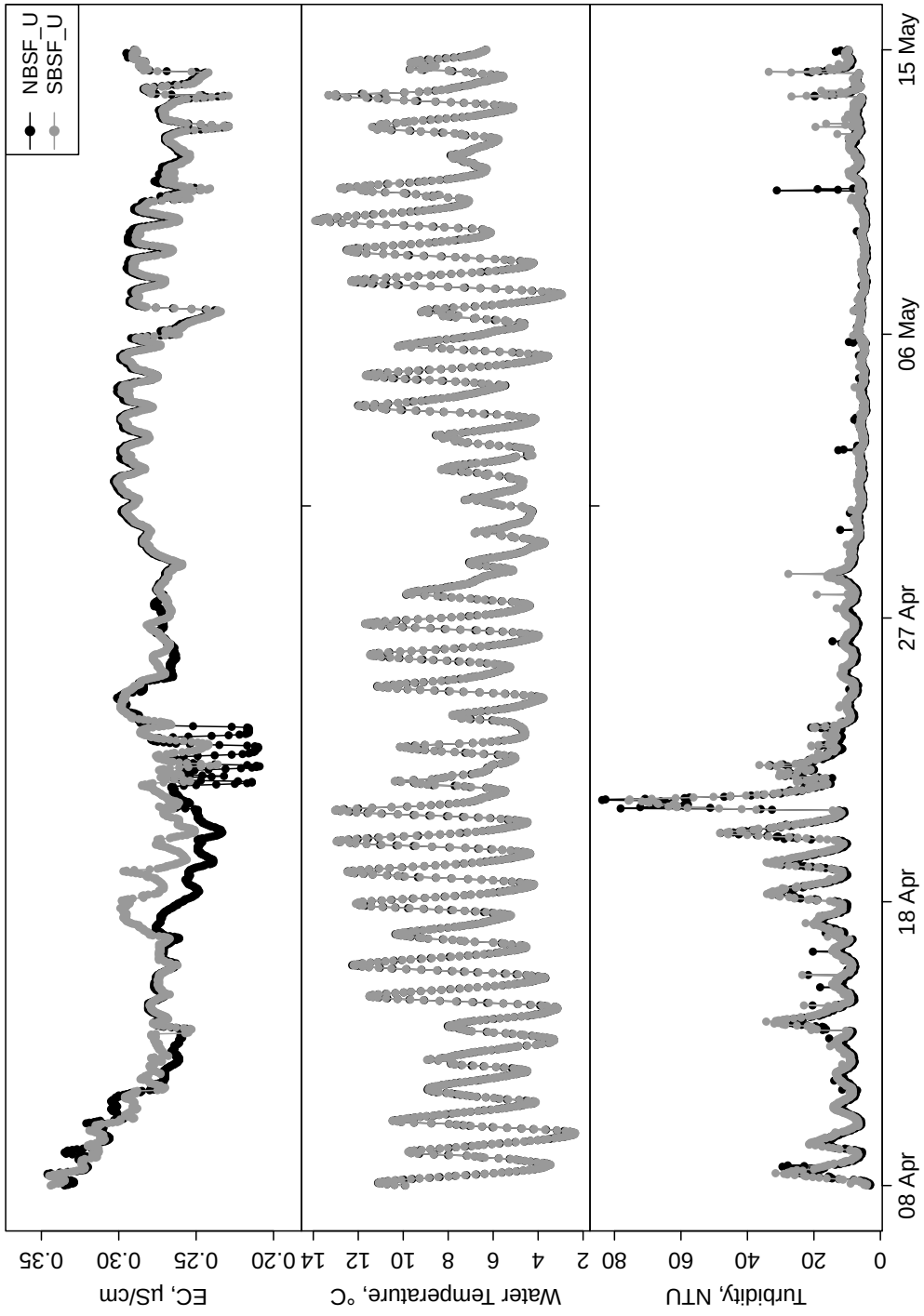

Fig. D.4: Comparison of high-frequency measurements at the upstream sites from 08 April to 15 May 2010.

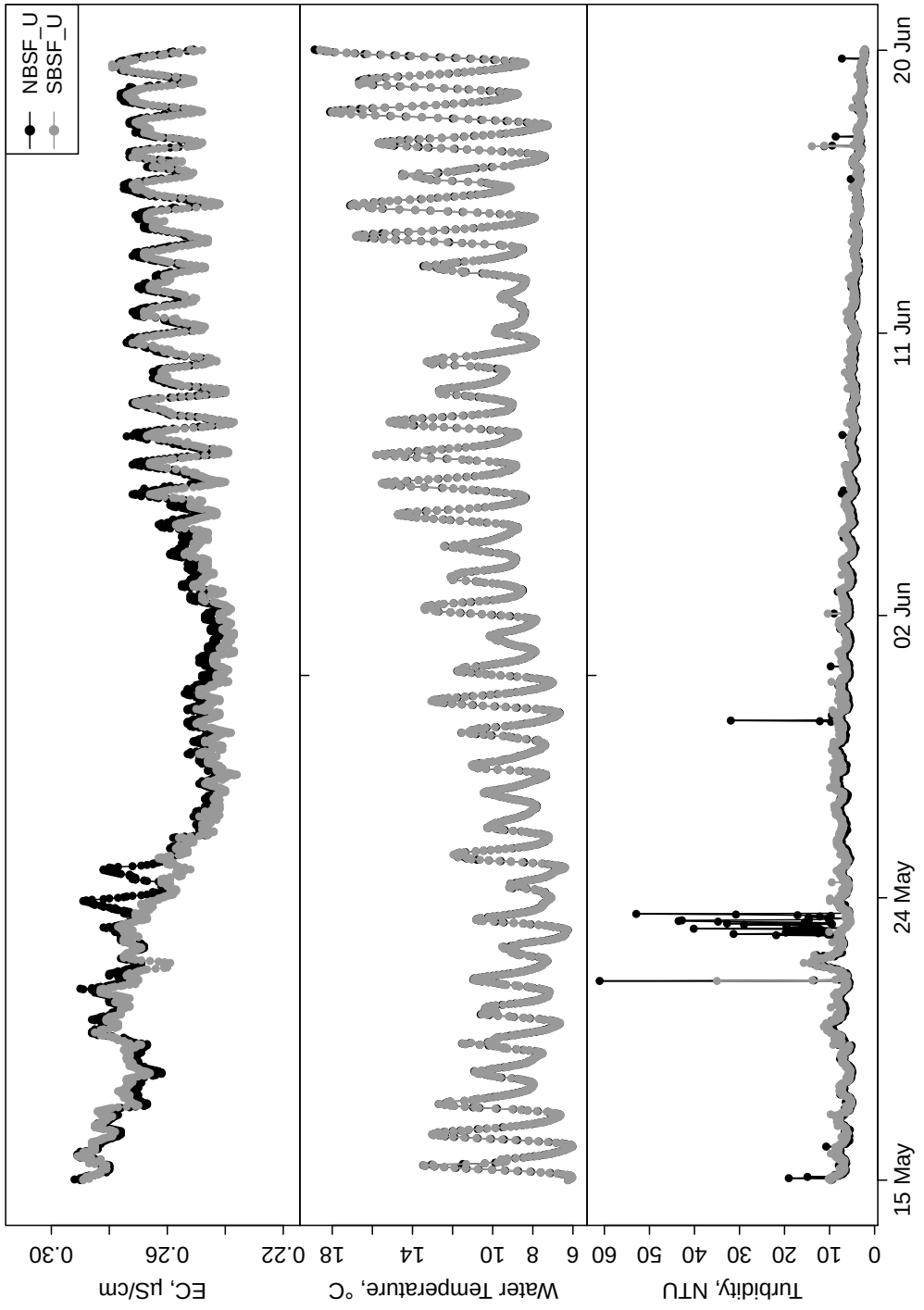

Fig. D.5: Comparison of high-frequency measurements at the upstream sites from 15 May to 20 June 2010.

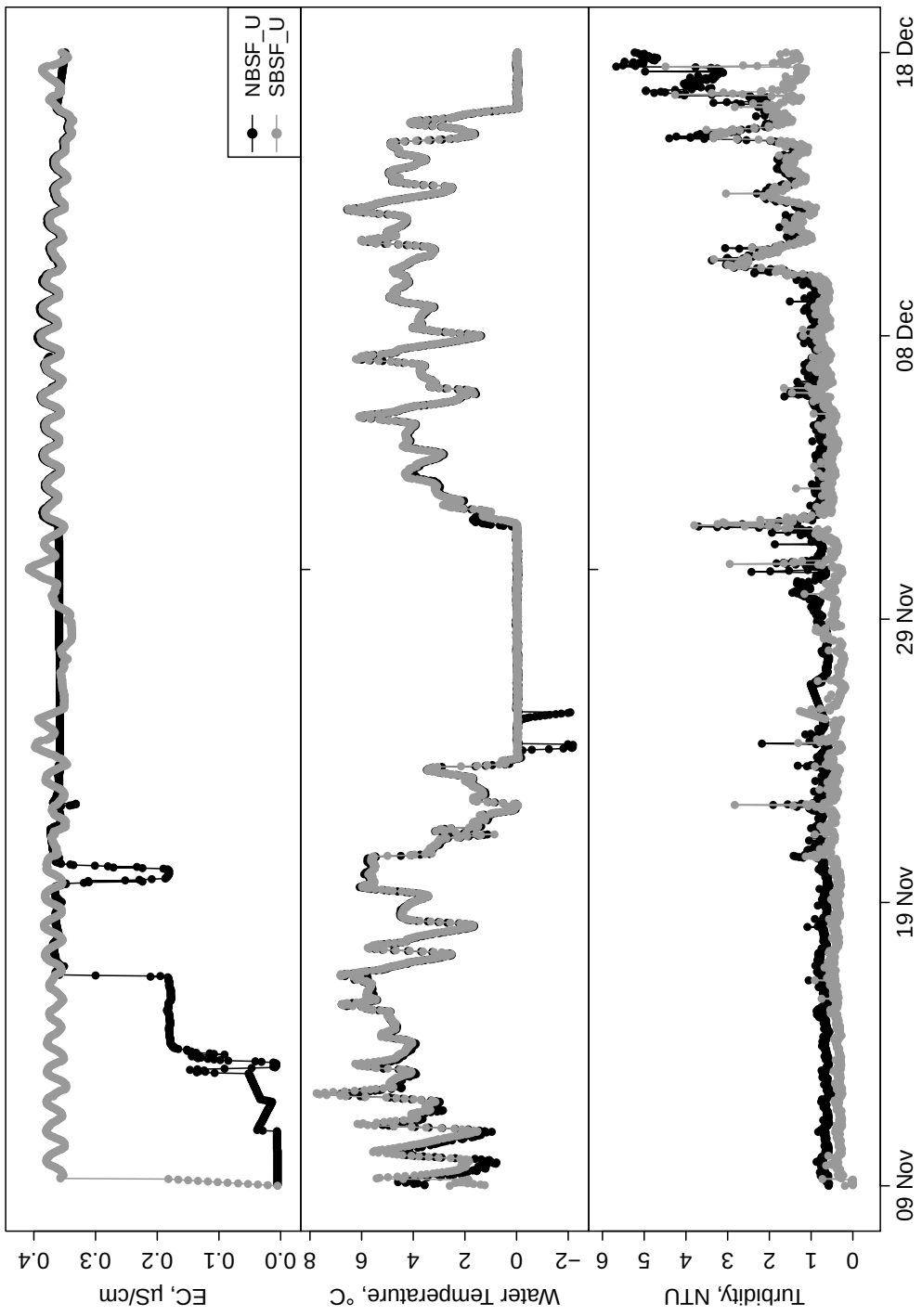

Fig. D.6: Comparison of high-frequency measurements at the upstream sites from 09 November to 18 December 2010.

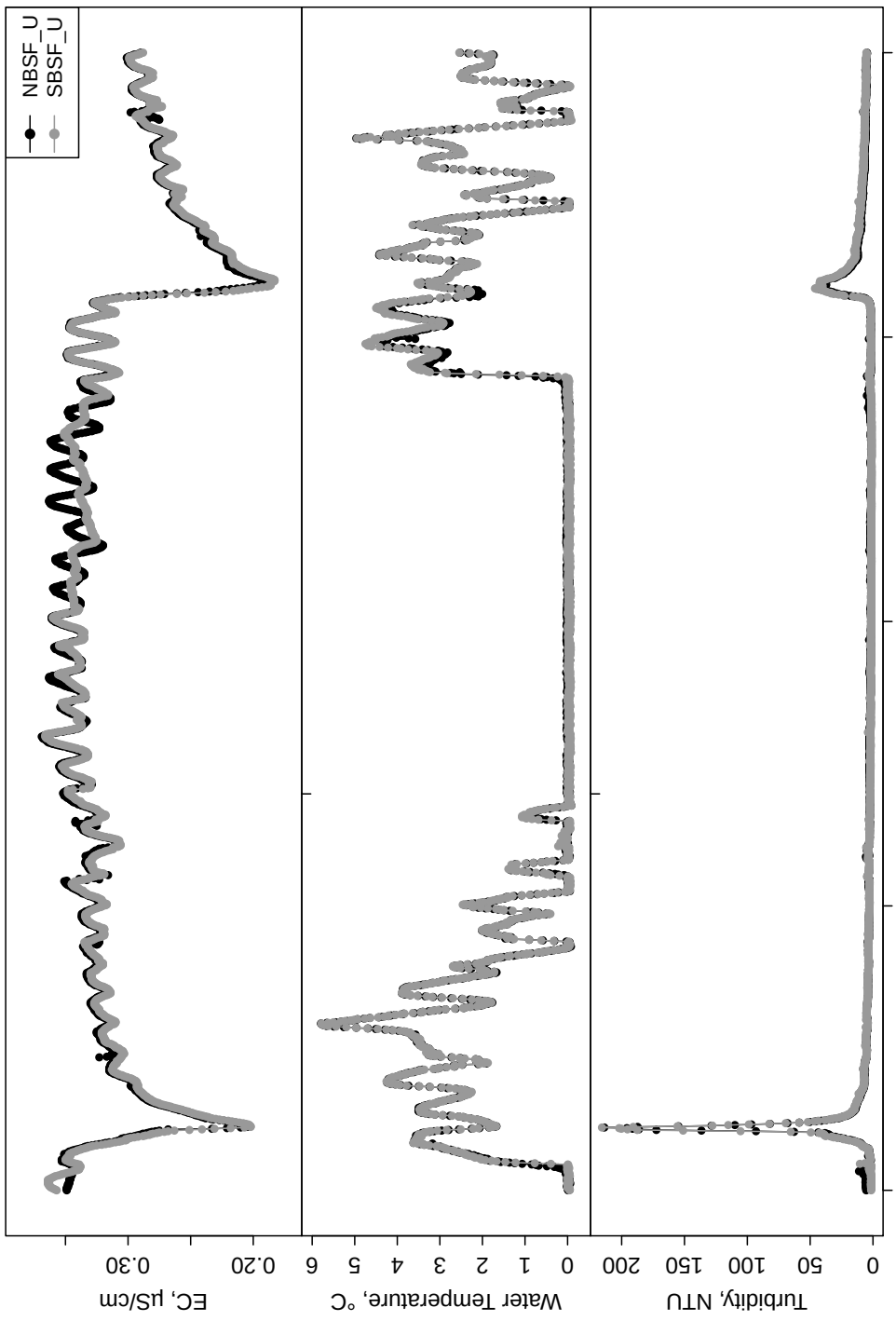

Fig. D.7: Comparison of high-frequency measurements at the upstream sites from 18 December 2010 to 25 January 2011.

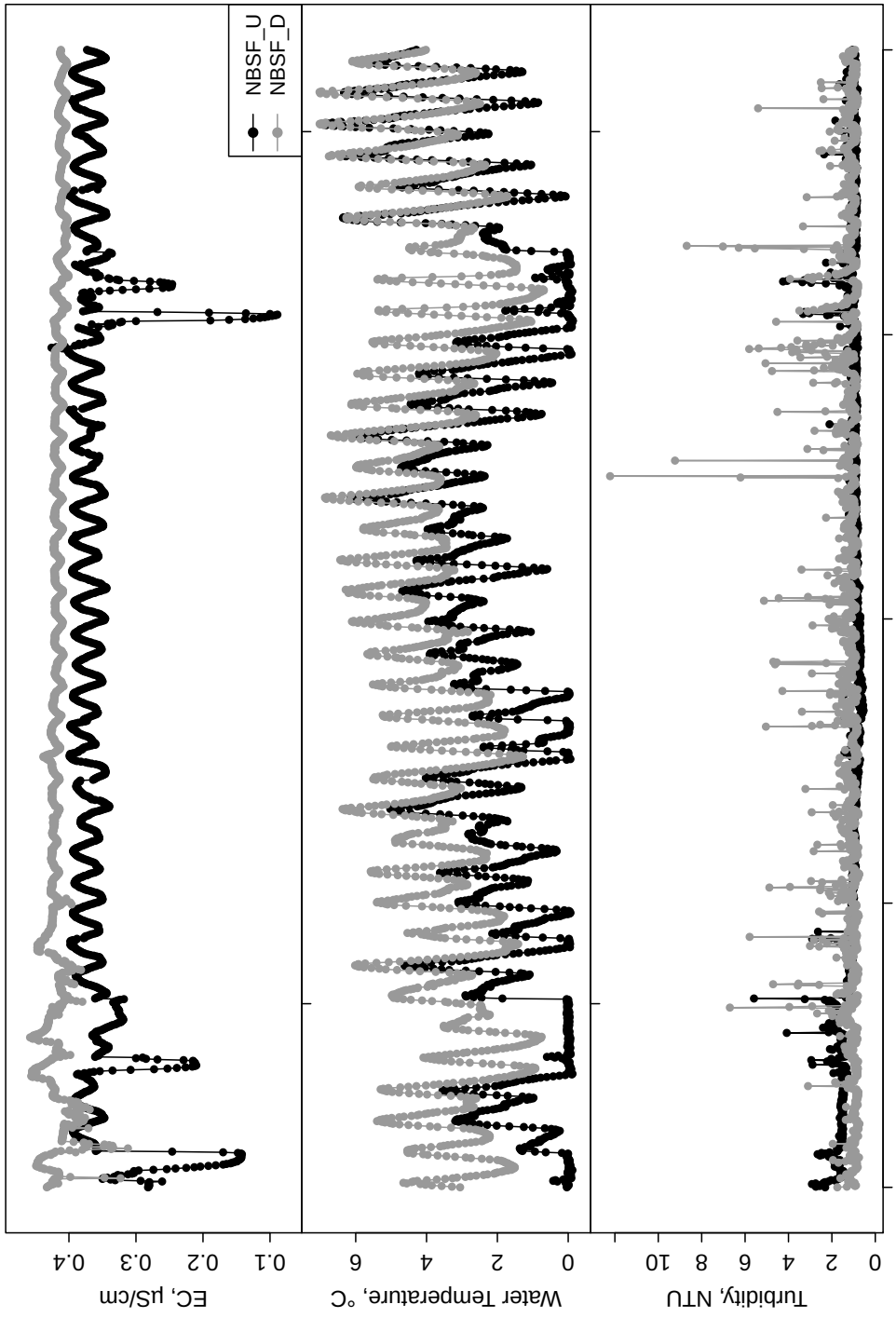

Fig. D.8: Comparison of high-frequency measurements at the North Branch sites from 25 January to 03 March 2010.

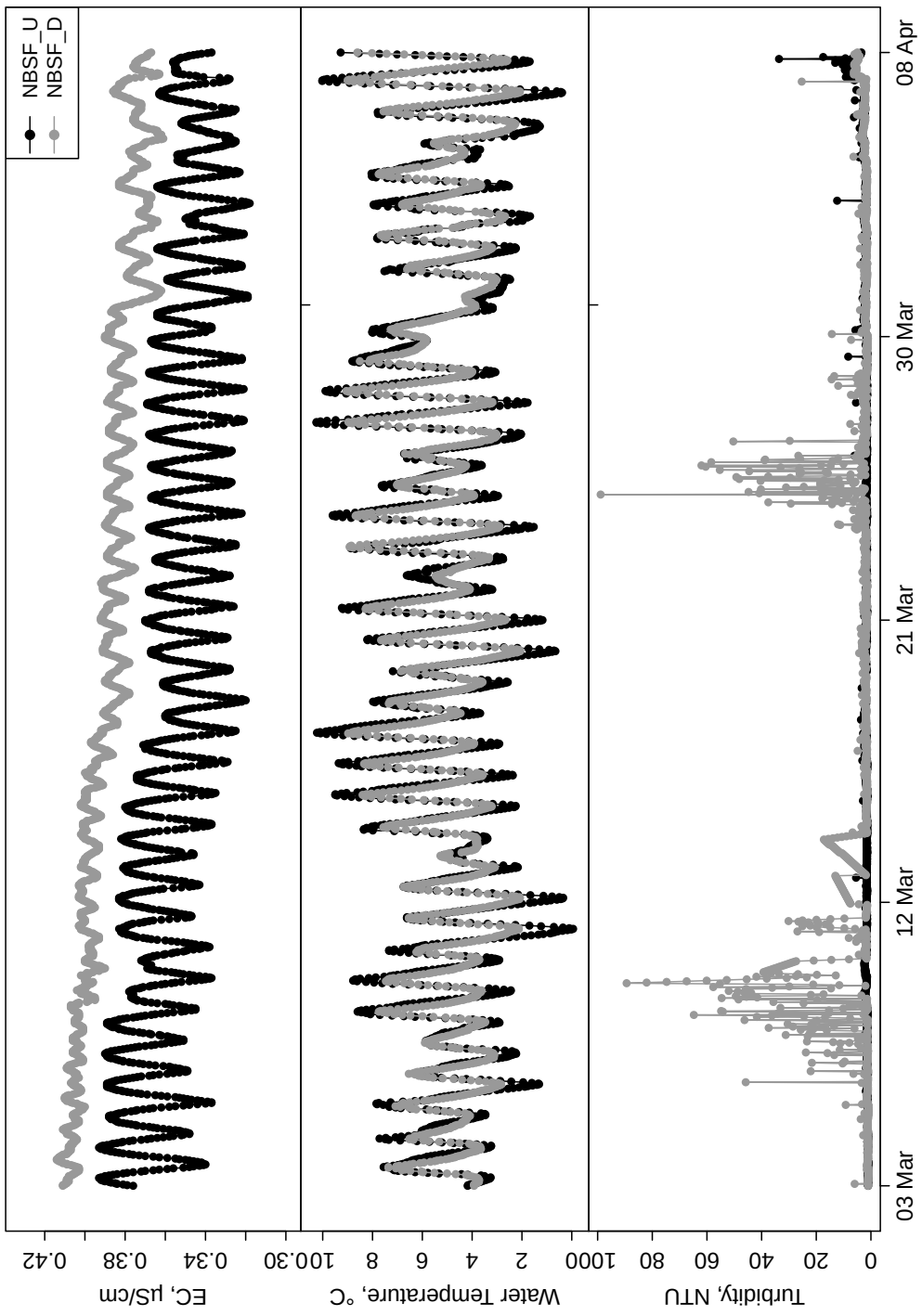

Fig. D.9: Comparison of high-frequency measurements at the North Branch sites from 03 March to 08 April 2010.

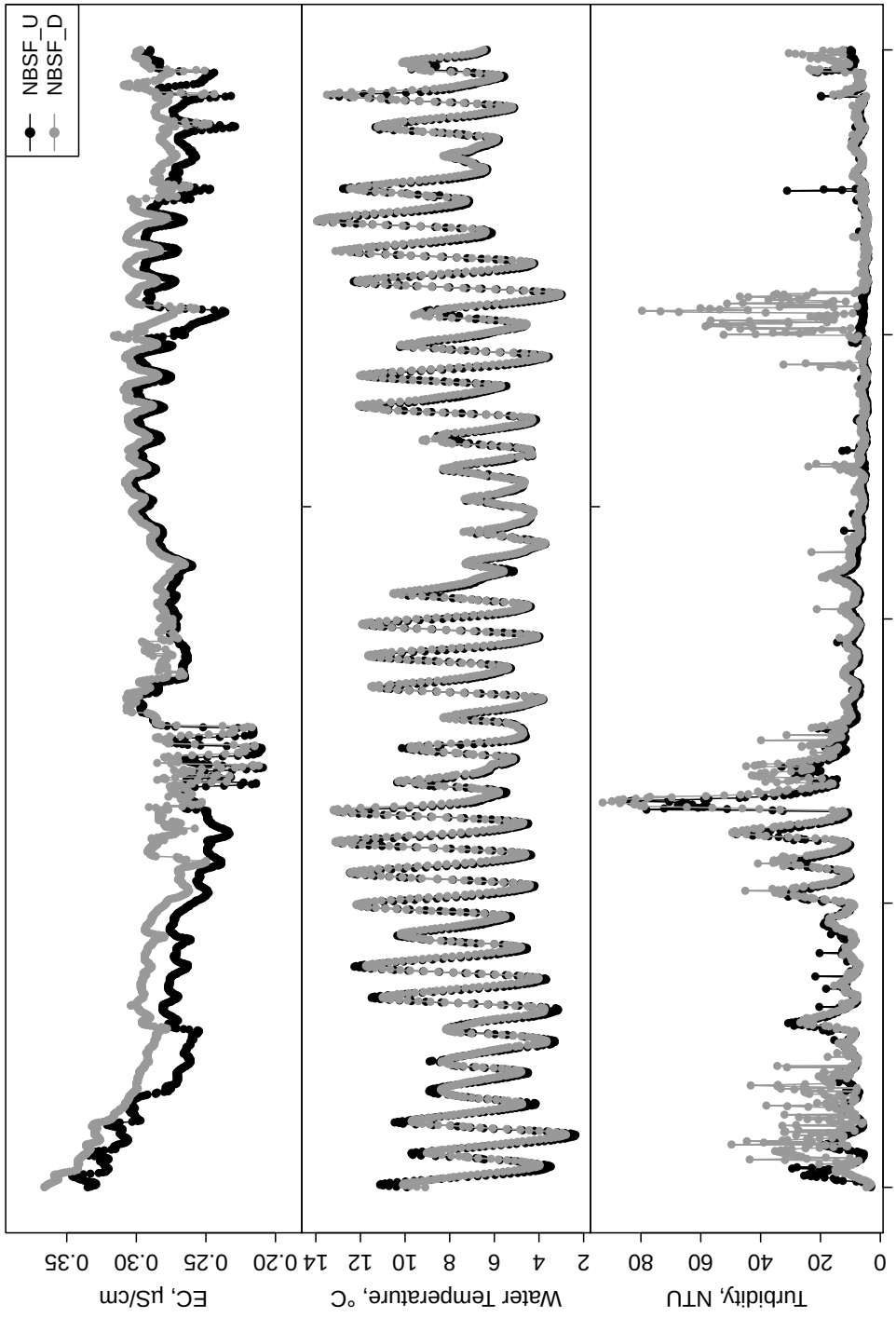

Fig. D.10: Comparison of high-frequency measurements at the North Branch sites from 08 April to 15 May 2010.

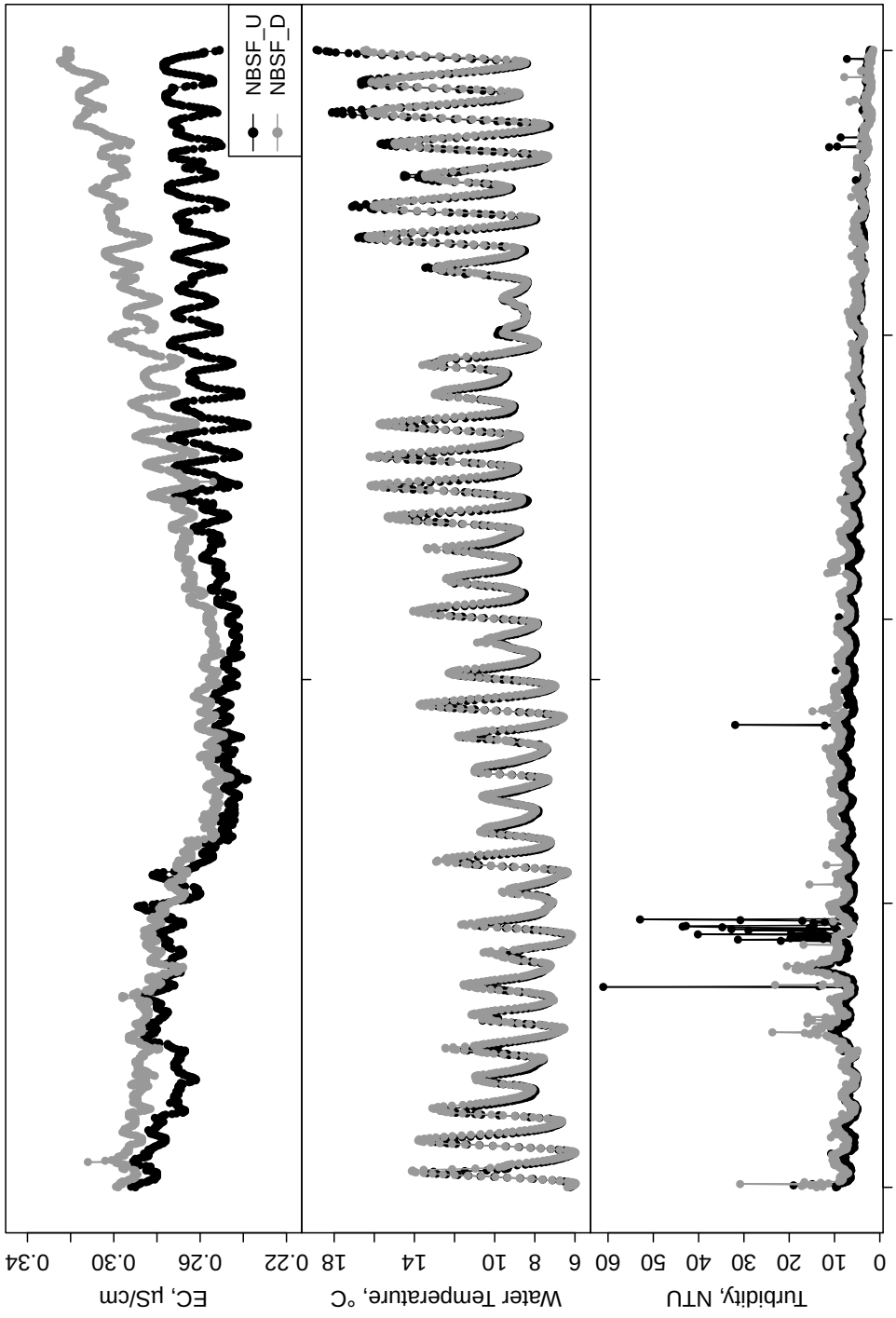

Fig. D.11: Comparison of high-frequency measurements at the North Branch sites from 15 May to 20 June 2010.

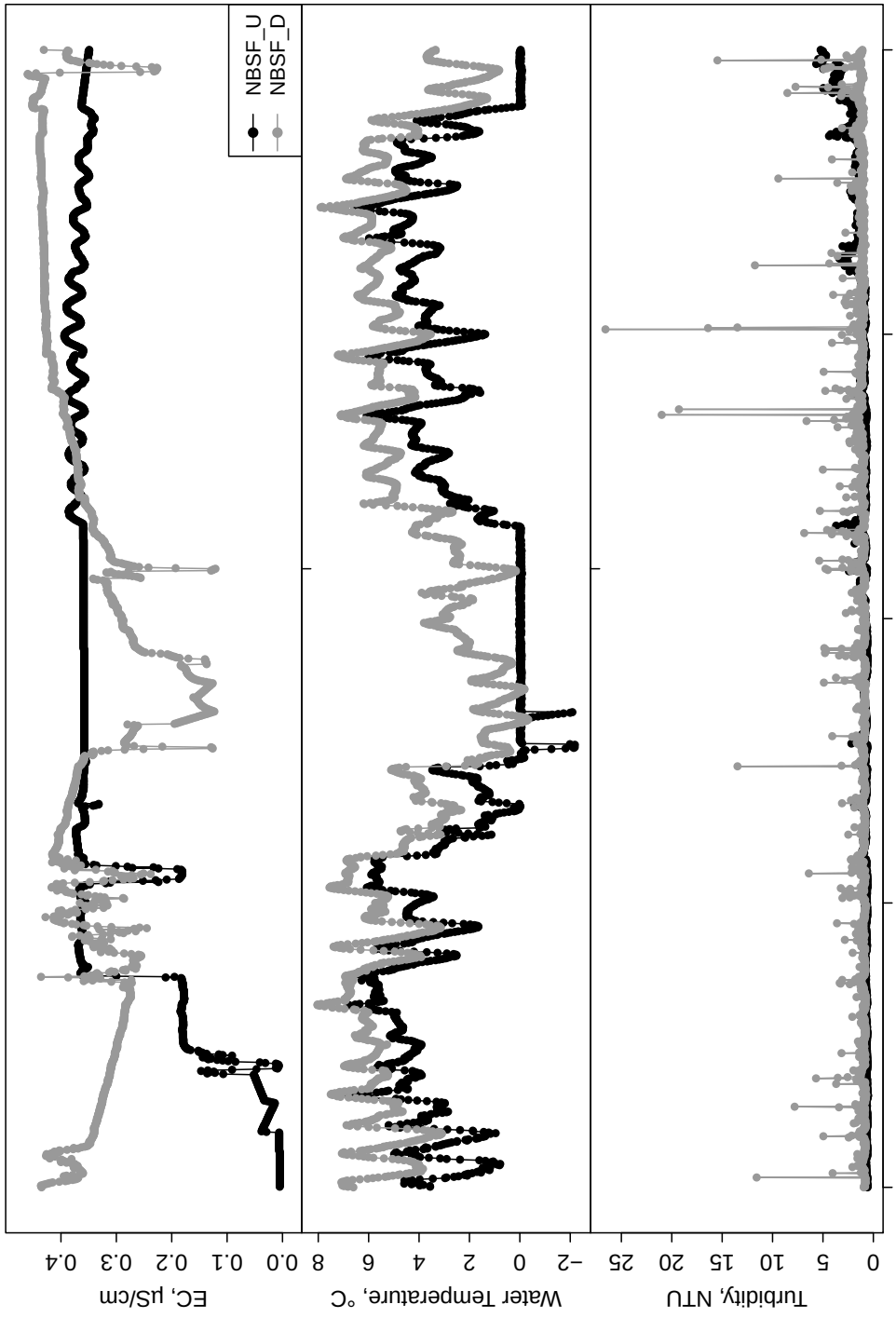

Fig. D.12: Comparison of high-frequency measurements at the North Branch sites from 09 November to 18 December 2010.

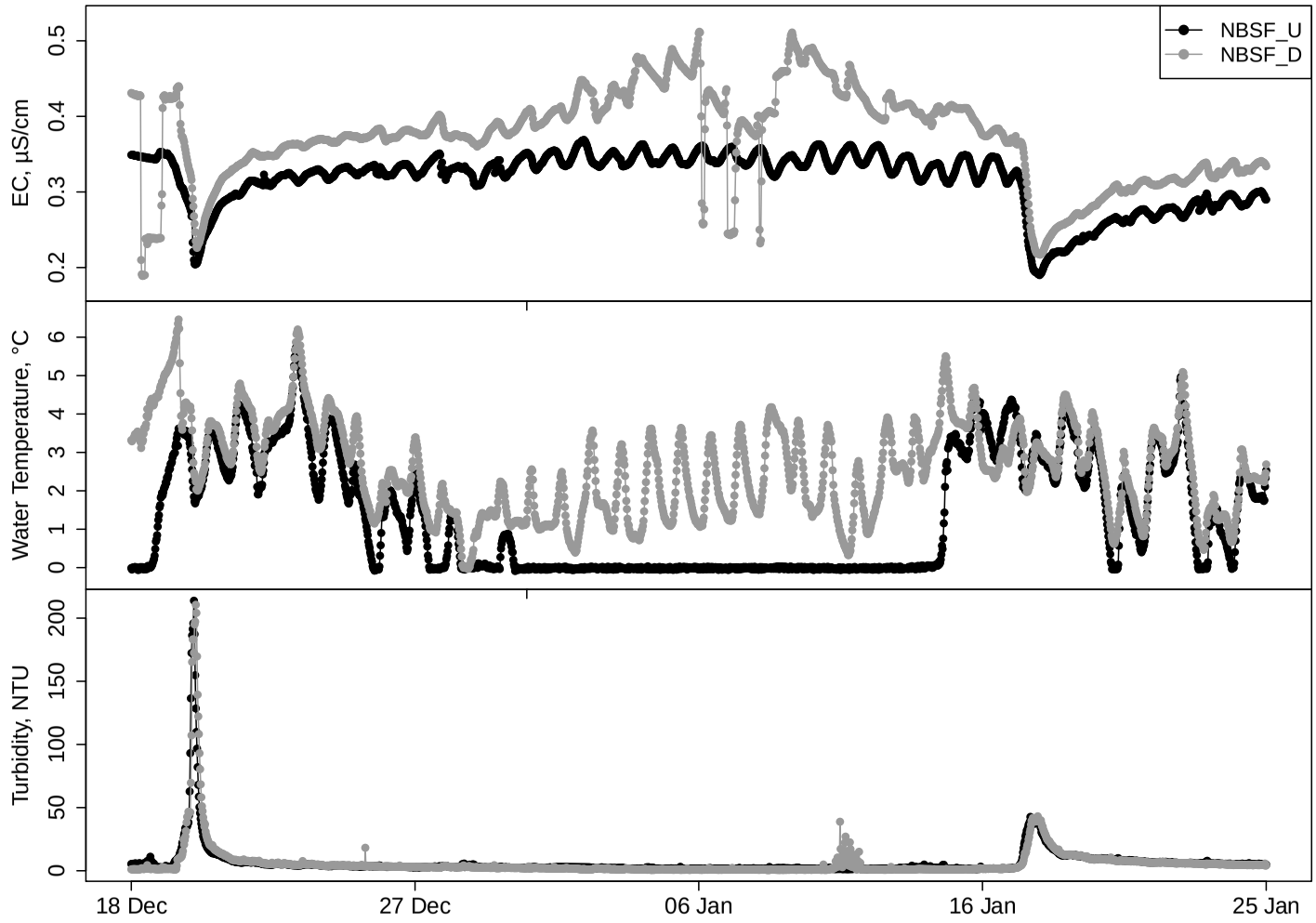

Fig. D.13: Comparison of high-frequency measurements at the North Branch sites from 18 December 2010 to 25 January 2011.

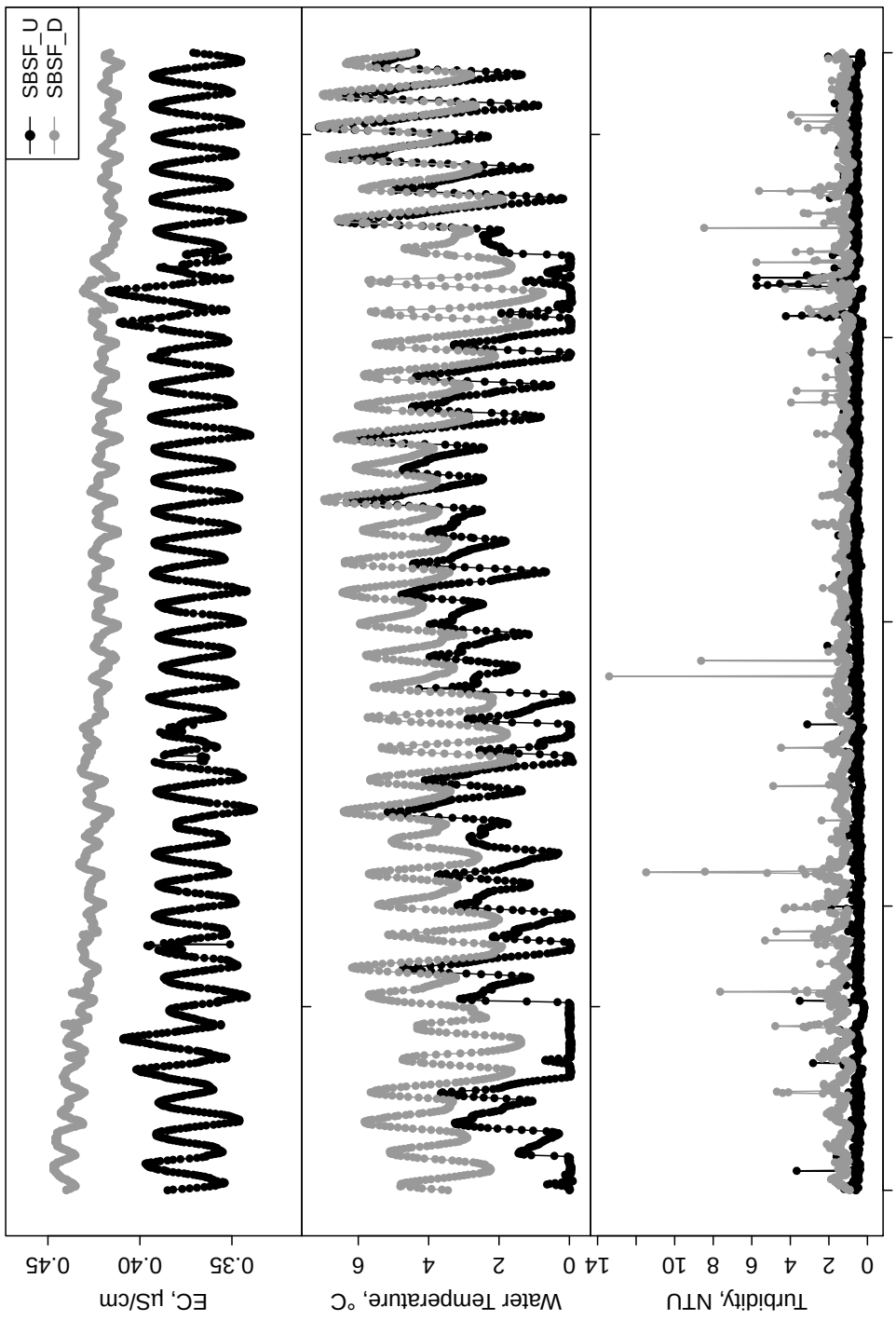

Fig. D.14: Comparison of high-frequency measurements at the South Branch sites from 25 January to 03 March 2010.

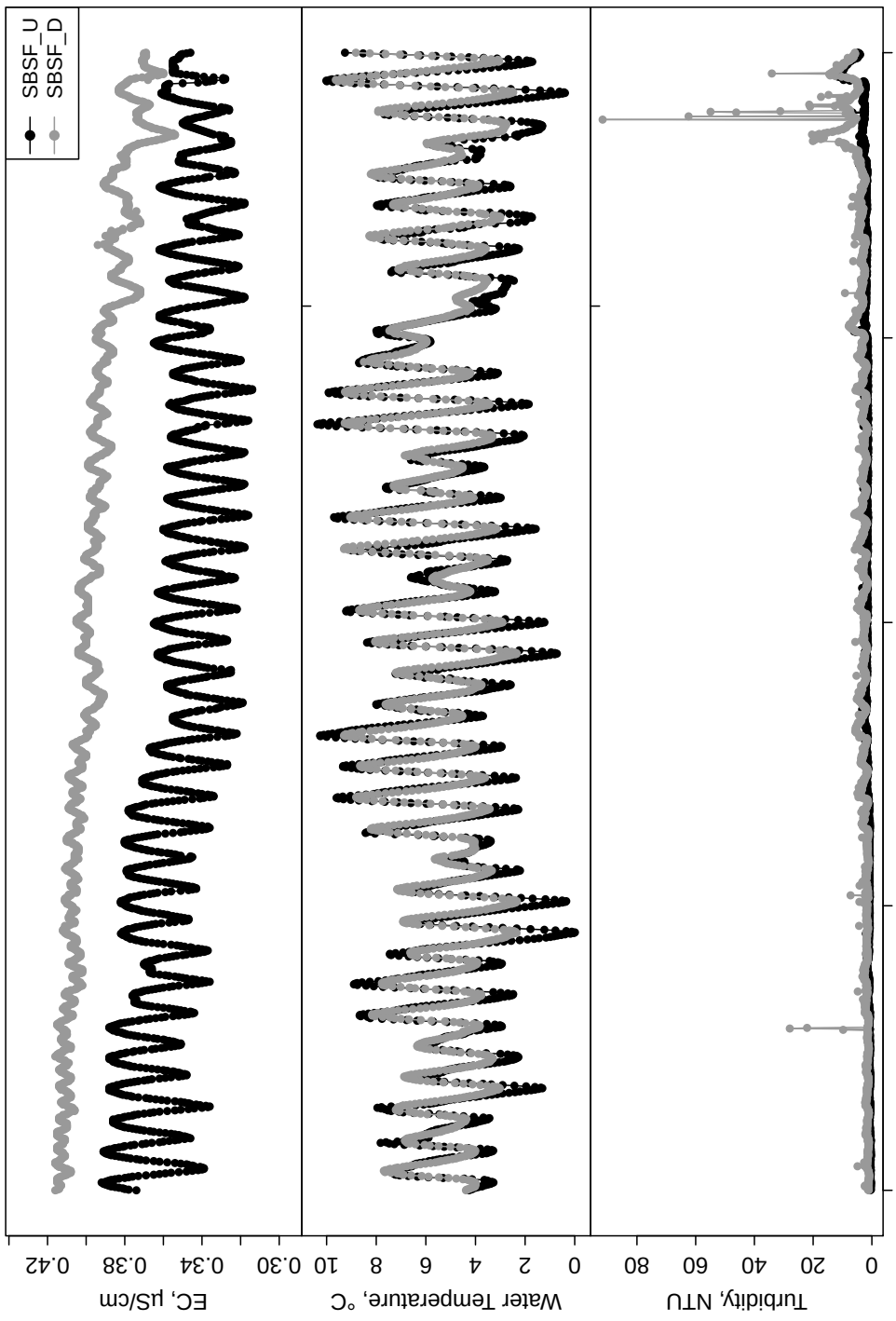

Fig. D.15: Comparison of high-frequency measurements at the South Branch sites from 03 March to 08 April 2010.

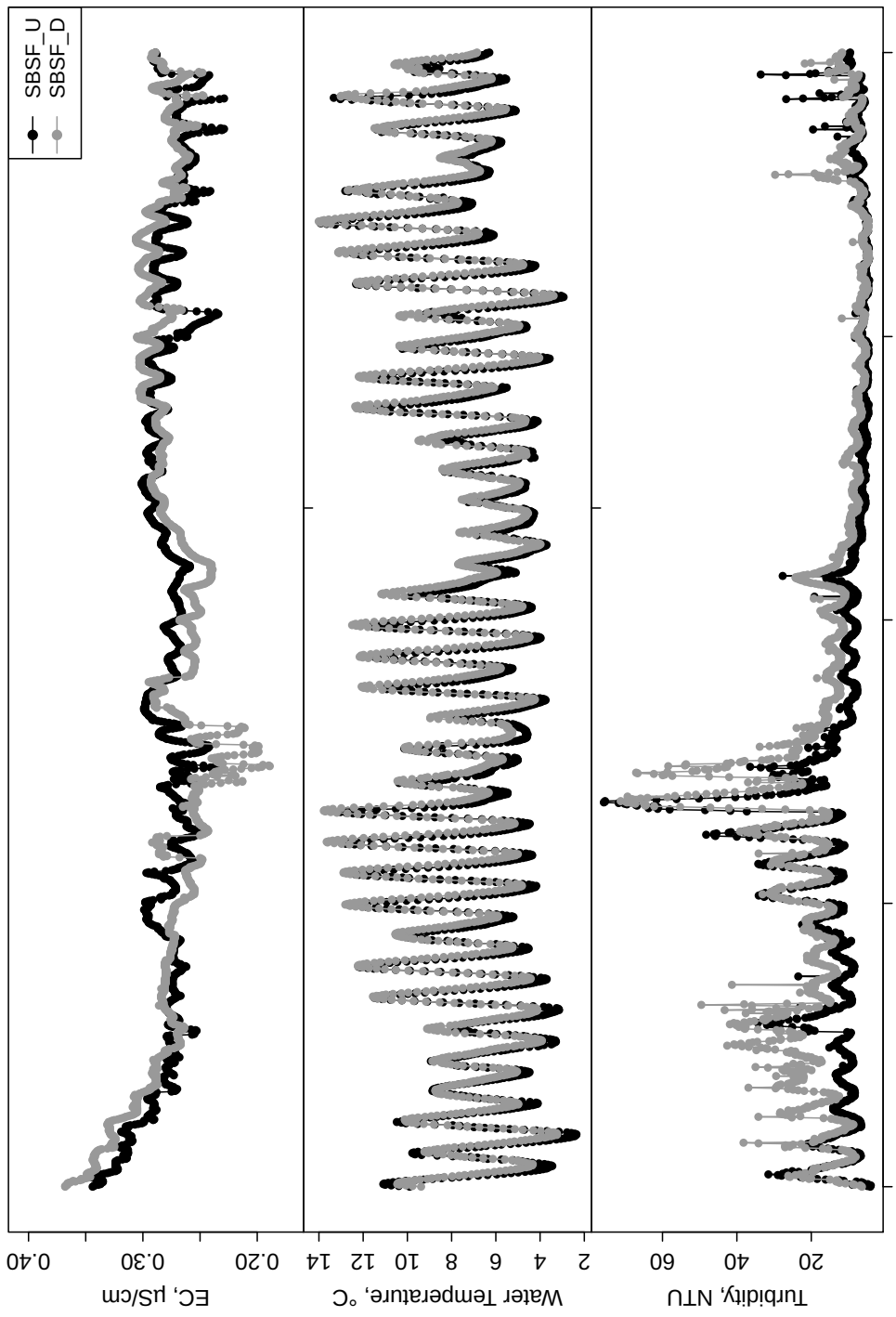

Fig. D.16: Comparison of high-frequency measurements at the South Branch sites from 08 April to 15 May 2010.

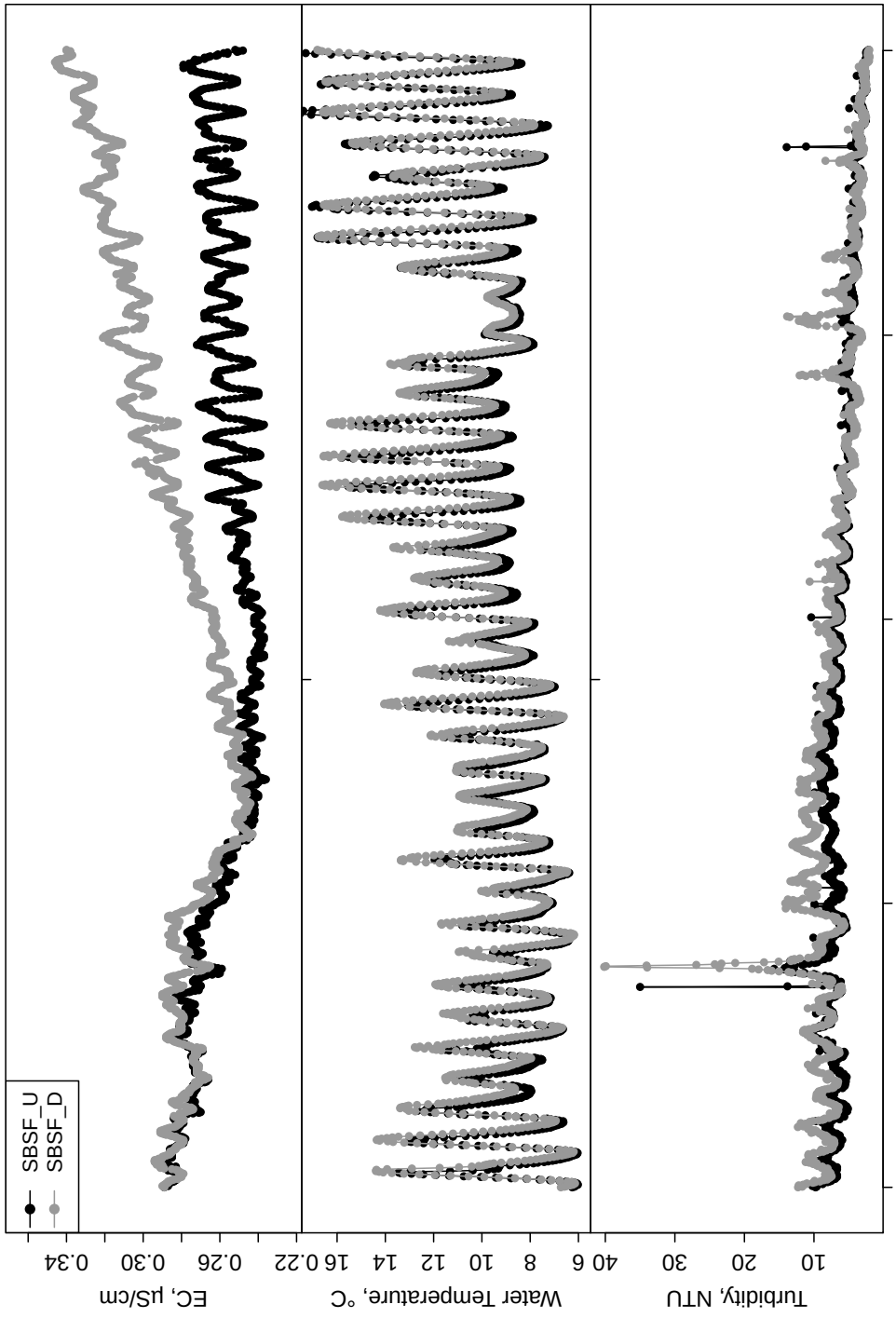

Fig. D.17: Comparison of high-frequency measurements at the South Branch sites from 15 May to 20 June 2010.

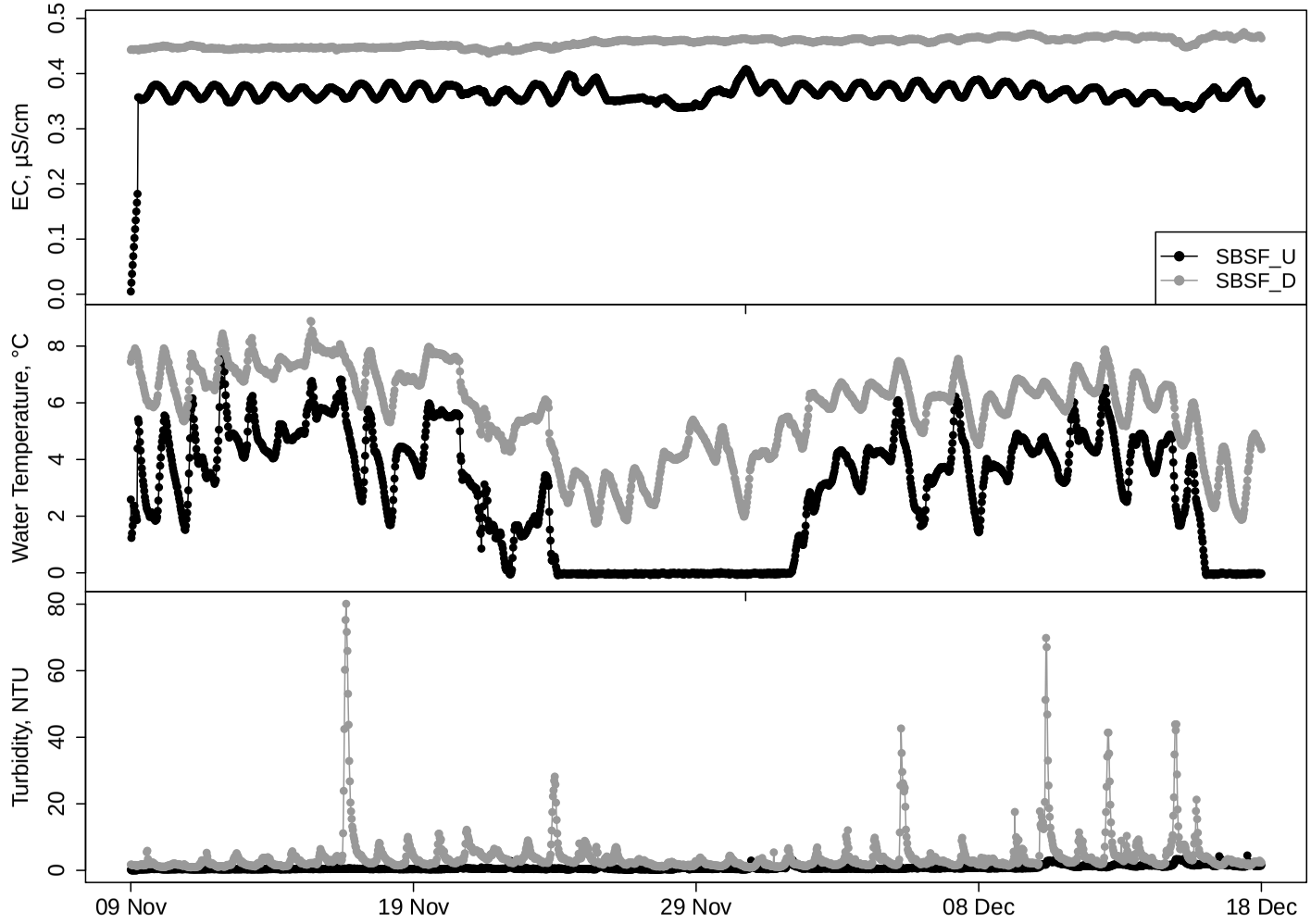

Fig. D.18: Comparison of high-frequency measurements at the South Branch sites from 09 November to 18 December 2010.

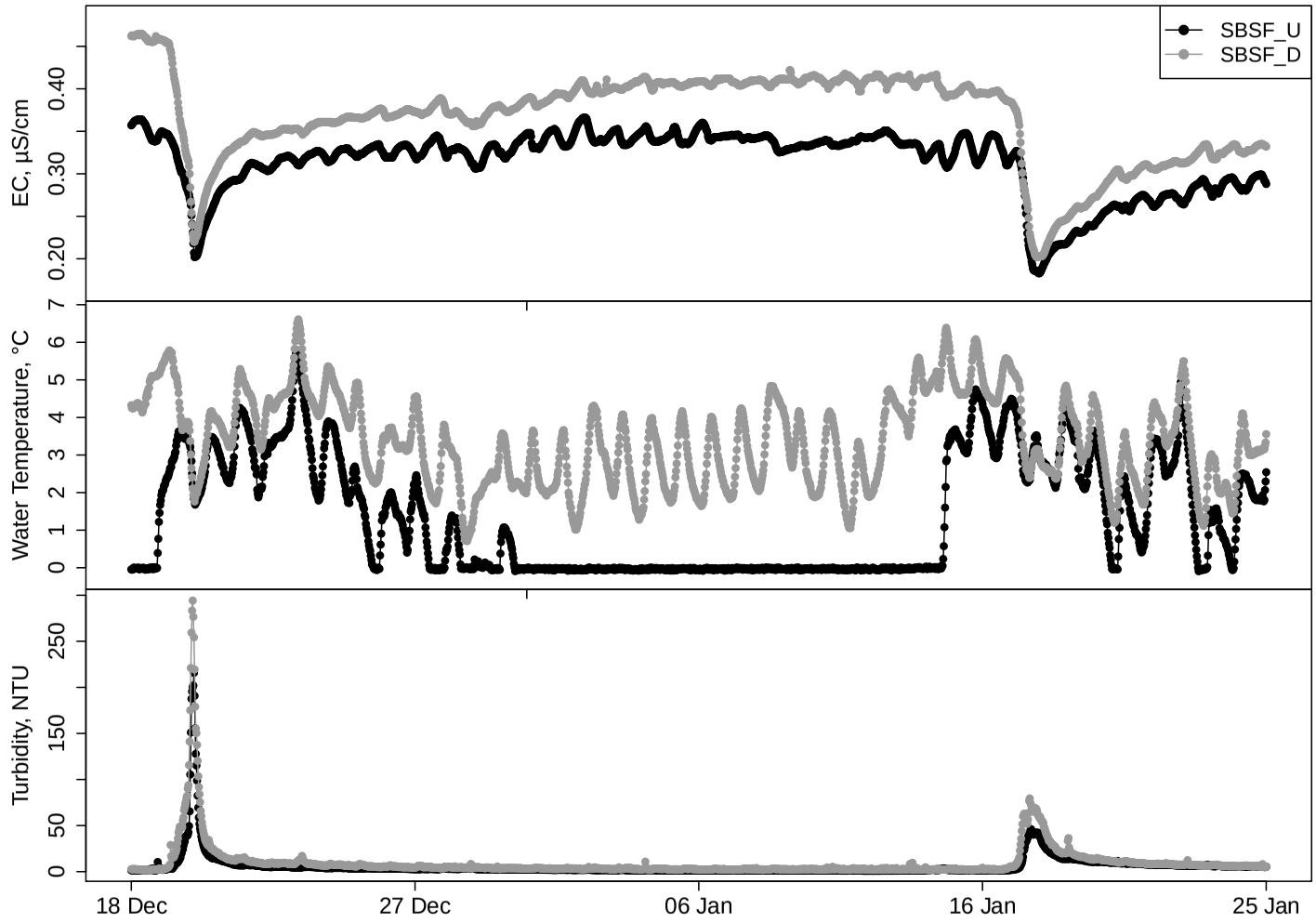

Fig. D.19: Comparison of high-frequency measurements at the South Branch sites from 18 December 2010 to 25 January 2011.